PONTIFÍCIA UNIVERSIDADE CATÓLICA
DO RIO DE JANEIRO

Anna De Falco

Activity evaluation and toxicological profile of new potential "Metal Protein Attenuating Compounds" in biological models of Alzheimer's disease

Tese de Doutorado

Thesis presented to the Programa de Pós-graduação em Química of PUC-Rio in partial fullfilment of the requirements for the degree of Doutor em Química.

Advisor: Prof. Nicolás Adrián Rey

Rio de Janeiro
August 2017

Anna De Falco

Activity evaluation and toxicological profile of new potential "Metal Protein Attenuating Compounds" in biological models of Alzheimer's disease

Thesis presented to the Programa de Pós-graduação em Química of PUC-Rio in partial fullfilment of the requirements for the degree of Doutor em Química. Approved by the undersigned Examination Committee

Prof. Nicolás Adrián Rey
Advisor
Departamento de Química - PUC-Rio

Prof. Ricardo Queiroz Aucélio
Departamento de Química - PUC-Rio

Profª Elene Cristina Pereira Maia
UFMG

Prof. Sérgio Teixeira Ferreira
UFRJ

Dr. Thomas Hermann Geriach
BIOZEUS

Profª Maria Lucia Vellutini Pimentel
Santa Casa de Misericórdia

Drª Ariane Leites Larentis
FIOCRUZ

Prof. Márcio da Silveira Carvalho
Vice Dean of Graduate Studies Centro Técnico Cientifico – PUC-Rio

Rio de Janiero, August 9th 2017

Anna De Falco

The author is graduated in Product and Process Biotechnology from Università degli Studi di Napoli Federico II (2006), validated in Brazilian territory by UFRJ, as Bachelor Microbiology and Immunology. She holds a specialization in Molecular and Industrial Biotechnology from the Università degli Studi di Napoli Federico II (2009), and a Master's Degree in Public Health and Environment from ENSP FIOCRUZ (2013) with emphasis on Environmental Toxicology

All'Arpa

Acknowledgments

To Prof. Dr. Ricardo Aucelio for the availability shown throughout all my PhD development, answering all kind of doubts, analytical or statistical, and for always being available to talk, discuss and laugh, even if in a rush in the middle of the hallway.

To Camilla and Daphne for allowing the use of H2QBS and HPCIH, respectively, and for their availability for their synthesis and all the practical help during the work.

To the group LABSO-Bio, present past and future: Ana Beatriz, Barbara, Carol, Cassiana, Catherine, Danilo, Daphne, Elio, Flavia, Guilherme, Isabela, Jesica, Juliana, Lisbet, Maria Victoria, Sergio: you made me feel good even in days when nothing worked, taught me every day that the union makes the force (may the force be with us), I would have been lost without you ... Did I hear OUTBACK?

To Daphne, my strong roommate during the period when I practically lived in the lab, may we'll never have the maturity to work with copper.

To Dr. Francinne Machado Ribeiro, more than a rheumatologist, a safe place, for being on my side in this daily struggle against this silent disease that is ankylosing spondylitis.

To Dr. Ana Clara Visconti, for the infinite scolding, and for teaching me that asking for perfection is too much, but asking for the best isn't.

To Marcello, Maria e Mario Leopoldo, because "you may leave Sala Consilina, but Sala Consilina never leaves you".

To Francesca, Giuseppe, Lalla and PeppePas, who showed me that friendship does not suffer from space-time changes.

To my volleyball families (Partenope, Revolution, Win & Wine, AABB and CescoPes), who in the course of my adult life have been the best therapy of all, indoor, and especially outdoor.

At 7x1, even close we had to maintain a virtual contact because of my experiments / congresses / articles / tests / works and everything that led to this thesis.

To Maira and Gustavo, despair together always gets better, make us understand that the problem isn't us, or is it???

To my Brazilian family, Bia, Druval and PH, because we will always be the "Republic of love", you all live in my heart.

To my family and my closest friends, who even with an ocean of distance alwa[...] made me feel close to home.

To my mother, aware that I had just done "half of my duty".

To my father (*in memoriam*), because I will never be able to make you proud, but I will always keep trying.

To my cats, Chewbacca and Wolverine (*in memoriam*), there will never be better study mates.

To my husband, Alan, we have evolved over several languages, even though I will never know enough words to thank you; define what you are in my life is beyond words: my refuge, my best friend, my biggest family. Even during our eternal "Samba em prelúdio".

And, finally, to me: against all odds I'm here after all.

Abstract

De Falco, Anna; Rey, Nicolás Adrián (Advisor). **Activity evaluation and toxicological profile of new potential "Metal Protein Attenuating Compounds" in biological models of Alzheimer's disease**. Rio de Janeiro, 2017. 156p. Tese de Doutorado - Departamento de Química, Pontifícia Universidade Católica do Rio de Janeiro.

Alzheimer's disease (AD) is currently the most common form of dementia worldwide. The synaptic loss at the neurotransmitter system level and the presence of extracellular amyloid plaques and intracellular neurofibrillary tangles are major events that identify AD among other dementias, at the cellular level. From a chemical point of view, it is well-known that Aβ peptide coordinates physiological metals, such as Cu and Zn, which, in AD patients' brain, are poorly distributed and concentrated in amyloid plaques. Despite the fact that aggregation of the Aβ peptide is one of the most important features of AD pathogenesis, the function of the extracellular plaques composed by this peptide is not fully understood. The hypothesis that Aβ neurotoxicity is best explained by its oligomeric form is well accepted. There are evidences supporting the link between physiological metals and oligomerization of Aβ. 'Metal-Protein Attenuating Compounds' (MPACs), a promising class of compounds for the management of AD and differ from strong chelating agents, once, instead of systematically removing metals, they correct abnormal interactions with Aβ, inhibiting the Aβ oligomerization, as well as preventing redox reactions that can ultimately generate harmful reactive oxygen species (ROS). In this context, the present work evaluates four compounds with potential to act as MPACs, namely, INHHQ, HPCIH, H2QBS and INHOVA. Among them, three substances (INHHQ, HPCIH and INHOVA) belong to the chemical class of aroylhydrazones. The stability of each compound was tested over 30 h in water/DMSO mixtures of different concentrations in order to define the best condition for the biological studies and a

suitable stability pattern was observed for all compounds, with the exception of INHOVA, which showed high sensibility to hydrolysis. INHHQ, HPCIH and H2QBS were analyzed *in vitro* in order to evaluate their ability to compete with Aβ for Cu and Zn, by ^{1}H and ^{1}H x ^{15}N HSQC NMR analyses: a similar metal-sequestering profile for INHHQ and HPCIH was observed, H2QBS, on the other hand, showed a higher capacity for the removal of metal ions from Aβ. Cell studies were performed in order to assess cytotoxicity. INHHQ and HPCIH showed the most promising profiles, suggesting that their toxicity was related to the amyloid precursor protein (APP) overexpression. Both substances were then evaluated concerning their capacity to affect the APP pathway by means of proteomic analyses in an exposed APP-overexpressing cell line. Results suggest possible interaction of both compounds with γ-secretases. *In vivo* acute toxicity assays were performed, showing no lethality at doses up to 200 mg kg^{-1}. Several biochemical parameters, such as GSH and Fe, Cu and Zn concentrations in brain, liver, heart and kidneys were evaluated. The results suggested that H2QBS present high capacity to displace biometals in rats, when high doses are administered. *In vivo* effectiveness studies were performed in order to evaluate the capacity of the most promising substance, *i.e.*, INHHQ, of affecting behavior in animal models. For this purpose, anxiety and memory were evaluated in mice, through Elevated Plus Maze, Open Field and Novel Object Recognition tests. The results indicated that INHHQ treatment does not alter the fear / anxiety-related defensive responses and that doses of 10 mg kg^{-1} or higher induce temporary cognitive impairment in healthy mice. Finally, it was proved that an innocuous INHHQ dosage of 1 mg kg^{-1} does prevent short- and long-term memory impairment induced by Aβ oligomers infusion7 in mice. The findings reported in this thesis definitively point to INHHQ as a good candidate for further pre-clinical trials, as a potential MPAC for AD treatment.

Keywords

Alzheimer's disease; metal hypothesis; Aβ; MPAC.

Resumo

De Falco, Anna; Rey, Nicolás Adrián; **Avaliação de atividade e perfil toxicológico de novos potenciais "Compostos Atenuadores da Interação Metal-Proteína" em modelos biológicos da doença de Alzheimer**. Rio de Janeiro, 2017. 156p. Tese de Doutorado - Departamento de Química, Pontifícia Universidade Católica do Rio de Janeiro.

A doença de Alzheimer (DA) é atualmente a forma mais comum de demência. A perda sináptica no nível do sistema neurotransmissor, a presença de placas amilóides extracelulares e emaranhados neurofibrilares intracelulares são importantes eventos que diferenciam, no nível celular, a DA dentre outras demências. Do ponto de vista químico, é bem conhecido que o peptídeo Aβ coordena os metais fisiológicos, como Cu e Zn, os quais, no cérebro de pacientes com DA, estão mal distribuídos e concentrados em placas amilóides. Apesar da agregação do peptídeo Aβ ser uma das características mais marcantes da patogênese da DA, a função das placas extracelulares composta por esse peptídeo não é totalmente compreendida. A hipótese que a neurotoxicidade de Aβ é melhor explicada pela sua forma oligomérica é bastante aceita pela comunidade cientifica. Há evidências que suportam a ligação entre metais fisiológicos e oligomerização de Aβ. Os compostos atenuadores de interação metal-proteína (MPACs, do inglês, *Metal-Protein Attenuating Compounds*) são uma classe promissora de compostos para o tratamento da DA que diferem dos agentes quelantes fortes, porque, ao invés de remover metais sistematicamente, esses corrigem interações anormais com Aβ, inibindo a oligomerização de Aβ, além de prevenir reações redox que podem gerar espécies reativas de oxigenio tóxicas. Neste contexto, o presente trabalho avalia quatro compostos com potencial para atuar como MPAC, a saber, INHHQ, HPCIH, H2QBS e INHOVA. Entre esses, três (INHHQ, HPCIH e INHOVA) pertencem à classe química de aroíl-hidrazonas. A estabilidade de cada composto foi testada durante 30 h em misturas de água/DMSO em diferentes concentrações, a fim de definir a melhor condição para os estudos biológicos, e um padrão de estabilidade adequado foi observado para todos os compostos, com

exceção do INHOVA, que se demonstrou muito sensível à hidrólise. INHHQ, HPCIH e H2QBS foram analisados *in vitro* para avaliar a capacidades de competir com Aβ para Cu e Zn, por análises de RMN ^{1}H e ^{1}H x ^{15}N HSQC: INHHQ e HPCIH apresentaram perfis de sequestro de metais similares e H2QBS mostrou uma maior capacidade para a remoção de íons metálicos do Aβ. Estudos celulares foram realizados a fim de avaliar a citotoxicidade. INHHQ e HPCIH apresentaram os perfis mais promissores, sugerindo que tais toxicidades sejam relacionadas à sobre-expressão da proteína precursora amiloide (APP, do inglês: *Amyloid precursor protein*). Ambas as substâncias foram avaliadas quanto a sua capacidade de afetar a rota do APP por meio de análises proteômicas em uma linha celular que sobre-expressa APP. Os resultados sugeriram a possível interação dos compostos com as γ-secretases. Foram realizados ensaios de toxicidade aguda *in vivo*, não apresentando letalidade em doses de até 200 mg kg^{-1}. Foram avaliados parâmetros bioquímicos, tais como as concentrações de GSH e Fe, Cu e Zn em cérebro, fígado, coração e rins. Os resultados sugeriram que H2QBS possui alta capacidade para deslocar os biometais em ratos, quando administrado em doses elevadas. Estudos de efetividade *in vivo* foram realizados para avaliar a capacidade da substância mais promissora, ou seja, INHHQ, de afetar o comportamento em modelos animais. Para esse propósito, ansiedade e memória foram avaliadas em camundongos, através dos testes de Labirinto em Cruz Elevado, Campo Aberto e Reconhecimento de Novo Objeto. Os resultados indicaram que o tratamento com INHHQ não altera a resposta defensiva relacionada ao medo/ansiedade e que doses de 10 mg kg^{-1} ou maiores induzem comprometimento cognitivo temporário em camundongos saudáveis. Finalmente, provou-se que uma dosagem INHHQ inócua de 1 mg kg^{-1} evita problemas de memória a curto e longo prazos induzidos pela infusão de oligômeros de Aβ em camundongos. Os resultados relatados nesta tese apontam para o INHHQ como um bom candidato para ensaios pré-clínicos adicionais, como potencial MPAC para o tratamento da DA.

Palavras-chave

Doença de Alzheimer; hipótese metálica; Aβ; MPAC.

Table of contentes

List of figures

List of tables

PUC-Rio - Certificação Digital Nº 1321699/CA

List of abbreviations

1D SDS-PAGE, one-dimensional sodium dodecyl sulfate polyacrylamide gel electrophoresis;

ACh, acetylcholine;

AChE, acetylcholinesterase;

AD, Alzheimer's disease;

AMPA, α-amino-3-hydroxy-5-methyl-4-isoxazolepropionic acid;

ApoE4, apolipoprotein E4;

APP, amyloid precursor protein

Aβ, β-amyloid peptide;

AβOs, Aβ oligomers;

BCA, Bicinchoninic Acid;

BSA, bovine serum albumin;

ChAT, choline acetyltransferase;

CI, Confidence interval;

CNs, coordination numbers;

CQ, Clioquinol;

DMSO, dimethyl sulfoxide;

DNA, deoxyribonucleic acid;

DTNB, 5,5 '-dithio-bis- (2-nitrobenzoic acid);

EOAD, early onset Alzheimer's disease;

EPM, elevated plus maze;

FAD, familial Alzheimer's disease;

GSH, L-γ-glutamyl-L-cysteinyl-glycine;

GST, glutathione S-transferase;

H2QBS, 4-(8-hydroxyquinoline-5-azo)-benzensulfonic acid;

HEK 293, human embryonic kidney cells 293;

HFIP, 1,1,1,3,3,3-hexafluoro-2-propanol;

His, histidine;

HPCIH, pyridyl-2-carboxaldehyde isonicotinoyl hydrazone;

HPLC, high performance liquid chromatography;

HSQC, heteronuclear single quantum correlation;

HVa, vanillin;

IC_{50}, half maximal inhibitory concentration;

ICP-MS, inductively coupled plasma mass spectrometry ;

i.c.v., intracerebroventricular

IGF, insulin-like growth factor;

INEPT, insensitive nuclei enhanced by polarization transfer;

INH, isoniazid;

INHHQ, 8-hydroxyquinoline-2-carboxaldehyde isonicotinoyl hydrazone;

INHOVA, 2-hydroxy-3-methoxy-benzaldehyde isonicotinoyl hydrazone;

IR, infrared;

K, lysine;

K_D, dissociation constant;

L, leucine;

LOAD, late onset Alzheimer's disease;

M, methionine;

MCI, mild to moderate cognitive impairment;

MPACs, metal-protein attenuating compounds

MTT, 3-(4,5-dimethylthiazol-2-yl)-2,5-diphenyltetrazolium bromide tetrazolium;

N, asparagine;

NFTs, neurofibrillary tangles;

NMDA, *N*-methyl-D-aspartate;

NMR, nuclear magnetic resonance;

NOR, novel object recognition;

OF, open field;

o-HVa*, ortho*-vanillin;

PAG, periaqueductal gray matter;

RNA, ribonucleic acid;

RNS, reactive nitrogen species;

ROS, reactive oxygen species;

SDS, sodium dodecyl sulfate;

SULT, sulfotransferase;

SW, Swedish mutation;

TTBS, Tween-20 / Tris-buffered saline;

UDPGT, uridine diphosphogluconosyltransferase;

UV-Vis, ultraviolet-visible;

β-APP, β-Amyloid precursor protein.

Only the peak matters. ACK

1.
Introduction

1.1.
Neurodegenerative diseases

Neurodegenerative diseases, such as Alzheimer's disease, Parkinson's disease, Huntington's disease and Amyotrophic Lateral Sclerosis, are pathologies characterized by a progressive loss of one or more nervous system's functions. They are disabling conditions currently treated, with very few results, by administering purely symptomatic drugs. Together, they are considered the biggest cause of dementia among the known diseases (Perry *et al.*, 1977; Wilcock *et al.*, 1982).

Dementia is a brain disorder characterized by a decrease in one or several cognitive functions, such as memory, intellect and personality, causing significant damage to the individual's quality of life. The most common symptoms associated with dementia are memory loss, delirium, psychosis, aggression, rage, insomnia and anxiety. Causes and molecular mechanisms underlying this disorder are not fully understood, but it is clear that it may be caused by different diseases that damage brain tissue, reversibly or not, by changing its operational mode (Mehan *et al.*, 2012).

1.1.1.
Diagnostic features of Alzheimer's disease

Alzheimer's (AD) is a disease that currently represents the most common form of dementia in the elderly. There are presently about 35 million people affected by AD in the world, and it is predicted that, by the year 2030, this number will reach 70 million (Reitz *et al.*, 2011).

The first report describing what would today be called Alzheimer's disease was published more than a century ago, by the German physician and pathologist Alois Alzheimer (Alzheimer *et al.*, 1995). The studied patient, A. Deter, began to

manifest dementia at the age of 51. These signs, at the time, did not correspond to any known disease. After six years of the onset of symptoms, which included memory loss, paranoia, and behavioral and language problems, the patient died. The autopsy showed an atrophic brain and signs of abnormal protein depositions, which were later called senile plaques and neurofibrillary tangles, NFTs (Maurer *et al.*, 1997).

In general, it is observed in AD patients the impairment of cognitive abilities, which tends to become more significant over the years. The short-term memory often is the first to be affected, but other skills are also engaged with the progress of the disease, such as, for example, the ability to perform calculations and to use common objects and tools (Small *et al.*, 1997).

Currently, there can be clearly distinguished two forms of AD: Late Onset AD (LOAD) and Familial AD (FAD). FAD, also known as Early Onset AD (EOAD), is characterized by its premature appearance, occurring before age 60; it is related to a Mendelian autosomal dominant transmission, representing 1% to 6% of all cases of AD (Crook *et al.*, 1998; Kawas, 2003). On the other hand, LOAD, the most common form of the disease, is characterized by a late appearance (after 60 years) and has a very complex etiological pathway (Perez *et al.*, 2014).

Despite the different causes, both forms of the disease are defined by the same pathological features, namely: decrease in cognitive function, particularly affecting memory of events, both remote and recent; language; judgment; attention and executive functions, such as capacity of planning and organization (Marien *et al.*, 2004; Bekris *et al.*, 2010). These behavioral changes progress as the disease advances (Kawas, 2003; Schwartz e Roth, 2008). They are complemented by changes in behavior and apathy in the earliest stages of the disease, followed, in the later stages, by psychosis and agitation (Lyketsos *et al.*, 2000; Guimaraes *et al.*, 2014). Changes of the motor and sensory system remain uncommon until the last phases of the disease (Mckhann *et al.*, 1984). Death usually occurs 6 to 12 years after the symptoms' onset, usually due to immobility complications or pulmonary embolism and pneumonia (Goodman *et al.*, 1996).

The most relevant neuropathological data in individuals affected by this disease are the presence of diffuse cortical atrophy, neurovascular degeneration and neuronal and synaptic losses, involving numerous neurotransmitter systems (Serrano-Pozo *et al.*, 2011). This starts in the cholinergic system of the basal forebrain, which plays a fundamental role in memory and learning processes (Winkler *et al.*, 1995), although significant changes are also observed at neuronal systems involving noradrenaline, serotonin, glutamate, P substance and somatostatin as neurotransmitters. On the other hand, the dopaminergic system and systems involving neuropeptides remain mostly unaffected. (Smiley *et al.*, 1999; Dringenberg, 2000; Marien *et al.*, 2004; González-Castañeda *et al.*, 2013; Toneff *et al.*, 2013).

Other common characteristics of the disease are: the presence of extracellular amyloid plaques and intracellular neurofibrillary tangles masses located primarily in the amygdala, hippocampus and entorhinal cortex of the temporal lobe, while the parietal and frontal portions of the association cortex appear to be less affected (Cardarelli *et al.*, 2010; Serrano-Pozo *et al.*, 2011). In Figure 1 a scheme of the brain's different regions is shown. The areas most affected by AD are highlighted in red (Amygdala, Hippocampus and Enthorhinal Cortex).
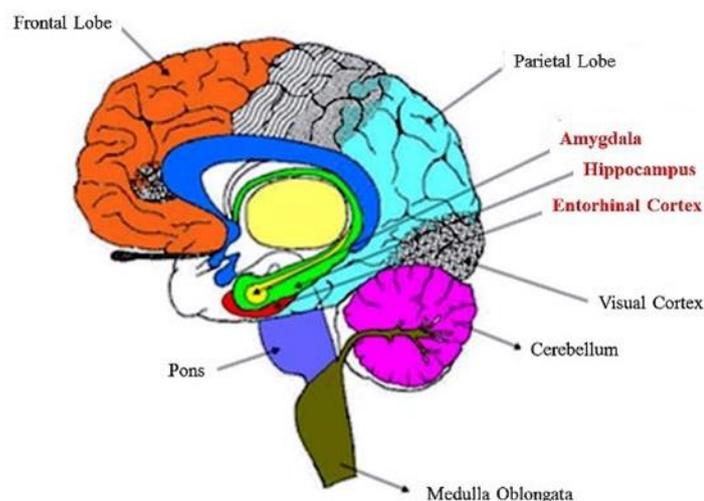
Figure 1. Different brain's regions. The most AD affected areas are highlighted in red.

The presence of extracellular senile plaques is the major pathological feature of AD (Mayeux & Stern, 2012) and is currently considered as the

fundamental sign that allows the differential diagnosis of AD at *post mortem* outcomes. These plaques are formed by extracts of composite masses of extracellular filamentous aggregates of the amyloid β protein (Jarrett *et al.*, 1993). Senile plaques may be individually found in the brain of healthy elderly people; however, deposition is not as intense as in patients suffering from AD (Smith, 1999).

Several other biochemical alterations are seen in AD patients, as widespread oxidative stress in the brain, neuroinflammation, calcium deregulation, deficiency and altered distribution of mitochondria, oligomerization of the Aβ peptide, intracellular accumulation of NFTs, synaptic toxicity and problems in metal homeostasis, which will be discussed below in more detail.

In AD diagnosis, the disease stages are determined according to the Braak scale. This approach mainly evaluates the distribution of NFTs in brain in correlation with the clinical symptoms of dementia. Stages are defined as I and II when NFTs involvement is confined mainly to the trans-entorhinal region, translated symptomatologically as normal and slightly affected cognition levels, respectively. In phases III and IV, limbic regions, such as the hippocampus, are also involved, leading to MCI (mild to moderate cognitive impairment), confusion and loss of memory, disorientation, problems with daily tasks, changes in personality and judgment on stage III and psychotic symptoms such as anxiety, mistrust, restlessness and sleep disorders in stage IV. Finally, in stages V and VI, there is great neocortical involvement, resulting in difficulty in recognizing family and friends, loss of speech, appetite and control of the bladder and bowel (Braak & Braak, 1991).

1.1.2.
Molecular bases of Alzheimer's disease

Different hypothesis concerning the molecular bases of AD have been proposed, and the most relevant are outlined below.

1.1.2.1.
Cholinergic Hypothesis

In the early 80s, Bartus introduced "The cholinergic hypothesis of geriatric memory dysfunction" (Bartus *et al.*, 1982). *Post mortem* studies in AD patients were fundamental to the development of the hypothesis. Bartus' research showed, in cortex and hippocampus of in-life affected individuals, a concentration decrease, from 60 to 90%, of choline acetyltransferase (ChAT), the enzyme responsible for the synthesis of acetylcholine (ACh), and a variable reduction, between 30 and 90%, of the cholinergic neurons in the *nucleus basalis* of Meynert, which is typically constituted by neuronal networks of cholinergic receptors (Davies & Maloney, 1976; Kása *et al.*, 1997).

A very interesting observation was the positive association between these depletions and the degree of severity concerning the patients' cognitive deficit (Wilcock *et al.*, 1982; Kása *et al.*, 1997). The importance of cholinergic function in learning and memory processes has been recognized since the early 70s (Deutsch, 1971). Confirming this theory, pharmacological studies with non-human primates indicate that blocking cholinergic transmission leads to a decrease in cognitive aptitudes that are extremely similar to those observed in people affected by dementia (Drachman & Leavitt, 1974; Drachman & Sahakian, 1980). Further studies showed that the administration of cholinomimetic substances strongly reduces the mnemonic difficulties presented by patients with AD (Drachman & Sahakian, 1980; Christie *et al.*, 1981).

In the experimental scenario, numerous studies with mammalian investigate the effects of irreversible inhibitors of acetylcholinesterase, AChE, the enzyme responsible for the catalysis of ACh present in the synaptic space, measuring ACh and AChE brain levels and the performance animals models in spatial recognition tests (Bennett *et al.*, 2007; Muthuraju *et al.*, 2009). These studies pointed to learning improvement due to the activation of the cholinergic system. The reduction of learning and memory performance in different animal models, when exposed to administration of the muscarinic antagonists atropine and scopolamine, corroborates this supposition (D'hooge & De Deyn, 2001).

Pharmacological studies in humans have shown that such substances hinder the formation of new memories without influencing the reacquisition of events from the remote past (Hasselmo, 2006). On the contrary, cholinomimetic substances promote the acquisition of new memory traces, both in humans and in animal models (Buccafusco *et al.*, 2005). This demonstrates the importance of cholinergic receptors' activation in the memory fixation process (Power *et al.*, 2003). Recently, it has been demonstrated that the antagonism between nicotinic and muscarinic receptors causes a severe cognitive deterioration, possibly indicating that this process is governed by the functioning of both receptors, activated by the modulation of the amnesic processes, interacting with each other (Green *et al.*, 2005).

Although the role of the prosencephalon (or forebrain) on the basis of memory regulation and learning processes is generally recognized, this concept is still matter of discussion among several researchers (Dunnett *et al.*, 1991; Muir *et al.*, 1993; Chappell *et al.*, 1998). This is probably due to the difficulty of assigning the full responsibility of these complex processes on a single neural system or on one brain area only.

1.1.2.2.
The Amyloid Cascade

Since the discovery of AD, it has been recognized that the symptoms of the disease may be associated with the development of numerous intraneuronal and extracellular filamentous lesions in the limbic and in the cerebral cortexes. Abnormal strands of cytoplasmic fibers, including NFTs, occur in neuronal cell bodies as well as in axons and dendrites. These signs are collectively called dystrophic neuritis.

In addition to these individualities, AD is characterized by another important histopathological finding: the widespread presence of plaques and aggregates formed mainly by Aβ in the brain tissue (Blanquet *et al.*, 1987; Jenkins *et al.*, 1988; Selkoe, 1996; Nie *et al.*, 2011). The production of this type of peptide is considered central in the pathology of AD, originating the so-called "amyloid cascade hypothesis".

As previously discussed, the presence of amyloid plaques, together with NFTs, in the hippocampus, amygdala, cerebral cortex and other regions of the brain constitutes the basis for a definitive pathological diagnosis of AD (Mayeux & Stern, 2012).

In Figure 2 some differences between a healthy neuron and a sick one are outlined.
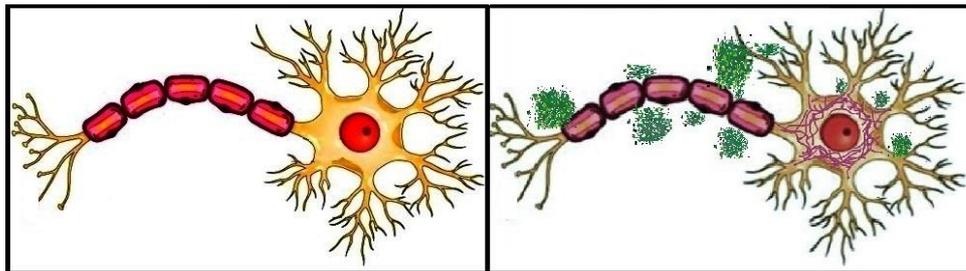
Figure 2. A healthy neuron (left) and neuron of an AD patient (right). Extracellular amyloid plaques (green) and intracellular NFTs (red fibers) can be observed in the sick cell. Adapted from (De Falco *et al.*, 2016).

The location of the gene encoding the β-amyloid protein precursor, β-APP, on the q-arm of chromosome 21, seems to explain the observation that patients with Down syndrome (trisomy 21) present β-amyloid peptide, Aβ, brain deposits in their late childhood or early adulthood, subsequently developing the classic neuropathological characteristics of AD, when they reach around the age of forty (Giaccone *et al.*, 1989; Iwatsubo *et al.*, 1995). This finding led to a specific search for families with autosomal dominant AD that had a genetic link in chromosome 21, resulting in the identification of six different missense mutations. This mutations lead to the synthesis of amino acids different from those encoded in the wild gene. Five of them are associated with FAD (Chartier-Harlin *et al.*, 1991; Goate *et al.*, 1991; Murrell *et al.*, 1991; Hendriks *et al.*, 1992; Mullan *et al.*, 1992) and one is associated with another pathology, the hereditary cerebral hemorrhage Dutch type syndrome (Levy *et al.*, 1990).

It is unclear why Aβ, although secreted by many types of cells in the body, is abundantly deposited in AD patients' brains, with only minor amounts of non-fibrillary Aβ deposits observed in the peripheral tissues (Joachim *et al.*, 1989; Ikeda *et al.*, 1993). Three secretases, α-, β- and γ-secretase, cleave the amyloid precursor protein, APP, at different sites (Figure 3). APP cleavage at the cell

membrane by α- and γ-secretases leads to the non-amyloidogenic pathway, *i.e.*, the final products of the pathway do not oligomerize. The cleavage by α-secretases produces two portions, extracellular sAPPα and the transmembrane peptide α-CTF (also known as C83); the latter is further cleaved by γ-secretases into two final products: extracellular P3 and the amyloid precursor protein intracellular domain, AICD. On the other hand, the APP cleavage by β- and γ-secretase leads to the so-known amyloidogenic pathway, which has as its final product Aβ, which is prone to undergo oligomerization. β-secretases, or BACE-1, cleave APP extracellularly, generating two portions, extracellular sAPPβ and the transmembrane peptide β-CTF (also named C99); the latter is further cleaved by γ-secretases into two final products: extracellular Aβ and AICD (Webb & Murphy, 2012).
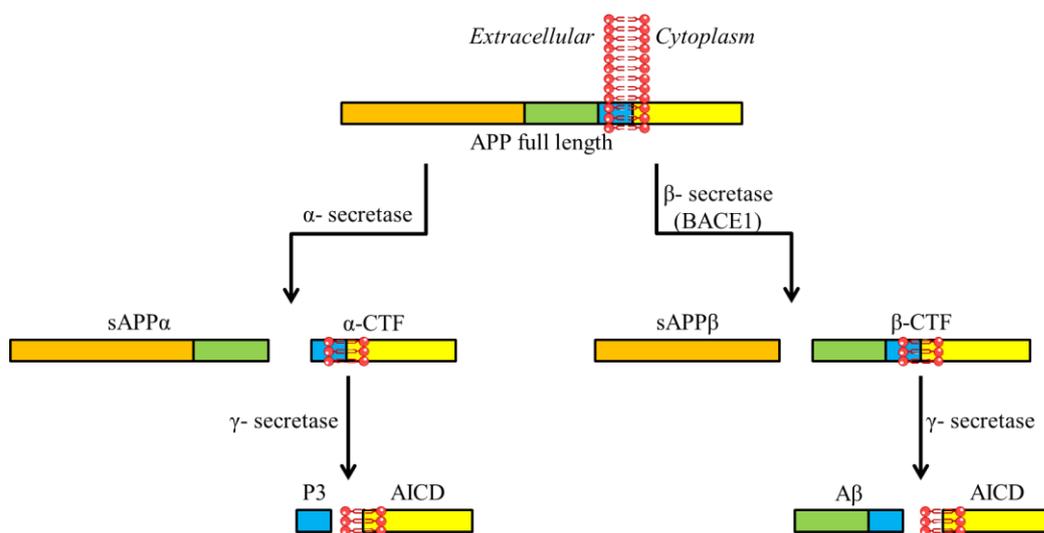
Figure 3. APP pathway.

The secretases cleavage inside the amyloidogenic pathway yields a pool of Aβ fragments of different lengths. Maybe the most important, and so far the most studied, are $A\beta_{1-40}$ and $A\beta_{1-42}$ (which comprise 40 and 42 amino acid residues, respectively). Although the former is more common, the latter, more hydrophobic, is considered to have a higher amyloidogenic potential, although both are capable of aggregating and originating oligomers, protofibrils, fibrils and, finally, insoluble plaques (Soreghan *et al.*, 1994; Urbanc *et al.*, 2011). Despite the fact that Aβ is one of the fundamental characteristics concerning the pathogenesis of AD, the role of the extracellular plaques of this peptide is not yet fully

understood. There are evidences in the literature that support $A\beta_{1-42}$ toxicity at high concentrations and also that its deposition activates the response of macrophages and neutrophils (Mattson *et al.*, 1993). These findings highlight that, in the presence of $A\beta_{1-42}$, neurons in the cortex and hippocampus suffer modifications that result in the induction of cognitive and mnemonic deficits, even though neuronal death does not occur (Selkoe *et al.*, 2012). Progressive accumulation of $A\beta$, as verified experimentally through the repeated intracerebroventricular (i.c.v.) administration of the 25-35 peptide fragment in mice, and the series of events leading to its formation are then considered important mechanisms in the early stages of memory loss (Yamada *et al.*, 2005).

1.1.2.2.1.
The Oligomeric Hypothesis

In the 90s, it was found that the $A\beta$ peptide, in addition to forming fibrils, shows the ability to group itself into soluble oligomers (Beyreuther *et al.*, 1996). A study published in 1998 showed that $A\beta$, when chemically forced to remain in its oligomeric form, immediately damages neuronal synapses, leading to neuronal death, although this does not occur with $A\beta$ fibrils (Lambert *et al.*, 1998). Other studies have demonstrated that oligomers rapidly induce synaptic plasticity failure (Walsh *et al.*, 2002; Bieschke *et al.*, 2012). Over the years, evidence corroborating the hypothesis that the oligomer form is the one that best explains the neurotoxicity of $A\beta$ has progressively been accumulated, both through *in vitro* studies and through the use of animal models for the disease (Lue *et al.*, 1999; Knobloch *et al.*, 2007; Puzzo *et al.*, 2008; Selkoe, 2008; Ferreira & Klein, 2011; Koffie *et al.*, 2011).

Over the last two decades, circumstantial evidence has been obtained on the direct correlation between $A\beta$ accumulation and tau protein aggregation, which would represent the last stage of the disease pathogenesis (Lacor *et al.*, 2004). $A\beta$ oligomers have also been considered directly responsible for tau oligomers formation in neuronal cells' cultures (Selkoe, 2011). The mechanism of synaptic damage brought out by oligomers, which lead to the death of certain neurons or specific neuronal regions (Ferreira & Klein, 2011), is still unknown, as are the dynamics of the self-propagation of fibrils and oligomers (Klein, 2013).

Thus, the fundamental questions in studies that approach this hypothesis are: (a) the elucidation, among the bewildering list of Aβ oligomer species identified so far, of which is(are) pathologically relevant (Benilova *et al.*, 2012); and (b) the investigation of the mechanism through which these soluble oligomeric species would be able to change the composition and the morphology of the synapses, causing rapid loss of plasticity (Schnabel, 2011).

1.1.2.2.2.
Correlation between a Amyloid and Cholinergic Hypotheses

The mechanism of APP processing regulation by the amyloidogenic pathway, as seen in the previous topic, is still under investigation. Different studies suggest that cholinergic inputs are presented in this process (Parikh *et al.*, 2014). The hypothesis that there may be a relationship between the neurochemical and histological aspects of AD is seen as an important area of study and the understanding of this relation can help to understand the causes and the possible treatments for this disease (Bartus *et al.*, 1982).

The formation of the extracellular aggregates seems to induce an inflammatory response capable of damaging cells of the cholinergic system (Giovannini *et al.*, 2002). On the other hand, it appears that the cholinergic system may also exert a regulatory function on the amyloid peptide processing (Kar *et al.*, 2004; Parikh *et al.*, 2014). The two aspects seem then to mutually influence each other, making difficult to understand what the triggering event of the pathology is. It is not known whether amyloid plaques are produced first, causing the death of cholinergic neurons, or whether the death of these neurons is the factor that triggers the onset or acceleration of plaque formation (Yan & Feng, 2004; Parikh *et al.*, 2014).

It has been observed that cholinergic activity is capable to influence amyloid processes. In the absence of muscarinic receptor activity, the amyloidogenic pathway is favored, whereas the opposite is the case with a normal receptor activity (Auld *et al.*, 2002; Yan & Feng, 2004).

It is necessary to specify that this evidence derives from studies conducted *in vitro* and that, of course, a more accurate verification of this

hypothesis with *in vivo* experiments is still required, in order to be able to analyze the complexity of the process within a complete organism. It is also evident that, in order to conduct this type of experiment, reliable animal models are required, which selectively and effectively replicate the pathological and behavioral signs typical of AD. In order to respond to these requirements, the model must reproduce cholinergic depletion in the cortex and hippocampus and also the diffuse presence in brain tissue of amyloid peptide plaques and NFTs (Yang *et al.*, 2000).

1.1.2.3.
Type 3 diabetes

The brain is, from a metabolic point of view, one of the most active organs of the human body. It processes a large amount of carbohydrates to produce cellular energy in the form of adenosine triphosphate, ATP. Despite its requirements, the brain does not have great flexibility in terms of substrates for the production of this energy, which relies almost exclusively on the use of glucose. This dependence puts the organ at risk if the supply of the substrate is poor or disrupted, or if the ability to metabolize glucose becomes faulty, a case in which the brain is unable to protect the synapses. In this situation, the cells may not function properly, resulting in cognitive changes. From this basic principle, a possible link between diabetes and Alzheimer's becomes apparent (Ferreira *et al.*, 2014; Lourenco *et al.*, 2015).

The investigation on the relationship between diabetes and AD started with the "Rotterdam study," an epidemiological inquiry which investigated more than 6,000 elderly people for two years. This study pointed to the positive correlation between the presence of diabetes mellitus and dementia development (Ott *et al.*, 1999). Another, more recent, epidemiological study has shown the incidence of increased AD in men who gained weight between the ages of 30 and 45 and in women with a body mass index above 30 in the 30-45 age group (Beydoun *et al.*, 2008). A Swedish study has shown the statistically significant increase in developing AD risk in men who develop type 2 diabetes around the age of 50. Researchers found that men with low insulin production at age 50 were 150 percent more likely to develop AD than those with normal insulin production.

This correlation was greater in patients with apolipoprotein E4 (ApoE4) deficiency, a strong genetic predisposition to AD, which makes them less efficient in disaggregating Aβ plaques. This fact makes diabetes a possible independent risk factor for AD (Rönnemaa *et al.*, 2008).

In the last two decades, human and preclinical studies have provided convincing evidence that AD is a degenerative metabolic disease mediated by impairments in brain insulin responsiveness, glucose utilization, and energy metabolism leading to increased oxidative stress, inflammation, and exacerbating insulin resistance (Hoyer, 2002; Craft & Watson, 2004; Rivera *et al.*, 2005; Steen *et al.*, 2005; Reger *et al.*, 2008; Talbot *et al.*, 2012; Butterfield *et al.*, 2014; Bedse *et al.*, 2015).

The term "type 3 diabetes" was developed in 2005 by Suzanne de la Monte. Her research group examined *post mortem* brain tissue of Alzheimer's patients, noting that the pathology demonstrates elements from type 1 and type 2 diabetes, in addition to the insulin production decrease and the resistance of insulin receptors. These observations suggested that AD may be a neuroendocrine disease associated with insulin signaling (Rivera *et al.*, 2005; Steen *et al.*, 2005). Those studies demonstrated that the insulin expression is inversely proportional to the Braak stage of the disease (see section: 1.1.1), with an 80% reduction in the number of insulin receptors in AD patients compared to normal subjects. Besides, the ability of insulin to bind its receptors was compromised, resulting in a reduction of the level of messenger RNA corresponding to insulin and its receptors, and a decrease in tau protein levels (Rivera *et al.*, 2005; De La Monte *et al.*, 2006). These results have inspired an animal model study, in which the intracerebral injection of streptozotocin, a drug for diabetes induction in rats, resulted in oxidative lesions appearance and also in the degradation of insulin and the alteration of the signaling mechanisms of the insulin-like growth factor. The combination of these changes ultimately resulted in neurodegeneration, including reduction in brain size and other neurological abnormalities typical of AD (Lester-Coll *et al.*, 2006).

Alzheimer's is characterized by early reduced glucose utilization. Insulin, which is important in memory processing, has the ability to cross the blood-brain

barrier and is produced constitutively in brain tissue. Patients with AD present a decrease in insulin concentration and a lower number of insulin receptors. In brain, the insulin / insulin-like growth factor (IGF) signaling is important for neuronal growth, synaptic maintenance and neuroprotection (Stockhorst *et al.*, 2004). Several studies, made by Dr. de la Monte group, propose that impairments in brain insulin / IGF signaling is associated with increased accumulation of Aβ, phosphorylated tau, ROS, RNS pro-inflammatory and pro-apoptosis molecules (De La Monte *et al.*, 2009; De La Monte, 2012a; b). When both restoration of insulin responsiveness and pharmacologically correction of insulin levels where performed, an improvement in patients' cognitive processes is observed. Most of the insulin's specific brain receptors are located in the cerebral cortex, hippocampus, olfactory bulb, cerebellum, and hypothalamus. Because these receptors are situated in areas of the brain relevant to cognition, it is logical to consider the association between insulin and cognitive studies (Craft & Watson, 2004). Several studies using intranasal, intravenous and intracerebral insulin administration, in rats and in human, have shown an improvement in cognition (Park *et al.*, 2000; Craft & Watson, 2004; Reger *et al.*, 2008).

1.2.
The metal hypothesis of Alzheimer's disease

1.2.1.
Coordination and metals

1.2.1.1.
Coordination Chemistry

The definition of a coordination compound refers to a neutral molecular set or to an ionic compound in which at least one ion is a complex, *i.e.* a substance whose metal center is coordinated by electron-donor atoms of molecules or ions, whether mono- or polyatomic, which have Lewis base characteristics (Kauffman & Lindley, 1974).

Modern coordination chemistry began in the late 19th century. In 1893, at the age of 26, the Swiss chemist Alfred Werner proposed the exact molecular structures for compounds containing complex ions. In 1913, he won the Nobel Prize for Chemistry "for his work on the linkage of atoms in molecules, by which

he has thrown new light on earlier investigations and opened up new fields of research, especially in inorganic chemistry" (*Op. cit*. de *Nobel Lectures in Chemistry,* 1966).

In the coordination chemistry scenario, metal ions interact with the ligands as a function of their oxidation state, the nature of the ligands, and the coordination numbers (CNs) and stereochemistry suitable for such an oxidation state. Three types of metals may form coordination compounds: the transition metals, using their partially occupied *d* orbitals; the internal transition metals, using partially filled *f* orbitals and, finally, the alkali and alkaline earth metals (Atkins & Shriver, 2006b).

1.2.1.2.
Metals involved in AD

In recent years, with a wide discussion about the amyloid cascade hypothesis, an increasing number of evidence has suggested that endogenous metal ions, particularly those with redox activity, such as copper(II)/copper(I) and iron(III)/iron(II), in addition to certain non-redox ions, such as zinc(II), may contribute to the development of AD, favoring Aβ aggregation and increasing its toxicity. Firstly, *in vitro* studies showed that zinc and copper induce the rapid aggregation of synthetic Aβ in an aqueous medium (Bush *et al.*, 1994; Miura *et al.*, 2000). This probably happens by binding histidine residues within the peptide (Huang *et al.*, 1997; Yang *et al.*, 2000). Secondly, transition metal concentrations, including those of zinc and copper, are elevated in brains of AD patients, particularly near the plaques (Deibel *et al.*, 1996; Danscher *et al.*, 1997; Lovell *et al.*, 1998). A metal chelation study resulted in the dissolution of Aβ aggregates from brain extracts of patients presenting AD, particularly those located in the hippocampus and amygdala, within the nucleus and in the peripheral areas of plaques (Deibel *et al.*, 1996; Danscher *et al.*, 1997; Lovell *et al.*, 1998; Cherny *et al.*, 1999; Sayre *et al.*, 2000).

Redox-active biometals induce increased oxidative stress in the brain due to their ability to produce reactive oxygen species (ROS), as hydroxyl radicals and hydrogen peroxide, and reactive nitrogen species (RNS), such as nitric oxide, via the Haber-Weiss and the Fenton reactions:

Haber-Weiss Reaction:

$$\bullet O_2 + {}^- H_2O_2 \rightarrow \bullet OH + OH + O_2$$

Fenton Reaction:

$$Fe^{2+} / Cu^+ + H_2O_2 \rightarrow Fe^{3+} / Cu^{2+} + \bullet OH + OH^-$$
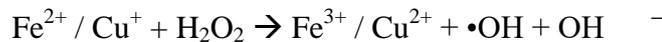
The cellular damage caused by ROS and RNS is extensive. For example, oxidation of iron through the Fenton reaction generates abnormalities in RNA, which in AD is particularly affected, causing a reduction in protein synthesis. The hydroxyl radical causes several damages to the biomolecules, attacking the nitrogenous bases and DNA deoxyribose, reacting with the amino acid residues in proteins (thus generating non-functional protein fragments), and also with membrane lipids (converting specific lipid sites into new free radical formation centers) (Barnham *et al.*, 2004; Barreiros *et al.*, 2006; Barnham & Bush, 2008).

Several studies have shown that zinc and copper compete for the same Aβ residues, with zinc having a greater relevance in the rapid aggregation of the peptide than copper, which, in turn, induces mainly conformational changes in the peptide (Hoernke *et al.*, 2010; Marino *et al.*, 2010). These data show the importance of metal determination in biological samples related to AD, as well as the use of chelation therapies (Leal *et al.*, 2012). For example, the work of the research group led by A. Bush suggests that the exacerbated deregulation of metal homeostasis would not only lead to aggregation and deposition of Aβ, but that in parallel would lead to the accumulation of iron within the neurons, causing oxidative damage and neurodegeneration (Bush *et al.*, 1994; Barnham *et al.*, 2004; Friedlich *et al.*, 2004; Adlard *et al.*, 2010; Adlard *et al.*, 2011; Sensi *et al.*, 2011; Bush, 2013). This research group also explored the functional interaction of metal transport systems and proteins involved in neurodegeneration, evaluating the hypothesis that these proteins are denatured in the presence of metals, due to the fact that they fail in their role of regulation of these, through a negative feedback mechanism, resulting in overload of those proteins due to the accumulation of metals. These studies present an unprecedented mechanism of toxicity, intrinsic to the process of Aβ formation, defining a pathological relationship between the accumulation of extracellular zinc in amyloid plaques and the accumulation of intraneuronal iron observed in AD. In Bush theory (Bush, 2013), when iron binds

to NFTs, inducing oxidative stress (Smith *et al.*, 1997), tau protein could present a physiological role in iron neuronal homeostasis, since it directs β-APP traffic to the neuron surface, to interact with ferroportin (Lei *et al.*, 2012).

In this context, the involvement of biometals in AD pathogenesis is increasingly being studied, because of their ability to cause oxidative stress and also due to their participation in secretion, transport and deposition of the Aβ peptide.

Zinc is involved in many different cellular metabolic pathways. It is necessary for the functioning of more than 300 different enzymes and plays a fundamental role in several biological processes (Sandstead, 1994). This element, for example, is a cofactor for copper-zinc superoxide dismutase (Cu/Zn-SOD) enzyme, and is present in many enzymatic reactions involved in the metabolism of both carbohydrates and proteins (Jurowski *et al.*, 2014). It has been shown that severe zinc deficiencies can suppress immune function (Shankar & Prasad, 1998), and even mild degrees of deficiency may impair macrophage and neutrophil functions (Wintergerst *et al.*, 2007), in addition to being necessary to develop and activate T-lymphocytes, CD4$^+$ cells and interleukin-2 (Rink & Gabriel, 2000). This metal also regulates the release of vitamin A stored in the liver and insulin activity and promotes the conversion of certain thyroid hormones (Jurowski *et al.*, 2014). Their ability to coordinate is critical to the three-dimensional structure of many biomolecules, through zinc fingers (Plum *et al.*, 2010; Chasapis *et al.*, 2012). Some studies have suggested that Zn may delay the progression of age-related macular degeneration, and loss of vision, possibly by avoiding retinal damage (Group, 2001; Van Leeuwen *et al.*, 2005; Evans, 2006).

On the other hand, zinc excess can cause various symptoms such as nausea, vomiting, loss of appetite, abdominal cramps, diarrhea and headaches (Lewis & Kokan, 1998). Consumption of 150-450 mg of zinc per day is associated with chronic effects such as lower copper levels, altered iron metabolism, decreased immune response, and reduced levels of high-density lipoprotein (Hooper *et al.*, 1980).

Copper is essential because of its ability to donate and accept electrons, which depends on its oxidation state, Cu^+ or Cu^{2+} (Atkins & Shriver, 2006b). It is, therefore, involved in various redox reactions of the metabolic processes, such as mitochondrial respiration, melanin synthesis, among others. It is an integral part of antioxidant enzymes such as Cu/Zn-SOD and plays a key role on iron homeostasis as a cofactor in ceruloplasmin. Copper from the circulatory system is primarily stored in the liver, where it is incorporated into the proteins that need it. Through the release of copper, the liver exerts its homeostatic control (Linder *et al.*, 1998).

Most of the elemental iron in adults is complexed in hemoglobin. Much of the remainder is stored by ferritin or in its degradation product, hemosiderin, in liver, spleen, and bone marrow, or is localized to myoglobin in muscle tissue (Whittaker *et al.*, 2001). Humans typically only lose small amounts of iron, through biological excretions. Loss of iron is higher in menstruating women. The hormone hepcidin is the major regulator of iron absorption and its distribution throughout the body (Drakesmith & Prentice, 2012). Most of the iron deficiencies, or anemias, are related to poor diet. Some diseases, such as rheumatoid arthritis, inflammatory bowel disease, as well as haematological malignancies can cause chronic anemia (Cullis, 2011). The clinical implications of iron deficiency in people with chronic diseases are unclear. It is known, however, that mild anemia associated with chronic diseases is correlated with an increased risk of hospitalization and mortality in the elderly (Riva *et al.*, 2009).

Intake of iron doses higher than 20 mg kg^{-1} of body weight may lead to gastric disturbance, constipation, nausea, abdominal pain, vomiting and fainting (Whittaker *et al.*, 2001), as well as to a reduced zinc absorption (Whittaker, 1998). Iron overdoses, defined as one-time ingestion of 60 mg kg^{-1} of body weight, can lead to multiple organ failure, coma, seizures and death (Chang & Rangan, 2011).

Not only the physiological metals have been implicated in the pathogenesis of AD, but also some metals considered toxic, such as aluminium, lead and mercury.

Several studies indicate that there is a direct relationship between aluminum and AD. This metal has been observed in higher concentrations in AD patients' brain affected by the disease. There are reports of statistically increased risks in populations exposed to aluminum levels above 0.1 mg L^{-1} in drinking water (Shcherbatykh & Carpenter, 2007; Frisardi *et al.*, 2010).

The aluminum absorptions is threefold greater in patients with AD compared to people without the disease (Rondeau, 2002). The hypothesis that Al is an environmental contributor to the pathogenesis of AD, termed the "aluminum hypothesis", was proposed in the 1960s based on various neurotoxicological, analytical, and epidemiological findings (Klatzo *et al.*, 1965; Crapper *et al.*, 1973; Martyn *et al.*, 1989). More recent studies showed that aluminum modifies brain structures, such as the number or distribution of charges present on the surfaces of the brain, with consequent alteration of the activity of the blood-brain barrier (Kawahara & Kato-Negishi, 2011). Also it has been shown that chronic exposure to this element through ingestion of drinking water increases inflammatory processes in the brain (Campbell *et al.*, 2004). Several mechanisms of action have been proposed to explain aluminum toxicity in AD. One involves its interaction with calmodulin, a modulating protein of several proteins and enzymes that binds to Ca^{2+}, inhibiting Ca-dependent inactivation of NMDA receptor channel (Levi *et al.*, 1998), while its involvement in indirect activation of serine proteases, such as α-quimiotripsin, has also been cited, with consequent increase in APP processing, Aβ peptide accumulation and amyloid plaque formation (Kawahara & Kato-Negishi, 2011). In addition, it was shown that aluminum alters AChE activity (Zatta *et al.*, 2002); it binds to polar portions of cell membranes; it impairs transportation processes and cellular metabolism; it promotes oxidative stress in brain by accelerating the lipid membranes peroxidation in the presence of Fe^{2+} and also modifies the homeostasis of this metal (Kawahara & Kato-Negishi, 2011). Aluminum also has toxic effects on the endoplasmic reticulum and mitochondria, inducing apoptosis of neuronal cells (Savory *et al.*, 2006), which certainly contributes to the progressive neuronal loss observed in AD. Interestingly, this cascade of apoptotic events has not been verified for other metals (Kawahara & Kato-Negishi, 2011).

Mercury is an extremely toxic metal in all its forms, and has also been the subject of AD-related hypotheses. For instance, exposure to mercury in rats has caused the inhibition of tubulin polymerization in microtubules (Pendergrass *et al.*, 1997). This identifies an important relationship between this metal and the disease, as this type of molecular injury is extremely similar to that observed in 80% of the brains of patients with AD. Other studies have shown that the presence of mercury also modifies neurite cell growth patterns *in vitro*, disintegrating the tubulin / microtubule structure, forming NFTs (Leong *et al.*, 2001). Some authors also postulate that, in presence of other metals such as zinc, cadmium and lead, mercury has exacerbated its toxicity due to synergistic mechanisms, leading to the belief that mercury is not required to be present at high levels in the brains of AD patients to be considered causal in the etiology of the disease (Haley, 2007). In addition, there is also the hypothesis that the susceptibility to AD in people carrying the *ApoE-ε4* gene may be related to the contamination by this metal (Ng *et al.*, 2013).

Recent studies indicate that exposure of rodents and primates to lead during childhood causes changes in AD-related genes and biomarkers expression when animals reach adulthood. Overexpression of APP and BACE-1, the presence of senile plaques with changes in intracellular Aβ distribution, increased methylation levels and oxidative DNA damage were observed (Basha *et al.*, 2005; Bolin *et al.*, 2006; Wu *et al.*, 2008).

1.3.
Oxidative stress

1.3.1.
Proteins and metalloproteins involved in oxidative stress in Alzheimer's disease

The free radicals present in biological systems are able to react with proteins, lipids or nucleic acids. When losing an electron, those biomolecules suffer modifications in its form and function, being a functionality loss possible. The cellular defense mechanisms may become incapable of acting on free radicals' scavenge or on their deleterious effects: such phenomenon is called oxidative stress (Valko *et al.*, 2007). Free radicals are naturally generated through

cellular processes, both enzymatic and non-enzymatic ones, from the reduction of molecular oxygen. For this reason, free radicals could be involved in cellular defense mechanisms, including the annihilation of invading microorganisms and tumor cells (Valko *et al.*, 2007). The oxidative condition promotes the formation of ROS, such as hydrogen peroxide (H_2O_2), which is able to react with reduced metal ions through the Fenton reaction. The hydroxyl radical ($OH^{\bullet}$), product of this reaction, is highly reactive and is able to capture hydrogen atoms from organic molecules and cause important oxidative damage (Valko *et al.*, 2007).

Nerve tissue has a high tendency to undergo oxidative damage. The main reason for that is the fact that brain has the highest aerobic activity in the body, lower levels of antioxidant elements, membranes containing lots of polyunsaturated fatty acids, and a natural tendency to accumulate metal ions, which is accentuated with age (Valko *et al.*, 2007; Moss *et al.*, 2009). Endogenous antioxidants constitute the first line of defense against oxidative damage. As an example of these, one can mention the glutathione system, which includes reduced glutathione, L-γ-glutamyl-L-cysteinyl-glycine, GSH (Figure 4). This tripeptide plays a crucial role in the biotransformation and elimination of xenobiotics, in addition to participating in cell defense against the oxidative stress. The reductive capacity of GSH is determined by the thiol group present in the cysteine residue, which has the primary function of serving as a substrate in redox reactions (Damasceno *et al.*, 2002). Several scientific studies have monitored this tripeptide with the purpose of evaluating the oxidative stress related to Alzheimer's disease (Saharan & Mandal, 2014; Subash *et al.*, 2014; Xu *et al.*, 2014).
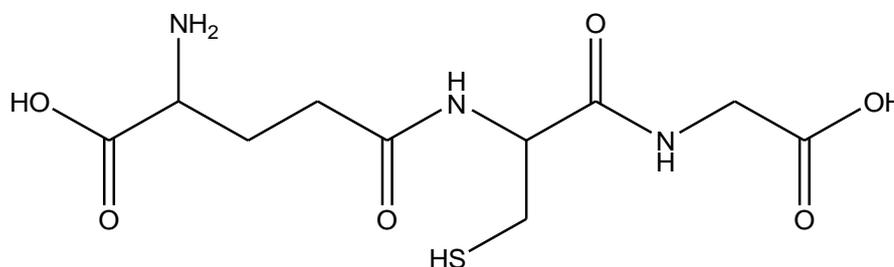
Figure 4. L-γ-glutamyl-L-cysteinyl-glycine (GSH) structure.

1.3.2.
Enzymes in Alzheimer's disease

In order to remove low polar molecules and their metabolites, organisms have improved, throughout evolution, reactions capable of rendering these compounds more polar so that they could be excreted (Habig *et al.*, 1974). Some enzymes present in the cytosol, mitochondrial membranes and rough endoplasmic reticulum of lung, kidney, heart, gastrointestinal tract, nasal mucosa, brain, blood, and liver cells are part of the set that acts in those metabolic processes, called biotransformation (Habig *et al.*, 1974).

Biotransformation generally involves two groups of reactions, which can be conceptually divided into two phases. In the first one, reactions of reduction, oxidation, or hydrolysis occur, leading to the loss of the toxic or pharmacological potential of the compound, and resulting in detoxification of the organism. Nevertheless, in some cases, metabolic activation may occur, that is, the xenobiotic can be converted into a molecule with a greater toxic or pharmacological potential than that it initially possessed. The metabolites of this phase may undergo biotransformation in the second phase, in stages that more often involve conjugation reactions, catalyzed by glutathione S-transferase (GST), uridine diphosphogluconosyltransferase (UDPGT), or sulfotransferase (SULT), in which the drugs bind to more polar molecules to be excreted mainly by the bile or urinary tract. In the case of glutathione conjugates, these can still be metabolized to the final production of mercapturic acid which is then dissolved in the urine (Habig *et al.*, 1974). Among all organs, the liver is the main metabolizing one (Hayes & Pulford, 1995; Liu & Klaassen, 1996). Studying alterations in enzymatic activities of animal models experimentally injected with potential MPACs may be useful in the evaluation of the biochemical effects of these compounds.

1.4.
Therapies for ad: state of the art

Currently, there is no cure for Alzheimer's. However, there are medications that help to control the symptoms, specifically agitation, depression, delusions, which are more frequent with the progression of the disease.

Commonly prescribed treatments include cholinesterase inhibitors, *N*-methyl-D-aspartate receptor antagonists and medications for anxiety, depression, and psychosis (Ellul *et al.*, 2007; Cunningham & Passmore, 2013; González-Castañeda *et al.*, 2013). In some cases, the use of vitamin E in combination with other drugs is also prescribed (Barnes & Yaffe, 2005). Recently, due to several researches on the correlation between AD and diabetes, as reported before (see section: 1.1.2.3), there was the advent of some treatment strategies based on the use of diabetes drugs (Morris & Burns, 2012).

1.4.1.
Acetilcolinesterase inhibitors

People suffering from AD have low levels of Ach, an important chemical in the brain involved in the communication of nerve cells (see section: 1.1.2.1). Cholinesterase inhibitors partially block the metabolic degradation of acetylcholine, improving the availability of this product for communication between cells, and slowing down the progression of cognitive dysfunction. This strategy may be effective for some patients in the early and intermediate stages of the disease (Anand & Singh, 2013).

There are four drugs in this class currently approved by the Food and Drug Administration (FDA, USA), designed to regulate and control the symptoms of mild to moderate AD. These are: tacrine, trade name Cognex®, donepezil, trade name Aricept®, rivastigmine, trade name Exelon® and galantamine, trade name Razadyne®.

The four treatments are approved for mild to moderate AD symptoms, and only memantine has been approved by the FDA for the treatment of severe symptoms in 2003 (Ellul *et al.*, 2007; Cunningham & Passmore, 2013).

Tacrine was approved by the FDA in 1993. This drug prevents the degradation of acetylcholine in the brain. The most common side effects are constipation, diarrhea, gases, loss of appetite, muscle aches, nausea, stomach pain, stuffy nose, vomiting, weight loss, with the possibility of liver damage. Due to these side effects it is no longer actively marketed (Anand & Singh, 2013; Rodrigues Simões *et al.*, 2014).

Donepezil was approved by the FDA in 1996. This drug also prevents the degradation of acetylcholine in the brain. The most common side effects are diarrhea, dizziness, loss of appetite, muscle aches, nausea, tiredness, trouble sleeping, vomiting and weight loss. The study by Barnes and Yaffe suggests that this drug may slightly retard the progression of MCI in AD. During the first year of a three-year study, people with MCI treated with donepezil shown a reduced risk of progression to AD compared to participants taking vitamin E or placebo (Barnes & Yaffe, 2005). However, there was no difference between the three groups, except for those who had the *ApoE-ε4* gene. The effect of donepezil lasted from two to three years for these participants. Previous studies indicate that those with the *ApoE-ε4* gene have a higher chance of developing AD than the general population (Molino *et al.*, 2013; Michaelson, 2014; Rodrigues Simões *et al.*, 2014).

Rivastigmine was approved by the FDA in 2000. This drug prevents the degradation of acetylcholine and also of butyrylcholinesterase, a cholinesterase that plays a minor role in the degradation of acetylcholine in human body. The most common side effects are nausea, diarrhea, increased frequency of bowel movements, vomiting, muscle weakness, loss of appetite, weight loss, dizziness, drowsiness and stomach pain. In 2007, FDA approved Exelon®Patch, a transdermal rivastigmine system, to deliver this medication through a skin patch as an alternative to the oral capsule (Anand & Singh, 2013).

Galantamine was approved by the FDA in 2001. This drug prevents the degradation of acetylcholine and stimulates nicotinic receptors to release more acetylcholine into the brain. The most common side effects are nausea, vomiting, diarrhea, weight loss, dizziness, headache, tiredness (Anand & Singh, 2013).

1.4.2.
N-methyl-D-aspartate receptor agonists

Memantine (trade name: Namenda®) was the first drug approved by the FDA to treat the symptoms of moderate to severe AD. It regulates the activity of glutamate, a chemical messenger, involved in learning and memory, which is released in large quantities by cells damaged by AD and by some other neurological disorders. When glutamate reaches *N*-methyl-D-aspartate (NMDA)

receptors on surface cells, calcium flows freely into the cell, which can lead to cell degeneration. Memantine can prevent this destructive sequence by adjusting glutamate activity (Danysz *et al.*, 2000). For many years, memantine has been available in some European countries, and has been available in the US since October 2003. This drug is generally well tolerated, with the most common side effects being pain, constipation, diarrhea, dizziness and drowsiness (Molino *et al.*, 2013).

In July 2010, Namenda XR®, a long-term drug release formulation, has been approved by the FDA. Its most common side effects are headache, diarrhea, dizziness and high blood pressure (Molino *et al.*, 2013).

1.4.3.
Depression control drugs

With the AD progression, patients often suffer from neuropsychiatric symptoms such as depression, agitation and psychotic symptoms such as paranoid thoughts, delusions or hallucinations. Symptoms may have an underlying medical origin, such as drug interaction or physical pain. The use of antidepressants is common in dementia, with a prevalence of 43.2% reported in a recent Danish study (Kessing *et al.*, 2007).

Several antidepressants have been studied in AD context, with ambiguous results. For example, a study of a serotonin reuptake inhibitor, sertraline hydrochloride, indicated positive results, in contrast to other studies on the same drug, as well as two other antidepressants: fluoxetine, citalopram (Reifler *et al.*, 1989; Nyth & Gottfries, 1990; Magai *et al.*, 2000).

1.4.4.
Vitamin E

Vitamin E has also been prescribed to treat the cognitive symptoms of Alzheimer's disease (Barnes & Yaffe, 2005). Vitamin E, also known as α-tocopherol, is an antioxidant. Antioxidants can protect brain cells and other body tissues from certain types of chemical wastage. Its use in AD was mainly based on a study carried out in 1997, which showed that high doses of this antioxidant, ingested over several months, cause a decrease in the loss of ability to perform

daily activities (Adelman, 1997). However, in the years following this study, evidence has been generated reporting that high doses of vitamin E may increase the risk of death, especially in patients with coronary artery disease (Spencer *et al.*, 1999).

Recently, in 2014, study results indicated that individuals with mild to moderate AD who received high doses of vitamin E had a 19% slower rate of functional decline than volunteers who received a placebo. Study participants were followed up for just over two years. Patients who received vitamin E in combination with memantine did not show the same benefit as participants who received only vitamin E, and none of the four study groups (placebo, vitamin E, memantine, vitamin E in conjunction with memantine) showed cognitive benefits (Dysken *et al.*, 2014).

1.4.5.
Diabetes drugs

In the last years, based on the correlation between diabetes and AD (see section: 1.1.2.3), different studies proposed the use of drugs against diabetes to treat the progression of AD (Park *et al.*, 2000; Craft & Watson, 2004; De La Monte *et al.*, 2006; Lester-Coll *et al.*, 2006; Reger *et al.*, 2008; Rönnemaa *et al.*, 2008).

A recent study evaluated the participation of insulin signaling, Aβ peptide regulation and the formation of NFTs by critically analyzing the promising field of some diabetes drugs, in order to verify their capacity to protect against dementia and AD, showing results on the Aβ formation rate and tau protein hyperphosphorylation (Sebastião *et al.*, 2014).

In 2011, a meta-analysis study gathered data from clinical trials of pharmacological therapies in use to treat diabetes mellitus type 2 and clinical trials of such therapy in progress. The analysis covered studies of peroxisome proliferator-activated receptor antagonists, which is increased in the brains of patients with AD, and has suggested that the use of these antagonists may render some therapeutic benefit to patients in the early stages of AD. In the study the effects of intranasal insulin administration were evaluated, by analyzing the

insulin ability to enter the brain within a short time by olfactory, trigeminal and axonal pathway transport, revealing that the efficacy of this exposure is directly dependent on *ApoE* genotype of the evaluated patients (Akter *et al.*, 2011).

A more recent analysis proposed, based on the molecular correlation data between inflammatory syndromes, deregulated insulin signaling and mitochondrial dysfunction in AD and diabetes, the development of new therapeutic strategies which rely on antidiabetic and / or anti-inflammatory agents. Results show the need for more studies aiming to find new ways and to clarify on the mechanisms involved in brain inflammation and deregulated insulin signaling in AD (Lourenco *et al.*, 2013).

1.4.6.
MPACs

Current drug therapies for AD cannot inhibit the neuropathological progression of the disease (Ellul *et al.*, 2007). New approaches propose to achieve what is now considered the underlying disease process: the accumulation of Aβ in the neocortex (Atwood *et al.*, 1999). As already mentioned, physiological metals such as Cu, Fe and Zn are concentrated around and bound to amyloid plaques in AD patients' brains (Deibel *et al.*, 1996). There is evidence that these metals interact with the Aβ peptide, even in its monomeric and oligomeric soluble forms, and can catalyze the production of hydroxyl radicals. This contributes to oxidative stress, generating amyloid fibers that are toxic, resistant to removal and more prone to aggregate (Bush *et al.*, 1994; Bush, 2003; Finefrock *et al.*, 2003; Bush, 2013). Zinc(II) appears to be the main factor responsible for adding the Aβ peptide. *In vitro* studies have shown that, at micromolar concentrations, this physiological metal ion rapidly induces precipitation of the soluble Aβ peptide in protease-resistant aggregates (Bush *et al.*, 1994). This aggregation is probably due to the formation of intermolecular bonds between two histidines and the Zn^{2+} ion (Miura *et al.*, 2000). Agglomeration can also be induced by Cu^{2+}, and, in a minor way, by Fe^{3+}, mainly in slightly acidic conditions (Atwood *et al.*, 1998).

The approach involving the use of Metal-Protein Attenuating Compounds, or MPACs, conceptually differs from that of traditional chelating agents, since they have a moderate affinity with metal ions. Thus, instead of binding and

systematically removing ions from tissues, they correct abnormal metal-protein interactions, resulting in subtle effects on metal homeostasis, which would lead to inhibition of Zn^{2+} and Cu^{2+} induced Aβ oligomerization. This helps with the removal of the Aβ peptide and inhibits redox reactions that ultimately lead to the generation of hydroxyl radicals. Therefore, MPACs represent a feasible therapeutic strategy to delay or even prevent the progression of Alzheimer's dementia (Cherny *et al.*, 2001; Barnham *et al.*, 2004; Sampson *et al.*, 2012) and other neurodegenerative diseases in which abnormal metal-protein interactions have been reported (Perry *et al.*, 2002; Mayeux & Stern, 2012).

2.
Compounds and description of fundamentals of some experimental methods used

As the metal theory of AD has gained visibility through the new evidence about it reported in the recent years, new strategies have been sought aiming to increase the pharmacological arsenal available for the treatment of this pathology. Thus, conducting syntheses, characterizations and *in vitro* and *in vivo* assays of new potential MPACs is part of an approach of fundamental importance.

In this context, the present work proposes to investigate a series of compounds belonging to the chemical classes of 8-hydroxyquinolines, aroylhydrazones, or both of them, regarding their potential to act as a MPAC as well as their toxicological profile.

2.1.
Potencial MPACs

Hydrazones belong to a class of organic compounds which have the functional group $R_1HC=N-NR_2R_3$ (Kostova & Saso, 2013). They are generally synthetized by the condensation reaction between hydrazides and carbonyl compounds, such as aldehydes.

Carbonylated hydrazones have been the focus of studies in many research areas due to their performance as bidentate ligands, coordinating metals through the azomethine nitrogen and the carbonyl oxygen. This chelating capacity is also explored in a broad spectrum of pharmacological applications: hydrazones are commonly associated with various biological uses, such as analgesics, antihypertensives, anticonvulsants, anti-inflammatories (Kajal *et al.*, 2014), anti-tuberculosis agents, antitumor agents (El-Hawash *et al.*, 2006; Vicini *et al.*, 2006), antiretrovirals (Savini *et al.*, 2004; Vicini *et al.*, 2009), antimalarials, anti-depressants and vasodilators (Silva *et al.*, 2005). These compounds have also been investigated as iron chelators for the control of neurodegenerative disorders such as Friedreich's ataxia and other diseases related to the excess of this metal.

2.1.1.
INHHQ

The class of 8-hydroxyquinolines was shown to be very interesting for the development of potential drug for AD therapy (Melov, 2002; Doraiswamy & Finefrock, 2004). Clioquinol (CQ, Figure 5), originally used as an anti-amoebic substance, was already adopted in a study using a transgenic rat AD model in order to decrease the formation of amyloid plaques, showing positive results. Its activity was attributed to the removal of metals from the plaques in the brain (Mancino *et al.*, 2009). Unfortunately, its use showed a strong correlation with subacute myelo-optic neuropathy (Doraiswamy & Finefrock, 2004; Levine *et al.*, 2009), which strongly encouraged the search for new analogues (Doraiswamy & Finefrock, 2004).
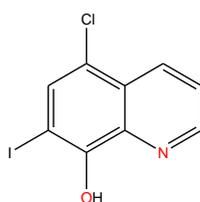
Figure 5. 5-chloro-7-iodo-8-hydroxyquinoline, clioquinol. Red labels show the potential complexation sites.

The compound 8-hydroxyquinoline-2-carboxaldehyde isonicotinoyl hydrazone (INHHQ, Figure 6), fits in this context (De Freitas *et al.*, 2013). The pharmaceutical potential of this compound for AD and Parkinson's disease, has already been confirmed with previous studies, also by our research group (Hauser-Davis *et al.*, 2015; Cukierman *et al.*, 2017).
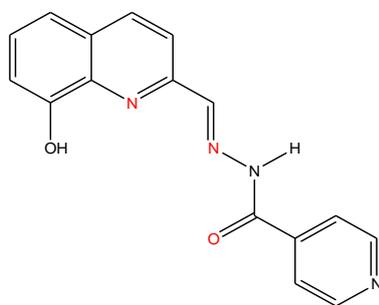
Figure 6. 8-hydroxyquinoline-2-carboxaldehyde isonicotinoyl hydrazone (INHHQ). Red labels show the potential complexation sites.

2.1.2.
HPCIH

Pyridyl-2-carboxaldehyde isonicotinoyl hydrazone, HPCIH (Becker & Richardson, 1999) is a particularly relevant compound in the context of this work. Its importance is due to its structure (Figure 7), completely contained in that of INHHQ. Actually, the only difference between them is the phenolic ring, absent on the structure of HPCIH.
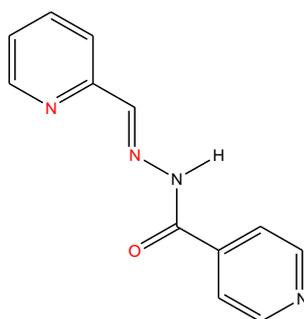
Figure 7. Pyridine-2-carboxaldehyde isonicotinoyl hydrazone (HPCIH). Red labels show the potential complexation sites.

Regarding HPCIH's metal complexes, in 2003, Armstrong *et al.* described a series of complexes with metals from the first transition series, *i.e.* from Mn to Zn. These metals are coordinated to the ligand in different ways, including a bidentate complex with Cu and a polymeric coordination structure with Zn, and with two and even three metal ions, bi- and trinuclear, respectively (Claire M. Armstrong *et al.*, 2003). Mono- and binuclear copper complexes were recently reported (Satyajit Mondal[a], 2013). From all these studies, it was well established that the aroylhydrazone HPCIH is mainly coordinated in a tridentate way through the N_{py}, N, O system, but may show a great variety of metal-ligand stoichiometries in their complexes.

2.1.3.
H2QBS

4-(8-hydroxyquinoline-5-azo)-benzensulfonic acid, H2QBS (Figure 8) is obtained by the azo coupling reaction between the diazotized sulfanilic acid and the precursor 8-hydroxyquinoline. Due to their physicochemical properties, azo compounds have a wide range of applications in the pharmaceutical, cosmetic,

food and textile industries. Their several biological activities make of them clinically attractive compounds as protease inhibitors, antibacterial and antifungals (Chen *et al.*, 2013).
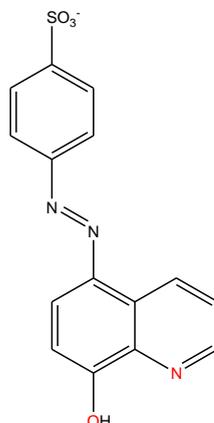
Figure 8. 4-(8-hydroxyquinoline-5-azo)-benzensulfonic acid (H2QBS). Red labels show the potential complexation sites.

2.1.4.
INHOVA

2-hydroxy-3-methoxy-benzaldehyde isonicotinoyl hydrazone, INHOVA (Figure 9) is obtained by the condensation of isoniazid with *ortho*-vanillin, *o*-HVa (González-Baró *et al.*, 2012a). HVa and its isomer, *o*-HVa, 2-hydroxy-3-methoxybenzaldehyde, have antioxidant activity due to the ability to capture free radicals. The therapeutic properties and the low toxicity of these aldehydes have made them good candidates for the preparation of hydrazones with a better pharmacological profile. Due to its structure, INHOVA can be considered a suitable ligand, as a consequence of its potential ability to coordinate several metal ions through its donor atoms, as shown in Figure 9. In addition, the toxicity of such a binder is expected to be low, since it is the condensation product of a human-approved drug, isoniazid (INH), with a compound frequently used in cooking, vanillin.
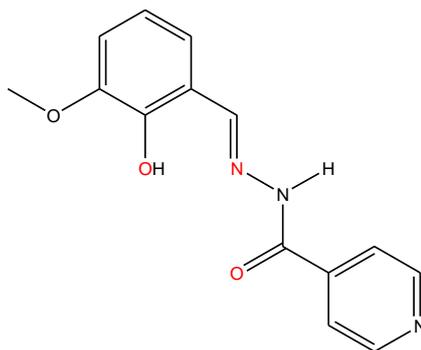
Figure 9. 2-hydroxy-3-methoxy-benzaldehyde isonicotinoyl hydrazone (INHOVA). Red labels show the potential complexation sites.

2.2.
Stability assays by UV-Vis spectrophotometry

The ability of molecules to absorb light can be used from a quantitative point of view through the Lambert-Beer law. Comparison between the absorption profiles of the same compound, obtained by spectrophotometric analyses over time of aliquots that are part of the same main solution containing the compound of interest, allows one to evaluate if and which changes may occur in the composition of the sample, for example, hydrolysis reactions that lead to the presence of more species in solution. Determining the stability of the four compounds, namely INHHQ, INHOVA, HPCIH and H2QBS, was the initial step to establish if the original form of each compound in solution is preserved and consequently to estimate the disponibility of the product over time after solubilization, before the *in vitro* and *in vivo* assays.

2.3.
In vitro studies

2.3.1.
^{1}H x ^{15}N HSQC NMR

The heteronuclear single quantum coherence experiment or, simply, heteronuclear single quantum correlation, HSQC, is a highly sensitive bidimensional NMR (Nuclear Magnetic Resonance) experiment used for the study of organic molecules, with strong application in molecular biology. The pulse sequence was first described in 1980 by Bodenhausen and Ruben, who claimed that "*The detection of NMR spectra of less sensitive nuclei coupled to protons may*

be significantly unproved by a two-dimensional Fourier transform technique involving a double transfer of polarization. The method is adequate to obtain natural abundance ^{15}N spectra in small sample volumes with a commercial spectrometer" (Bodenhausen & Ruben, 1980).The data obtained from this technique is two-dimensional (2D) with one axis for hydrogen, ^{1}H, and the other for a heteronucleus, ^{15}N in the case of this work.

The basic scheme of this experiment involves the transfer of magnetization on the proton to the second nucleus, via an INEPT (Insensitive Nuclei Enhanced by Polarization Transfer) step. After a time delay (t_1), the magnetization is transferred back to the proton via a retro-INEPT step and the signal is then recorded. In HSQC, a series of experiments is acquired, in which the time delay t_1 is incremented at each step. The ^{1}H signal is detected in the directly measured dimension of each experiment, while the chemical shift of ^{15}N is recorded in the indirect dimension, which is constituted from the series of experiments. Although the ^{1}H x ^{15}N HSQC experiment can be performed using the natural abundance of the ^{15}N isotope, for protein NMR, normally, isotopically labeled proteins are used. These proteins are biologically produced by cells grown in ^{15}N-labelled media. Each amino acid, with the exception of proline (which is technically an immino acid), has an amide proton attached to a nitrogen in the peptide bond. In this case, the technique provides the correlation between this nitrogen and amide proton, and each amide yields a peak in the bidimensional contour plot.

2.3.2.
Cell studies

The use of cell cultures in research dates back to the 1950s, but only in the last decades this practice became commonplace. The reason for this is the ability of keeping cells cultivated for long periods due to the development of modern sciences, in particular molecular biology, and the sensitive enhancement of technologies, sterility techniques and the most complete and complex formulation of cell culture media (Mariottini *et al.*, 2010). Currently, a remarkable amount of stabilized cell lines derived from different species is available, whose phenotypic, genotypic and biochemical characteristics are well known; these factors allow to

an almost complete standardization and validation of laboratory tests. These tools allow the study of numerous aspects of cellular biology (Mariottini *et al.*, 2010).

The possibility of studying the toxicological effects derived from exposure to substances in human cells is one of the biggest advantages of cell cultures. For instance, they allow the analysis of expositions which are ethically impossible to be studied *in vivo*, thus reducing the problem of validation of results for the human species, without, however, eliminating the problems of interspecific extrapolation of the obtained data. An enormous limitation in this point is related to the different organization between an experimental system composed of cells isolated from each other, thus being deprived of both, communication and three-dimensional structure, and an organism in its totality, presenting structural and functional complexity. Other limitation is related to the loss of components involved in homeostatic regulation *in vivo*, mainly component of the nervous and endocrine system (Mariottini *et al.*, 2010). Despite these limitations, *in vitro* studies are fundamental for understanding molecular biology phenomena, when it is necessary to study them with total control of all environmental conditions and all interactions. Over the last decades *in vitro* studies on cell lineages of tissues and / or genetically modified unicellular organisms have greatly aided in pharmaceutical research, reducing the need for studies in animal models, or at least reducing the number of animals required for statistical significance in biological studies. In pharmaceutical research the study of *in vitro* phenomenon has the advantage of being able to observe processes isolated from the context, which could create significant interferences rendering events distinction impossible (Mariottini *et al.*, 2010).

A large number of studies, contributed to gain new insights into the molecular mechanisms leading to AD pathology (Haass *et al.*, 1992; Seubert *et al.*, 1992; Haass *et al.*, 1994; Huang *et al.*, 1997; Atwood *et al.*, 1998; Cherny *et al.*, 1999; Cherny *et al.*, 2001; Mekmouche *et al.*, 2005; Mancino *et al.*, 2009; Squitti & Salustri, 2009; Chen *et al.*, 2011; Sampson *et al.*, 2012), either using mammalian cell lines or using genetically modified unicellular organisms cultures programmed to simulate the pathology of AD, *i.e.* cells expressing the amyloid

beta peptide (Tan *et al.*, 2012; O' Neill, 2013; Jackrel & Shorter, 2014; Nair *et al.*, 2014).

2.3.2.1.
Cell lines

SH-SY5Y is a human derived cell line widely used in scientific research. The original cell line, called SK-N-SH, from which it was subcloned was isolated from a bone marrow biopsy taken from a four-year-old female with neuroblastoma. SH-SY5Y cells are often used as *in vitro* models of neuronal function and differentiation. This cell line is highly valued to be N-type (neuronal), given its morphology and the ability to differentiate the cells into along the neuronal lineage, and is widely used as cell model for neuroscience research (Biedler *et al.*, 1973).

Human embryonic kidney cells 293, also often referred to as HEK 293, HEK-293, 293 cells, or less precisely as HEK cells, are a specific cell line originally derived from human embryonic kidney cells grown in tissue culture. HEK 293 cells have been widely used in cell biology research for many years, because of their reliable growth and propensity for transfection.

HEK 293 cells were described for the first time in 1977 obtained on an experiment numbered as 293. This experiment carried the transformation of cultures of normal human embryonic kidney (HEK) cells with sheared adenovirus 5 DNA, derived from a single, apparently healthy, legally aborted fetus (Graham *et al.*, 1977). Graham and co-workers provided evidence that HEK 293 cells and other human cell lines generated by adenovirus transformation of human embryonic kidney cells have many properties of immature neurons (Shaw *et al.*, 2002).

The Aβ peptide is a product of APP digestion (see section: 1.1.2.2). In 1993 was reported for the first time the transfection of a neuroblastoma cell culture with mutant APP gene. The transfection regarded the mutated form of APP that was discovered in two large Swedish families who were found to be connected genealogically, therefore called the Swedish mutation (SW). The SW is immediately adjacent to the β-secretase site in APP. It is actually a double

mutation, resulting in a substitution of two amino acids, lysine (K) and methionine (M) to asparagine (N) and leucine (L). *In vitro*, this mutation repeatedly has been shown to increase total Aβ levels. Specifically, there is increased production and secretion of Aβ$_{40}$ and Aβ$_{42}$. The ratio of Aβ$_{40}$/Aβ$_{42}$ is generally not affected (Cai *et al.*, 1993).

In 1995 the APP pathway was studied in HEK 293 cells for the first time, expressing APP Swedish Mutation (Schrader-Fischer & Paganetti, 1996). Due to the wide use, and the great knowledge of HEK 293 cells, the SW APP HEK 293 became, over the year, an *in vitro* model for AD research.

2.3.2.2.
Cytotoxicity

Cytotoxicity tests are *in vitro* bioassay methods used to predict the toxicity of substances in tissues and cell lines. The *in vitro* cytotoxicity test provides a crucial tool to evaluate safety assessment and screening, and for ranking compounds. The cytotoxicity evaluation allows one to calculate parameters such as IC$_{50}$ (half maximal inhibitory concentration), which is the concentration of a unique dose compound which causes death of 50% of analyzed cells population sample.

The decision to use a specific cytotoxicity analysis technique is based on specific research objectives. Thus, four major classes of assays are used to monitor the response of cultured cells after treatment with potentially toxic molecules, measuring vitality, cell membrane integrity, cell proliferation, and metabolic activity, respectively.

3-(4,5-dimethylthiazol-2-yl)-2,5-diphenyltetrazolium bromide tetrazolium, MTT, reduction colorimetric assay aims to evaluate the intracellular effects of metabolic activity (Tolosa *et al.*, 2015). The MTT colorimetric assay determines the number of active cells in proliferation based on the mitochondrial cleavage of the yellow tetrazolium salt, MTT, to form a soluble blue formazan product. This formation happens because the amount of formazan produced is directly proportional to the number of vital cells present during the MTT exposure. Since the MTT test is fast, convenient and economical, it has become a very popular

technique for quantifying vital cells in culture. However, several parameters have been identified that may affect cellular metabolism and other factors that significantly modify the specific MTT activity and may result in low or false accounting calculations. Therefore, it is essential to establish analytical parameters with the appropriate controls for each cell line and / or pharmacological treatment in order to optimize test conditions and minimize confusion effects. These parameters should include the appropriate density of the cell, culture medium optimal concentrations, MTT exposure times and composition of the fresh culture medium at the time of dosing. These are needed in order to avoid the exhaustion of nutrients and the control of the effects of pharmacological treatment that can affect cellular metabolism, as well as, possible direct reaction or colorimetric interferences of tested molecules with the specific absorbance of MTT and its enzymatic product. By checking these important parameters, the MTT colorimetric assay provides accurate and reliable quantification of the number of vital cells (Sylvester, 2011). This helps to determine the parameters, such as improvement, tolerate and toxic dose for each compound, which are important for decision-making in the next steps of the research and to determinate de IC_{50} dose, for universal classification of the toxicity of each compound (Klaassen *et al.*, 2008).

2.3.2.3.
Proteomic Screening

Proteomic screening of biological samples allows the analysis of differential expression of proteins in order to evaluate the biochemical effects of pathologies or experimental treatments. Currently, the technique most used for this purpose is the, one or two dimension electrophoretic separation in polyacrylamide gel. In this technique, an electric field is applied forcing the protein samples to migrate through the gel pores containing sodium dodecyl sulfate, SDS.

SDS is an anionic surfactant that interacts with protein peptide chains acting as reducing agent and forming negatively charged complexes of SDS and proteins. β-mercaptoethanol is commonly used to denature the protein performing the disruption of disulfide bonds found between the protein complexes.

Application of an electric field forces these complexes to migrate towards the cathode, with migration speed inversely proportional to complex size (Ninfa *et al.*, 2010).

One-dimensional sodium dodecyl sulfate polyacrylamide gel electrophoresis (1D SDS-PAGE) consists of migration of denatured solubilized proteins into a polyacrylamide electrophoresis system, in the presence of SDS. One of the advantages of SDS-PAGE compared to a native-PAGE is the fact that SDS-PAGE denatures and separates the oligomeric form into its monomers resulting in bands proportional their molecular weights. This type of gel separation is usually associated with immunochemical analysis techniques, with the purpose of identifying and quantifying proteins of interest; the most used technique is western blot (Ninfa *et al.*, 2010).

The name western blot was given to the technique by W. Neal Burnette (Burnette, 1981), it is actually a joke on the eponymously-named Southern blot, which is a technique for DNA detection developed earlier by Edwin Southern (Southern, 2015). Western blot is a process by which proteins separated in the acrylamide gel are electrophoretically transferred to a stable membrane such as a nitrocellulose, nylon, or PVDF membrane. The proteins, immobilized on the membrane, are available by the application of immunochemical techniques with artificial antibodies created with a specific target protein. This allows one to visualize the transferred proteins, as well as to accurately identify relative increases or decreases on the protein of interest. After the protein transference, and before the use of the artificial antibodies, a "blocking" step is performed, done to prevent the direct interactions between the membrane and the antibody. This step is normally achieved by placing the membrane in a diluted solution of protein, typically bovine serum albumin, BSA, or non-fat dry milk in tris-buffered saline, TBS, with a minute percentage of detergent such as Tween 20 or Triton X-100 (Green & Sambrook, 2012).

The incubation step is normally composed by two parts, first the incubation with primary antibody and then incubation with secondary antibody. Primary antibodies are generated by exposing host species or immune cell culture to the interest protein, or part of it. After removing unbound primary antibody, the

membrane is exposed to another antibody, steered to a species-specific portion of the primary antibody, known as a secondary antibody, which is usually linked to biotin or a reporter enzyme, such as alkaline phosphatase or horseradish peroxidase, which allows enhancing a specific quantifiable signal. Most commonly, a peroxidase-linked secondary is used to cleave a chemiluminescent agent, the reaction product produces then luminescence in proportion to the amount of protein (Green & Sambrook, 2012).

2.4.
In vivo studies

2.4.1.
Acute toxicity tests

Acute toxicity tests allow evaluating, in mammals, the biochemical behavior of potential drugs. The complete study of complex physiological phenomena related to organs or whole systems requires the use of suitable models, which presently can only be provided by animal experimentation. Animal studies provide valuable data from which it is possible to estimate the level of exposure in which the risk of health impairment is acceptable. As far as possible, animal studies should use species for which the metabolic pathways and disease process reflect those of humans. Guidelines and protocols for experimentally evaluation of xenobiotic toxicity are formulated by various national and international agencies. These tests include local and systemic acute toxicity tests, among others (Klaassen *et al.*, 2008).

Acute and short-term toxicity tests are usually performed to find out whether the compound under investigation has immunotoxic and cumulative characteristics. This type of test provides information on xenobiotic overdose and observation of the parameters of interest, *i.e.* the drug target organs. Extreme exposure conditions allow the evaluation of small doses events that would not result in signals intense enough to be recognized (Klaassen *et al.*, 2008).

2.4.1.1.
Physiological Metals Quantification

The physiological metals quantification in different organs allows evaluating the possible biochemical changes due to the chelation of the physiological metals, or to the redistribution of the same ones. The determination of metals can be performed quickly and multielementarily by Inductively Coupled Plasma Mass Spectrometry technique, ICP-MS, with a quadrupole analyser. This technique is highly sensitive, allows multi-element and multi-isotope detection, showing a large dynamic range. The ionization process is almost independent of the matrix and the compound analyzed. This technique combines some desired characteristics, namely the easy introduction of the sample, the speed of analysis (typical of ICP), the low limits of detection, and the accuracy of a mass spectrometer (Warra & Jimoh, 2011). The components of the sample are decomposed to positive ions in high temperature argon plasma and analyzed based on their mass to charge ratios (Snook, 1992; Jarvis *et al.*, 2003).

2.4.2.
Effectiveness studies

Behavioral phenomena cannot be studied in cellular systems. Nevertheless it is impossible to study the underlying mechanisms of sensations, such as pain, or psychological situations, such as depression, without using *in vivo* models. More specifically, studies on the neuronal transmission pathways of stimuli cannot be developed in isolated cells, despite the problem of transferring the data obtained by the animal model to man. The need for *in vivo* experimental models is important in human pathology studies, both for etiopathogenesis and for therapy. The existence of experimental models available for some diseases allows evaluating the effect of new drugs with more comprehensiveness. The experimental models of human disease in animal models are divided into two main groups: natural and induced (Monamy, 2009).

The advent of genetic engineering in animals has resulted in significant progress and new perspectives for studies of hereditary diseases and diseases with a strong genetic component. In this sense, knock-out mice and other transgenic animals represent preclinical models of great interest. Knock-out mice are animals

with engineered genomes in order to selectively lose the function of one or more genes. Transgenic animals are characterized by the insertion into the genome of one or more functionally active genes, called transgenes that would not normally be part of the genetic baggage of the species. In this sense, the transgene may be a mutated version of a gene leading to the corresponding pathology, or a heterologous gene, *i.e.* from other species of animals, such as of human origin (Austin *et al.*, 2004). Induction may also not involve genetics, but rather the use of drugs with the ability to induce disease or mimic its symptoms, *i.e*. streptozotocin-induced diabetes in rats (Szkudelski, 2012).

Although rats represent the main experimental animal species to conduct studies on AD, studies on flies (Kong *et al.*, 2014; Sofola-Adesakin *et al.*, 2014) and guinea pigs (Bates *et al.*, 2014) have been described. In this scenario, it is worth noting that mice and rats, unlike other mammalian species, do not develop amyloidogenic pathologies with advancing age (Vaughan & Peters, 1981). Therefore, for *in vivo* studies of AD, one has to chemically induce AD on them, or to use transgenic mice. All amyloidogenic effects will depend only on the induction performed, which can be controlled.

2.4.2.1.
Anxiety

Fear and anxiety are normal emotions that increase the chance of survival in the face of different types of stressful stimuli and therefore have an important adaptive value (Nesse, 1999; Blanchard *et al.*, 2003). In addition, anxiety can be identified under two general aspects. The first, commonly termed trait anxiety, refers to the individual's predisposition to react with a greater or lesser degree of anxiety in the face of a potentially threatening situation. The trait is determined by genetic and environmental factors (Graeff & Del-Ben, 2008). The second aspect, called state anxiety, is related to the individual life moment, that is, a transient emotional state. This varies according to a stress event (Lister, 1990). The elevated plus maze, EPM, explained below, is one of the most used models in anxiety and fear studies and evaluation of drugs that could alter these states.

The neural circuit involved in fear and anxiety (normal and pathological) involves, firstly, the perception and integration of sensory information from

danger signaling stimuli. During and after sensory processing, the resulting information is sent to the thalamus, which projects it to the amygdala. The latter events can occur in two distinct ways; a direct pathway (thalamus-amygdala) and an indirect one, connected with cortical regions (thalamus-cortex-amygdala). The information coming from the first route reaches the lateral nuclei of the amygdala, which organize a series of physiological and behavioral reactions for the defense of the organism. Information from the thalamus-cortex-amygdala pathway is sent by the thalamus to the cerebral cortex, which, after a more refined analysis of the hazard information, projects to the amygdala which is responsible for processing the mnemonic and emotive aspects. The amygdala, in turn, gives a command for two other structures: the periaqueductal gray matter (PAG) and the hypothalamus. The PAG is responsible, among other aspects, for the deflagration of the main behavioral components of the fight-or-flight response. The hypothalamus, however, commands several neuroendocrine reactions (Fanselow & Ledoux, 1999). As discussed above (see section: 1.1.2.2) the amygdala is strongly affected in AD, since this is probably the reason why panic and anxiety states increase during the progression of the disease.

The EPM experiment was developed by Handley and Mithani (Handley & Mithani, 1984) and validated pharmacologically, physiologically and behaviorally for rats by Pellow in 1985 (Pellow *et al.*, 1985) and for mice by Lister (Lister, 1990). The EPM is an animal test model ethologically based on the natural fear of rodents to open spaces and heights. Because of its simplicity, ecological validity and bidirectional sensitivity (used to test the anxiolytic and anxiogenic properties of drugs), this model has several advantages in the study of anxiety (Pellow *et al.*, 1985). Namely, no training of the animals is required, shortening the experiment duration, low experimental cost. It is thus considered a useful and valid instrument to measure anxiety, investigating behavioral, physiological and pharmacological aspects (Pellow *et al.*, 1985; Cruz *et al.*, 1994; Anseloni & Brandão, 1997). Exposure to EPM consists of introducing rats at the crossroads of four arms, two open and two closed, arranged perpendicular to each other and elevated from the ground. When rats are exposed to this experimental situation, they tend to avoid the open arms, remaining longer in the closed arms.

The animal defense behavior in the EPM model is evaluated from traditional indexes of exploitation: analyzing the frequency of inputs and time spent on each type of arm, and, in some cases, other behaviors such as displacements, getting up, stretching, etc. The animal explores the two types of arm but enters more and stays longer in the closed arms. The percentage of preference (inputs and time spent) for open and closed arms is a reliable index of anxiety: the higher the anxiety levels, the lower the percentage of open arms input and the time spent in them (Handley & Mithani, 1984; Pellow *et al.*, 1985).

Despite the apparent simplicity of the test situation, many factors influence open-arm aversion (Hogg, 1996). Some of them are inherent to the subject, such as sex and age (Johnston & File, 1991; Imhof *et al.*, 1993) and nutritional status (Almeida *et al.*, 1996). Others are linked to the experimental procedure, such as a single or multiple exposures to the labyrinth and the time of day the test is performed (Gentsch *et al.*, 1982; Griebel *et al.*, 1993; Treit *et al.*, 1993). In addition, experimental manipulations also alter the behavior of animals in the labyrinth test, such as the type of transport to the test room, individual or group housing and time in the vivarium before the test (Maisonnette *et al.*, 1993; Morato & Brandão, 1996).

The cause of open-arm aversion has been explained by different hypotheses. Initially, it was proposed that this aversion would result from the natural avoidance of rodents in relation to novelty (Montgomery, 1955; Montgomery & Monkman, 1955). Grossen and Kelly justify this behavior as an evolved strategy to avoid predators, especially aerial predators (Grossen & Kelley, 1972). Later, it was suggested that aversion to open arms would result from fear of height, and / or open spaces (Barnett, 1975; Pellow *et al.*, 1985; Pellow, 1986). Treit and Fundytus however, proposed that the animal's inability to perform the thigmotaxis behavior - the tendency of the animal to remain with the body close to or in contact with vertical surfaces - would be the associated aversive stimulus to the open arms of the labyrinth (Treit & Fundytus, 1988).

2.4.2.2.
Memory

According to Squire and Kandel there is no unique brain region responsible for memory (Squire & Kandel, 2009). Not all encephalon regions are equally involved in the process of storing information, because different areas store different aspects of memory. According to Cammarota *et al.*, we can define memory as a process of formation, conversion, evocation and gathering of innumerable information (Cammarota *et al.*, 2005). The act of memorizing includes some processes, such as acquisition, consolidation, storage, evocation and extinction. Memory is classified according to its nature and its retention time.

Working memory is an instant memory; it is used as long as the information will be useful to us, and soon after it may be forgotten. This type of memory is fed by the electrical activity of neurons in the prefrontal cortex that interact with others through the entorhinal cortex, including the hippocampus, during perception, acquisition, or recall. The areas responsible for working memory are the anterolateral prefrontal cortex, the orbitofrontal cortex, and their connections via entorhinal cortex to the hippocampus, the amygdala, the inferior temporal cortex, and the associative parietal cortex. The work memory does not form long-lasting files and leaves no biochemical traits. It depends on glutamatergic transmission by AMPA (α-amino-3-hydroxy-5-methyl-4-isoxazolepropionic acid) receptors and the electrical activity of pyramidal cells in the prefrontal cortex (Dworetzky, 2001).

Declarative memory is an explicit memory, stored in the temporal lobe and diencephalon. It is any memory that we can recall thought some word (Ullman, 2004). It is related to memory for skills, which does not have to be verbalized to be remembered. It is subdivided into 4 types of memories: memory of perceptual representation, a type of memory that stores some object; memory of perceptual form, which does not need to know the meaning of the object to be kept and is a memory that can be remembered through tips; memory of procedures, which is stored in striate nucleus; and associative and non-associative memories, which are stored in the amygdala and are related to the response to some type of behavior (Schacter, 1987).

Based on memory retention, it is possible to classify memory into three: ultra-fast, short-term and long-term. Ultra-fast memory is a type of memory that lasts from fractions to a few seconds and is preconscious and sensory. Short-term memory, which lasts from 3 to 6 hours, allows to remember each memory while its definitive form is not yet consolidated. The short duration of this memory is necessary to the formation of long-term memory, this duration allows the gradually replacement from short to long-term memory. The difference between short- and long-term memories occurs in the underlying mechanisms of each of them. Although short-term memory requires the same nerve structures (hippocampal region, entorhinal cortex and parietal cortex, see Figure **1**) than long-term memory, short-term memory involves its own biochemical mechanisms. The long-term memory guarantees the record of the individual's autobiographical past and knowledge, its duration is hours, days, or years. This memory is based on morphological alterations of the synapses. Inside this type of memory it is found the working and declarative memory mentioned above (Izquierdo *et al.*, 1998; Roesler *et al.*, 2004; Cammarota *et al.*, 2005; Izquierdo, 2015).

As seen before cognitive decline and the consequent memory loss, is one of the major problems associated with AD. The progression of this symptom is used as indicator of AD progression (Braak stages, see section: 1.1.1). The most-used effectiveness AD animal test to investigate the drugs ability to alter memory mechanics is the Novel Object Recognition, NOR, through which it is possible to analyze both short- and long-term memory. When rodents are introduced to familiar and new objects, they spend more time exploring the new object. This behavior has been used in the design of a behavioral paradigm known as an object recognition task (Ennaceur & Delacour, 1988), which has been widely used to evaluate the mechanisms involved in the formation of declarative memories (Moses *et al.*, 2005).

2.4.2.3.
Alzheimer's disease experimental model

Based on the hypothesis of the toxicity of soluble Aβ peptide oligomers (Lambert *et al.*, 1998; Walsh *et al.*, 2002; Ferreira *et al.*, 2007) (see section:

1.1.2.2.1) the experimental model used in the present study aims to mimic the observed cognitive and metabolic effects in AD by the i.c.v. administration of $A\beta_{1-42}$ peptide oligomers in healthy adult Swiss mice (Figueiredo *et al.*, 2013; Ledo *et al.*, 2013; Lourenco *et al.*, 2013).

3.
Objectives

3.1.
General objective

The general objective of this work was to evaluate the potential, reactivity and activity, and toxicological profile of new promissing MPACs in biological models of AD.

3.2.
Specific objectives

- To perform synthesis and characterize four potential MPACs produced in the "Laboratório de Síntese Orgânica e Química de Coordenação Aplicada a Sistemas Biológicos" LABSO-Bio;

- To conduct solution stability tests over time for all the compounds, using pure DMSO or different water:DMSO mixtures as the solvent;

- To perform acute toxicity assessments on healthy male Wistar rats by intraperitoneal (IP) injection of high concentrations of each potential MPAC and, after dissection and removal of the organs of interest (brain, kidneys, liver and heart), compare some biochemical parameters obtained from the animals with those found for a control group and a group injected only with the vehicle solution;

- To determine the concentrations of metals in the organs of interest by ICP-MS;

- To measure the concentrations of reduced glutathione (GSH) in the organs of interest by ultraviolet-visible molecular absorption spectrophotometry.

- To evaluate the *in vitro* MPAC-like potential of the compounds through the study of their interaction, in solution, with the $A\beta_{1-40}$ peptide and the Zn/Cu-$A\beta_{1-40}$ systems;

- To verify the cytotoxicity of the compounds in different mammalian cells lines;

- To evaluate, *in vitro*, the effect of the most promising MPACs on the APP pathway in the SW APP Swedish Mutation HEK 293 cell line, which overexpresses APP;

- To evaluate, *in vivo*, the anxiogenic effects of the most promising compound on an established mouse model of Alzheimer's disease;

- To evaluate, *in vivo*, the effects of the most promising compound on memory using an established mouse model of Alzheimer's disease;

- To correlate the tested compounds' structures with their performances as MPACs.

4.
Material and methods

4.1.
Compounds: syntheses and characterization

All the reagents and solvents purchased were of analytical grade and were used without previous purification, with exception of pyridyl-2-carboxaldehyde, which was distilled before its use in the synthesis of HPCIH. None of the syntheses presented in here was conceived by the author of the thesis.

4.1.1.
Syntheses of the studied compounds

INHHQ was obtained according to the procedure described by De Freitas *et al.* following the synthesis scheme showed in Figure 10, where INHHQ is obtained through the Schiff base condensation reaction between 8-hydroxyquinoline-2-carboxaldehyde and isoniazid (De Freitas *et al.*, 2013).
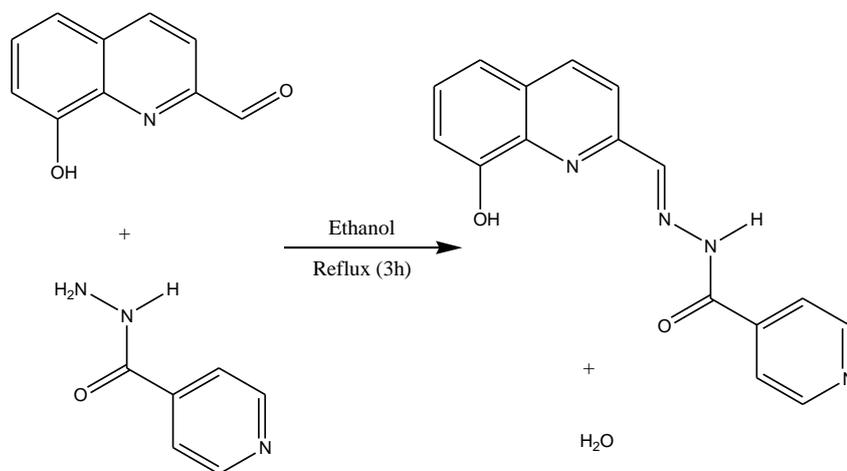
Figure 10. Reaction scheme for INHHQ synthesis.

HPCIH was prepared according to the procedure described by Richardson *et al.* following the synthesis scheme showed in Figure 11, where HPCIH is obtained through the reaction between pyridine-2-carboxaldehyde and isoniazid (Richardson *et al.*, 2006).
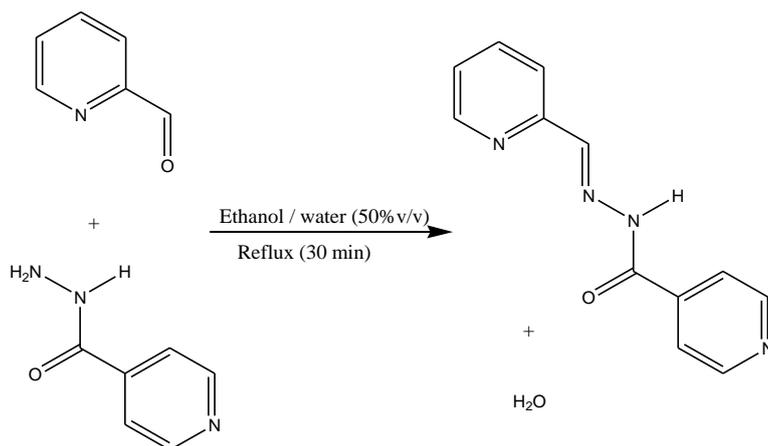
Figure 11. Reaction scheme for HPCIH synthesis.

H2QBS was prepared according to the procedure described by La Deda *et al.* following the synthesis scheme showed in Figure 12, where H2QBS is obtained through azo coupling reaction between the diazonium derivative of sulphanilic acid and the chelating agent 8-hydroxyquinoline according to the procedure described by Chen *et al.* (La Deda *et al.*, 2004; Chen *et al.*, 2013).
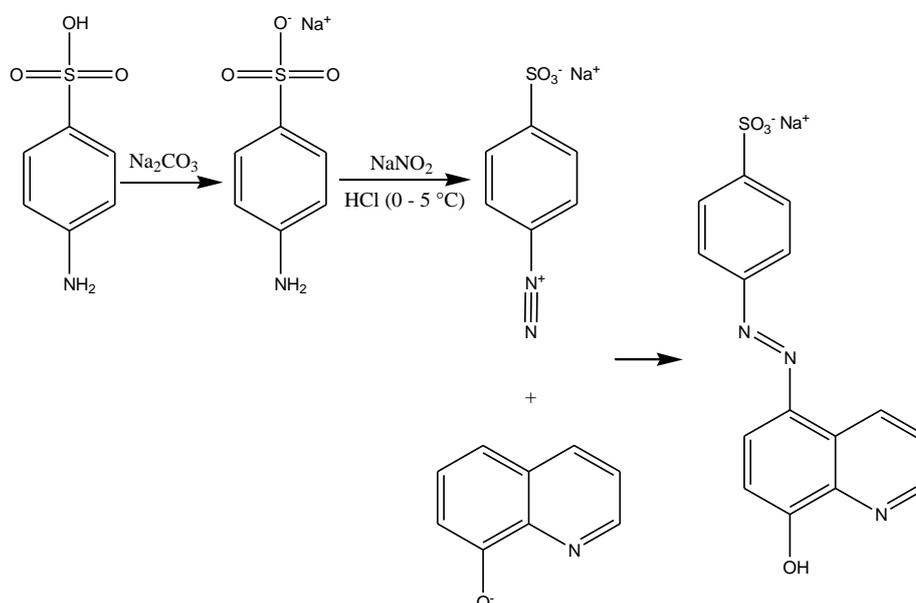
Figure 12. Reaction scheme for H2QBS synthesis.

INHOVA was prepared according to the procedure Gonzáles-Baró *et al.* following the synthesis scheme showed in Figure 13, where INHOVA is obtained through the reaction between *o*-HVa and isoniazid (Oga, 2010; González-Baró *et al.*, 2012b).
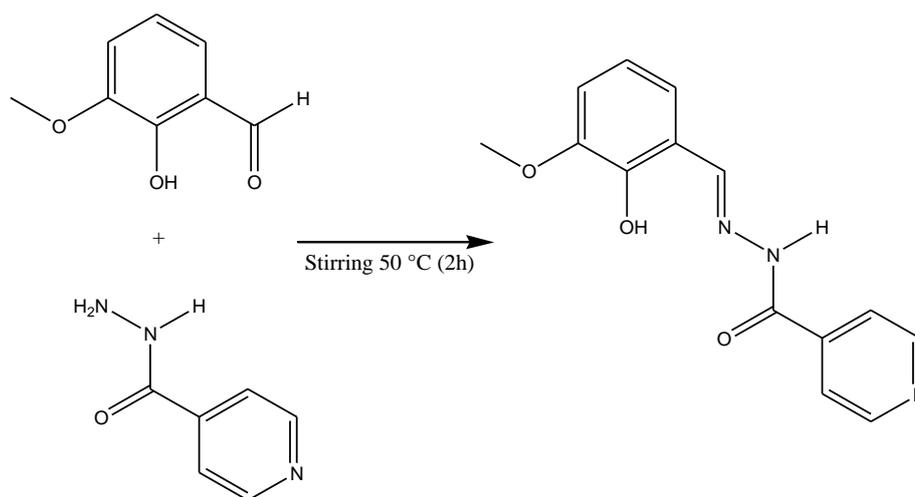
Figure 13. Reaction scheme for INHOVA synthesis.

4.1.2.
Identification

All the products were identified by other members of the research group, before being delivered to the author, through infrared (IR) analysis. When the syntheses were performed by the author, the identity of the compounds was also confirmed by IR. IR spectra were obtained on a Perkin Elmer 2000 FT-IR spectrometer, using KBr pellets. The vibrational spectra of all compounds were analyzed in the range of 4000-450 cm^{-1}. The main characteristic bands were compared with a standard spectra and / or literature data in order to ratify the identity of the synthesis products.

4.2.
In vitro studies

4.2.1.
Stability characterization

Stability tests were performed for all the studied compounds, with the purpose of establishing the susceptibility to hydrolysis of each potential MPAC over time using pure DMSO (control) or different DMSO:water mixtures as the solvent.

Assays were executed in a molecular UV-Vis absorption spectrophotometer (Perkin Elmer Lambda 35, USA) in the range from 200 to 800 nm at room temperature. The compounds were analyzed in DMSO:water mixtures

(dimethyl sulfoxide 99.9% UV/HPLC, #V002021, Vetec, Brazil), varying from 100 to 0.1% DMSO, along 30 h.

The intensity variation of the signals was evaluated, indicating the concentration percentage decrease of the initially dissolved quantity of compound, in order to estimate the disponibility of the product over time after solubilization.

4.2.2.
$A\beta_{1-40}$-MPACs interaction (^{1}H NMR)

The ^{1}H-NMR experiments were performed by the author in collaboration with the research group of Prof. Dr. Claudio O. Fernández, at the "Laboratorio de Biología Estructural y Molecular de Enfermedades Neurodegenerativas (IBR-CONICET)", Max Planck Institute, Rosario, Argentina.

For the 1D NMR titration experiments, non-labeled $A\beta_{1-40}$ samples were used. NMR spectra were acquired on a Bruker Avance II 600 MHz spectrometer using a triple-resonance probe equipped with z-axis self-shielded gradient coils. ^{1}H experiments were measured using 50 mM $A\beta_{1-40}$ dissolved in TRIS buffer 20 mM, pH 7.4, at 5 ^{o}C. To this solution was added 1 equivalent of each compound and the resultant spectrum was acquired, as described in Hauser-Davis *et al.*, (2015).

4.2.3.
^{1}H x ^{15}N HSQC NMR

Heteronuclear ^{1}H x ^{15}N HSQC NMR experiments were performed by the author in collaboration with the research group of Prof. Dr. Claudio O. Fernández, at the "Laboratorio de Biología Estructural y Molecular de Enfermedades Neurodegenerativas (IBR-CONICET)", Max Planck Institute, Rosario, Argentina.

Heteronuclear ^{1}H x ^{15}N HSQC NMR experiments were performed on a Bruker Avance II 600 MHz spectrometer, with pulsed-field gradient enhanced pulse sequences, using 50 mM ^{15}N-isotopically enriched peptide samples in TRIS buffer 20 mM, pH 7.4, at 5 ^{o}C. Amide cross-peaks affected during Zn^{2+} or Cu^{2+} addition were identified by comparing their intensities, I, with those of the same cross-peaks in the data set of samples lacking the divalent metal ions, I_0.

In the same way, amide cross-peaks affected during each compound titration, in Aβ-metal solution, were identified by comparing their intensities, I, with those of the same cross-peaks in the data set of samples of free Aβ, I_0. The experiments were performed, unless otherwise specified, by adding to each Aβ – Cu/Zn system 1, 3, 5 and 10 equivalents for the titration of each compound, in order to obtain the recovery profile of amide cross-peaks of labeled Aβ.

For all mapping experiments, I/I_0 ratios of well-resolved cross-peaks were plotted as a function of the peptide sequence to obtain the intensity profiles as described in Hauser-Davis *et al.*, 2015.

Spectrum acquisition, titration data processing and visualization were performed using the CcpNmr Analysis 2.4.1 software (Python, Germany).

4.2.4.
Cell studies

Cell studies were performed by the author in collaboration with the research group of Prof. Dr. Fabio Di Domenico, at the "Laboratory of Redox Biochemisty in Neuroscience – LRBN", at the Department of Biochemical Sciences A. Rossi Fanelli of "Sapienza" University of Rome, Italy.

4.2.4.1.
Cytotoxicity

For cytotoxicity experiment in the three different cell lines two control groups are presented: cells treated only with medium and cells treated with medium containing 1% DMSO. All the data were normalized to the values related to the cells treated with medium containing 1% DMSO. The threshold of 80% of vital cells was defined as a tolerance limit of accepted vitality. Based on this threshold, three fundamental doses where highlited:

- The improving dose, defined as the dose where cellular vitality is higher than 100%, this dose is capable of parcially repair to DMSO toxicity;

- The tolerated dose, defined as the last tested dose before the threshold of 80% of vital cells was reached;

- The toxic dose, defined as the first tested dose capable to decrease cellular vitality lowers than the threshold of 80%.

Each cells line were seeded in a 96-well plate, with specific cells density in specific culture medium and incubated for 24 h at 37 °C, 5% CO2.

The specific conditions for each cells line were:

- SH-SY5Y cells were seeded at 20'000 cells per well density in 150 μL of complete culture medium (DMEM / HAM 1:1, 10% FBS, 1% penicillin);

- SW APP HEK 293 cells were seeded at 5'000 cells per well density in 150 μL of complete culture medium (DMEM, 10% FBS, 1% penicillin; G418 3 μL mL^{-1});

- HEK 293 cells were seeded at the density of 5'000 cells per well in 150 μL of complete culture medium (DMEM, 10% FBS, 1% penicillin);

The lowest cells density for SW was chosed due to lack of adhesion for higher density in this cell line.

After 24 h the culture medium was removed and replaced with complete culture medium containing 1% FBS under different concentration of each compound, according to the following scheme:

- 8 wells were treated with 1% FBS complete medium for control (CTRL);

- 8 wells were treated with 1% FBS complete medium with 1% DMSO to control the effects of the vehicle (0 μL);

- 8 wells were treated with 1% FBS complete medium containing five concentration of the compound of choice (10, 50, 100, 250 and 500 μmol L^{-1} respectively).

Each plate was incubated for 24 h at 37 °C, 5% CO_2. After 24 h of treatment the medium was withdrawn from each well, the 100 μL complete medium containing 1% FBS and 10% MTT was added in each well and the plate was kept under incubation for 1h at 37 °C, 5% CO_2. After 1 h the medium containing MTT was removed, and 100 μL of isopropanol were added in each well, the plate was covered to protect from light and held in oscillation for 10 min, the plates were analyzed by UV-Vis microplate reader spectrophotometer (Multiskan EX, Thermo Scientific, USA) at 570 and 690 nm wavelengths, to quantify the formation of the purple precipitates. The experiments were always repeated, at least in duplicates.

Parametric data with normal distribution were analyzed by Analysis of Variance (ANOVA) followed by *t*-test. Values were plotted as mean ± standard deviation. The significance level in all experiments was p <0.05.

The obtained data were analyzed with GraphPad Prism software, the outlier presence was evaluated by Grubb's test. The statistical significance between the different conditions was evaluated by the *t*-test.

For all the experiments IC_{50} was calculated as interpolation in dose-response curve.

4.2.4.2.
Proteomic screening

SW APP HEK 293 cells were plated at a density of 165'000 cell per T25 flask in 5 mL of complete culture medium (DMEM, 10% FBS, 1% penicillin; G418 3 µL mL^{-1}) in five different T25 flask.

After 24 h the culture medium was removed and replaced with complete culture medium containing 1% FBS under different concentration of each compound, according to the following scheme:

- 1 flask was treated with 1% FBS complete medium for control (CTRL);
- 1 flask was treated with 1% FBS complete medium with 1% DMSO to control the effects of the vehicle (0 µL);
- 3 flasks was treated with 1% FBS 1% complete medium containing a different concentration of the specific compound. The dose for the proteomic screening cells treatment was chosen from the cytotoxicity result for INHHQ and HPCIH, in SW APP HEK 293, establishing, for each compound, three concentrations doses: the improvement, the tolerated and the toxic one.

Each flask was incubated for 24h at 37 °C, 5% CO_2. After 24 h the culture medium was removed and 500 µL of trypsin (Trypsin 0.05%, #IK5062, Immunological Science, USA) was added to each flask to detach the cells from the flask wall. After 3 minute at 37 °C, 2 mL of complete medium was added to each flask to suspend the cells and annul the enzymatic effect of trypsin. The solution containing the treated cells was collected in 15 mL centrifuge tubes and centrifuged for 5 min at 2700 rpm, at room temperature. The supernatant was

completely discarded and the tubes with pellet were stored in ice. The surface of the pellet was thoroughly washed with PBS, minutely avoiding cell pellet resuspension, to remove the culture medium residues. 80µL of RIPA buffer containing protease and phosphatase inhibitors was added to each tube and the pellet was resuspended using micropipettes. The function of RIPA is to break cellular membrane and make cytosol content available for proteomic screening. Each suspension was transferred in 1.5 mL centrifuge microtube and in ice sonication was applied for 3 cycles of 10 second each interspersed by a 10 second pause to distrupt cellular membranes. The samples were centrifuged at 4 $^{\circ}$C for 1 h at 14'000 rpm. The supernatant was collected and stored at -80 $^{\circ}$C for at least 12h. All the experiments were repeated in triplicate.

4.2.4.2.1.
Total Protein Quantification

Protein quantification was performed through BCA (bicinchoninic acid) assay for each group of treatment.

2 µL of each sample was transferred to a 96 multiwell plate in duplicate. On the same plate seven different concentration of BSA standard (BSA standard, # 52_11920, SERVA, Germany), in duplicate, were transferred (0; 5; 10; 15; 20; 25 and 30 µg µL^{-1} of BSA) to obtain the analytical reference curve. To each well, containing sample or BSA, were added 100 µL of BCA solution (Pierce™ BCA Protein Assay Kit, #23223, Thermo Scientific™, USA), and the plate was covered, to protect from light, and held in oscillation for 10 min. Then the plates were analyzed by UV-Vis microplate reader spectrophotometer (Multiskan EX, Thermo Scientific™, USA), at 540 nm wavelengths, to quantify the BCA reaction. The obtained data were analyzed with GraphPad Prism software, and sample concentration was obtained through interpolation with BSA curve.

4.2.4.2.2.
SDS-PAGE

SDS-PAGE was performed in order to separate protein in each sample.

For each sample, 20 µg of proteins were buffered to 10 µL with PBS, and then 10 µL of sample buffer (2x Laemmli Sample Buffer, #1610737, BIORAD, USA) was added, to a final volume of 20 µL. The sample were boiled for 10 min

to complete the denaturation, and then were resolved on a 4–12% Criterion™ XT Bis-Tris Protein Gel (BIORAD, USA). The run was performed in TGS buffer (25 mM Tris, 192 mM glycine, and 0.1% SDS, pH 8.3, in ultrapure water) for about 1 h at 150 mA with a running system (Criterion™ Vertical Electrophoresis Cell, BIORAD, USA). The Precision Plus Protein™ All Blue Prestained Standard (#1610373, BIORAD, USA) was used as protein weight marker.

Before immunoblot analysis the gel image was acquired as standard to be subsequently used to normalize blot analysis.

4.2.4.2.3.
Western blotting

For immunoblot analysis, gels were transferred onto Trans-Blot® Turbo™ Mini PVDF Transfer Packs nitrocellulose membranes (BIORAD, USA) through Trans-Blot® Turbo™ Transfer System (BIORAD, USA).

Membranes were blocked with 3% BSA 0.5% in Tween-20 / Tris-buffered saline (TTBS) and incubated overnight at 4 °C with the following antibodies:

APP (1:5'000, rabbit, #A8717, Sigma-Aldrich, USA)

BACE-1 (1:1'000, rabbit, #5606, Cell Signaling Technology®, USA)

6e10 (1:1'000, mouse, #SIG-39320, BioLegend®, USA)

After 3 washes with TTBS the membranes were incubated for 60 min at room temperature with anti – rabbit / mouse IgG secondary antibody conjugated with horseradish peroxidase (1:5000; Sigma-Aldrich, USA). Membranes were developed with the Clarity™ Western ECL Substrate (BIORAD, USA), and the images were acquired with Chemi-Doc MP (BIORAD, USA) and analyzed using ImageLab software (BIORAD, USA) which allows the normalization of a specific protein signal with the total proteins load.

4.3.
In vivo studies

4.3.1.
Ethical aspects

All experiments involving the use of animals were approved by an Ethics Committee of PUC-Rio and collaborating universities (protocol in CEUA / 036/2013), and are in accordance with the Ethical Principles on Animal

Experimentation adopted by the Brazilian Society of Science in Laboratory Animals / Brazilian College of Animal Experimentation in conformance with the Guide of the North American Society of Neurosciences and Behavior for Care and Use of Laboratory Animals.

4.3.2.
Acute toxicity assays

Acute toxicity experiments were performed by the author in collaboration with the research group of Prof. Dr. J. Landeira-Fernandez, at the Psychology Department of PUC-Rio, Rio de Janeiro, Brazil.

The compounds were injected to healthy adult male Wistar rats of between 180 and 240 days of age, weighting between 260 and 420 g. Only males were used to avoid the influence of the estrous cycle of the females on the parameters to be analyzed. Animals were housed in polycarbonate cages measuring 18 x 31 x 38 cm, at controlled temperature (24 ± 1 °C), with circadian cycles maintained (12 h / 12 h light-dark). All experiments took place during the light phase of the cycle.

For each experiment, 8 rats were injected intraperitoneally, IP, with a 10% DMSO / saline solution vehicle containing 20 mg mL^{-1} of the compound to be tested, maintaining the dose ratio at 200 mg of compound per kg of animal body weight. The animals were kept under observation, with feed and water supplied *ad libitum* to verify any behavioral changes. Subjects were sacrificed after 72 h. Noble organs, *i.e.*, brain, liver, heart and kidneys were removed, cleaned and weighed before being aliquoted for the different analyses and frozen at −20 °C. Any macroscopic changes in internal anatomy of the animals were observed and taken into account in the data treatment.

All data obtained for each compound were compared with a control group (n=11), not submitted to any treatment, and a "vehicle" group (n=11), injected only with the vehicle solution, *i.e.*, 10% DMSO / saline solution.

Since most of data reported in this section did not present a parametric distribution, all the data were treated as non-parametric, in order to allow comparing them. Statistical differences between the groups medians were detected through Kruskal-Wallis test (confidence interval=95%). Dunn's multiple comparison test was performed to determinate the presence of significant difference between each group: only difference between the following pairs are

evaluated here (p<0.05): (i) MPAC-injected and non-injected, (ii) MPAC-injected and vehicle-injected.

4.3.2.1.
Oxidative Stress Evaluation

4.3.2.1.1.
GSH extraction and quantification

GSH was extracted from a frozen portion of brain and liver. The portion was weighed in triplicate and homogenized in 0.1 mol L^{-1} sodium phosphate buffer containing 0.25 mol L^{-1} sucrose at pH 7.0 in a partially inert atmosphere (nitrogen flow) to minimize protein oxidation. The samples were centrifuged at 13'500 rpm for 30 min at 4 °C, and the supernatants were separated, stored in sterile 2 mL microtubes, passed through the nitrogen stream again and frozen until analysis.

The GSH concentrations were calculated using GSH (Sigma-Aldrich, USA) as an external standard plotting an analytical curve of at least 5 points. Samples were quantified according to the literature (Ellman, 1959). 5,5 '-dithio-bis- (2-nitrobenzoic acid) (DTNB) 0.25 mmol L^{-1} and 0.1 mol L^{-1} phosphate buffer of pH 8.0 were added to samples and to curve points 1:1 volume ratio. After incubation for 15 min, without light incidence, the samples were analyzed in a spectrophotometer (Perkin Elmer Lambda 35, USA) at 412 nm wavelength.

4.3.2.2.
Metals Quantification

Metal quantification was performed on aliquots of lyophilized samples from rats' organs. Approximately 100 mg of each sample were acidified with 1 mL of sub-distilled nitric acid (Vetec, Brazil), and were kept overnight. The reference material used was the DORM-4 (Dogfish muscle, NRC, Canada), in duplicate. The samples were heated at 80-100°C for approximately 4 h for digestion. After cooling at room temperature, the samples and the reference material were brought to 10 mL in volume, and two dilutions (10x and 100x) were prepared. Three solutions without any sample were prepared in the same way for each analysis. The elements of interest were determined by ICP-MS, ELAN DRC II model (Perkin Elmer, USA) in standard mode, without reaction cell. Samples

were introduced using a Meinhard nebulizer with a twister cyclone chamber. During the analysis, ^{103}Rh was used as the internal standard at 20 mg L^{-1} concentration. The results were obtained by averaging the three readings made for each sample after external calibration with multi-element calibration solutions obtained by appropriate dilutions of standard solution (Merck IV).

4.3.3.
Studies of effectiveness

Effectiveness studies were performed by the author in collaboration with the research group of Prof. Dr. Sérgio T. Ferreira, at the "Leopoldo de Meis Institute of Medical Biochemistry/CCS/UFRJ", Rio de Janeiro, Brazil.

4.3.3.1.
Alzheimer's disease experimental model

Three-month-old healthy male Swiss mice weighting between 30 and 50 g were employed in this study. During the whole period, the animals were kept in controlled temperature environments (22 ± 2 ^{o}C), with a normal light / dark cycle of 12 h and water and standard feed *ad libitum*.

The mice, previously weighed, were exposed to the compound by IP injection of a saline solution containing 10% by volume of DMSO and different concentrations of INHHQ, reported by each experiment.

The oligomers were prepared from the synthetic peptide Aβ_{1-42} (American Peptide, Sunnyvale, CA). The peptide was resuspended in ice-cold 1,1,1,3,3,3-hexafluoro-2-propanol, HFIP (Merck, Germany) and the obtained colorless solution was incubated at room temperature for 60 min. The solution was placed on ice for 10 min and aliquoted, in laminar flow, into microtubes. The microtubes were left open in the laminar flow hood for 12 h for HFIP evaporation. Complete elimination of HFIP was done by centrifugation in "SpeedVac" for 10 min. The aliquots containing the Aβ_{1-42} films thus obtained were stored at -20 °C for further use. The AβOs preparations were made from these Aβ_{1-42} film stocks and, at each AβOs preparation, an Aβ_{1-42} aliquot (film) was resuspended in DMSO (Sigma, USA) in order to obtain a 5 mmol L^{-1} solution. This solution was diluted to 100 μ mol L^{-1} in sterile PBS and incubated at 4 °C for 24 h. A sample of the same volume of 2% DMSO in PBS was prepared and incubated at 4 °C for 24 h, and

used experimentally as control. After incubation, the preparation was centrifuged at 14'000 g for 10 min at 4 °C to remove insoluble aggregates of $A\beta_{1-42}$. The centrifugation supernatant, containing the Aβs, was maintained at 4 °C until use within a maximum period of up to 48 h after preparation. To determine the concentration of AβOs in the preparations, the BCA assay for protein dosing was used (see section:4.2.4.2.1). Since they are metastable, the AβOs preparation, performed weekly in the laboratory, are routinely analyzed by gel-filtration chromatography to characterize the oligomeric species present and occasionally also by Western blotting (De Felice *et al.*, 2009; Brito-Moreira *et al.*, 2011).

HPLC analyses were done with a SynChropak GPC 100 silica column with the following characteristics: column size: 250 x 4.6 mm; pore size: 100 Å; limit of exclusion for proteins: 3-300 kDa. The mobile phase used was PBS pH 7.0, filtered through Millipore nitrocellulose membrane (Billerica, USA) (0.45 µm), kept on ice throughout the analysis. The analyses were performed using high performance liquid chromatography (HPLC), with simultaneous detection of absorption at 280 nm and fluorescence with excitation at 275 nm and emission at 305 nm.

Prior to the injection of the AβOs sample, the column was washed for 1 h with Milli-Q water and equilibrated for 1 h with the mobile phase, both with flow rate of 0.5 mL min^{-1}. Initially, 50 µL of vehicle (2% DMSO in PBS) were injected, with flow rate of 0.5 mL min^{-1} and run time of 15 min. Then, the column was rebalanced with the mobile phase for 15 min and 50 µL of AβOs were injected, analysis done with the same parameters used for the vehicle.

For Aβ oligomers, AβOs, or vehicle i.c.v. injection, the animals were anesthetized using a vaporizer system with 2.5% isoflurane (Cristalia, Brazil) and rapidly restrained during the injection. For the administration of a final volume of 3 µL of vehicle or AβOs at a dose of 10 pmol, a needle of 2.5 mm length was inserted unilaterally 1 mm to the right of the midline point equidistant from both eyes and 1 mm posterior to a line drawn through the anterior base of the eyes (Laursen & Belknap, 1986).

4.3.3.2.
Behavioral measures

4.3.3.2.1.
Elevated plus maze

The EPM equipment used consists of four wooden arms arranged in a cross shape, these arms are aligned, two arms closed by walls (30 x 5 x 15 cm) opposite two open arms (30 x 5 cm). The test lasted 5 min and was performed in a room with fluorescent lighting, with intensity set at 44 lux. The animals were placed directly on the central platform of the raised cross maze with the head facing one of the closed arms and the behavioral parameters recorded were: frequency of animals entering the open arms and closed arms of the labyrinth; and length of stay of the animals in the open arms and in the closed arms of the labyrinth.

4.3.3.2.2.
Object recognition test

Initially, the animals were habituated in the open field (OF) boxes, where the tests were performed with the support of Any Maze® software. The apparatus consists of a wooden arena with black floor (30 x 30cm) and 40 cm walls. The luminous intensity at the center of the OF was 50 lux.

The object recognition test consisted of allowing the animals to freely explore an OF containing two identical objects for 5 min. The retention test was performed 30 min, 4 h or 24 h after the training session. In these 5-min test sessions, the animals were individually reintroduced in the OF, and one of the objects presented during training was randomly replaced by a new object, the difference resides on the shape of the object, not on its color. The time spent exploring each object was measured by an observer and expressed as a percentage of the total exploration time.

Parametric data with normal distribution were analyzed by Analysis of Variance (ANOVA) followed by Bonferroni *post hoc* test or *t*-test. Values were plotted as mean ± standard deviation. The significance level in all experiments was $p < 0.05$.

5.
Results and discussion

5.1.
Identification of the synthesized compounds

All the products were identified through IR analysis in the range 4000-500 cm^{-1}. The main characteristic bands were compared with a standard spectra and / or literature data in order to ratify the identity of the synthesis products.

The INHHQ spectrum was compared to that reported in the literature, allowing to conclude that the product obtained corresponded to the expected compound (Figure 14) (De Freitas *et al.*, 2013).
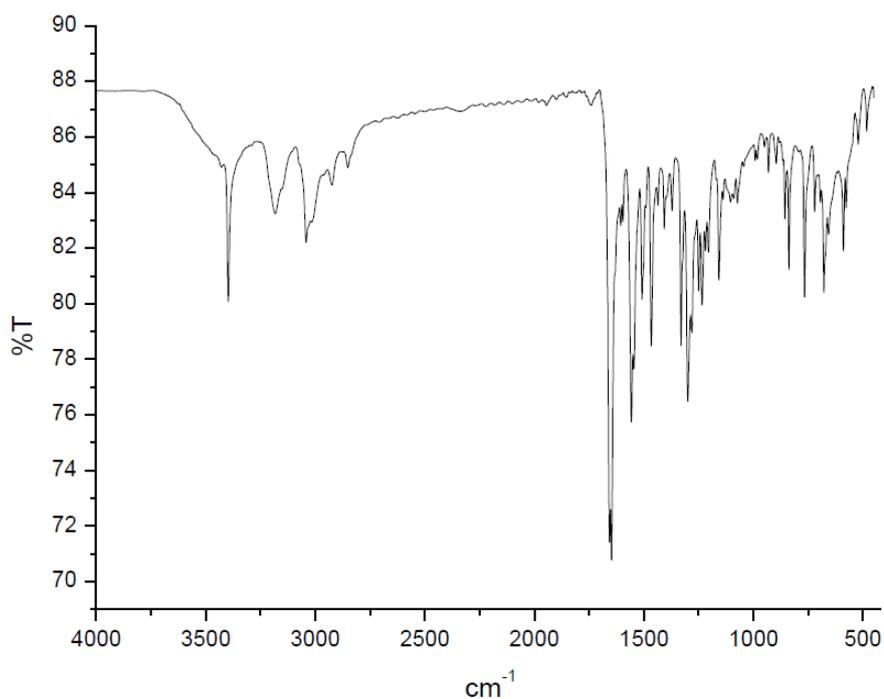
Figure 14. IR spectrum of INHHQ in KBr pellets.

The HPCIH spectrum was evaluated in order to conclude that the product obtained corresponded to the expected compound (Figure 15) (Nakamoto, 2009).
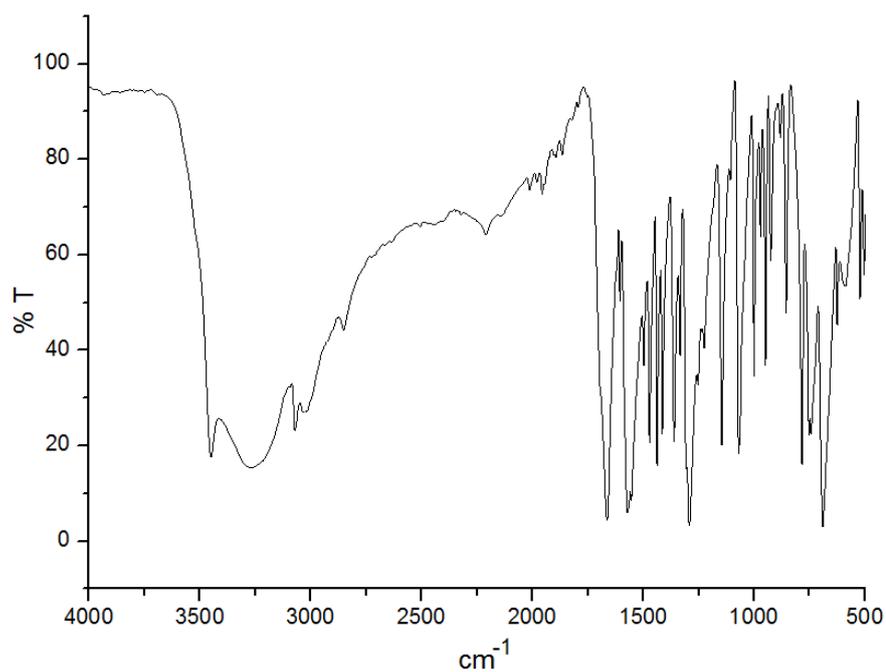
Figure 15. IR spectrum of HPClH in KBr pellets.

The H2QBS spectrum was evaluated in order to conclude that the product obtained corresponded to the expected compound (Figure 16) (Nakamoto, 2009).
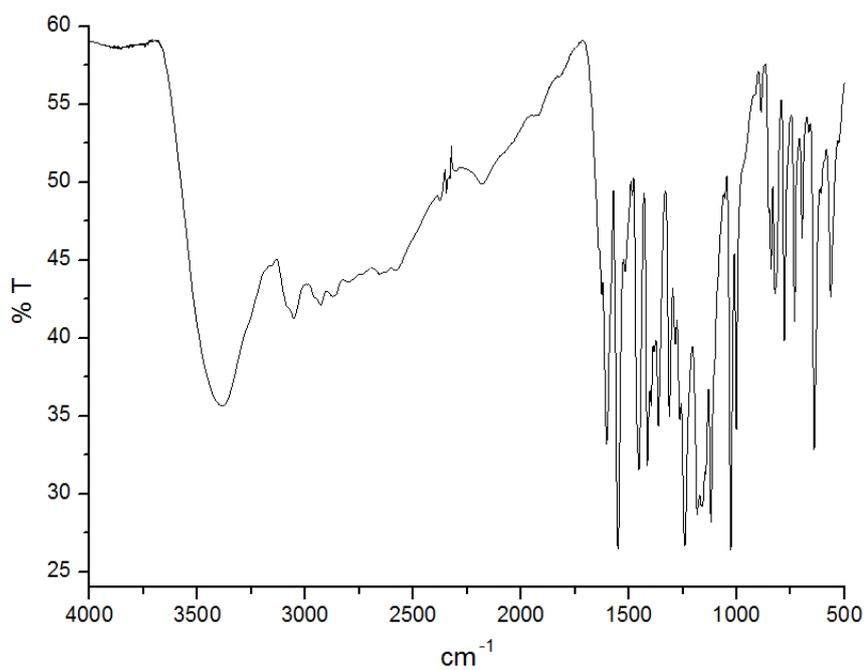
Figure 16. IR spectrum of H2QBS in KBr pellets.

The INHOVA spectrum was compared to that reported in the literature, allowing to conclude that the product obtained corresponded to the expected compound (Figure 17) (González-Baró *et al.*, 2012a).
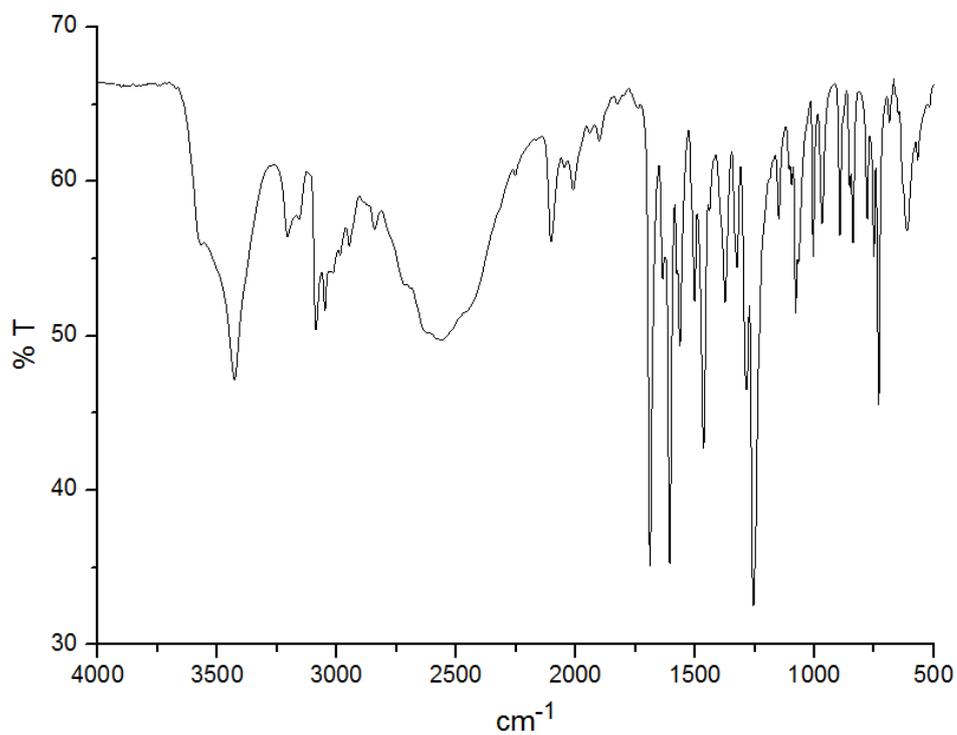

Figure 17. IR spectrum of INHOVA in KBr pellets.

The main bands of the four compounds and their attributions are summarized in Table 1.

Table 1. Main IR bands of the four compounds and their assignments:

Assignment	INHHQ (cm^{-1})	HPCIH (cm^{-1})	H2QBS (cm^{-1})	INHOVA (cm^{-1})
v(OH) phenol	3397	-	*	3015
v(NH) hydrazone	3182	**	-	3158
v(C=O) carbonyl	1657	1663	-	1689
v(C=N) azomethine	1647	1621	-	1606
v(N=N) azobenzene	-	-	1551	-
δ(C−O−H) phenol	1371	-	1312	1374
v(C−OH) phenol	1233	-	1241	1324
v(SO$_3^-$)	-	-	1119 1028	-

* The intense water band did not allow the attribution in the 3500-3250 cm^{-1} region.

** The spectrum showed a relatively complex pattern in the 3500-3150 cm^{-1} region, and for that reason it was not possible to completely attribute these bands.

5.2.
Stability characterization

Each compound was evaluated, regarding its stability in solution, by observing the UV-Vis absorbance profile changes, in the 200-800 nm range, and each system was monitored for 30 h. The solvents used were pure DMSO or mixtures containing specific DMSO / bidistilled water ratios. Tests at 100% DMSO were performed to evaluate the stability in an aprotic environment, and to define a control profile for each compound, assuming no hydrolysis take place in such a medium. Tests at 10% DMSO were performed to evaluate the stability at the same DMSO concentration used as vehicle for the *in vivo* injection. Tests at 1.0%, 0.5% and 0.1% DMSO were performed in order to define the best condition for the *in vitro* experiments involving cells, due to the high DMSO cytotoxicity. Tests at concentrations of 0.5 and 0.1% DMSO indicated a very low stability

profile for all the analyzed compounds. Therefore, the 1.0% DMSO solution was established as the most suitable condition for *in vitro* cellular assays.

5.2.1.
INHHQ

After 30 h at 100% DMSO, the absorbance profiles data for INHHQ were obtained for each time. In Figure 18 is presented the absorbance profile of the compound, showing two major bands, 330 nm and 290 nm. The absorbance decreasing after 30 h for these bands were 2.2% and 2.4%, at 330 and 290 nm, respectively: this indicates a good INHHQ stability in 100% DMSO.
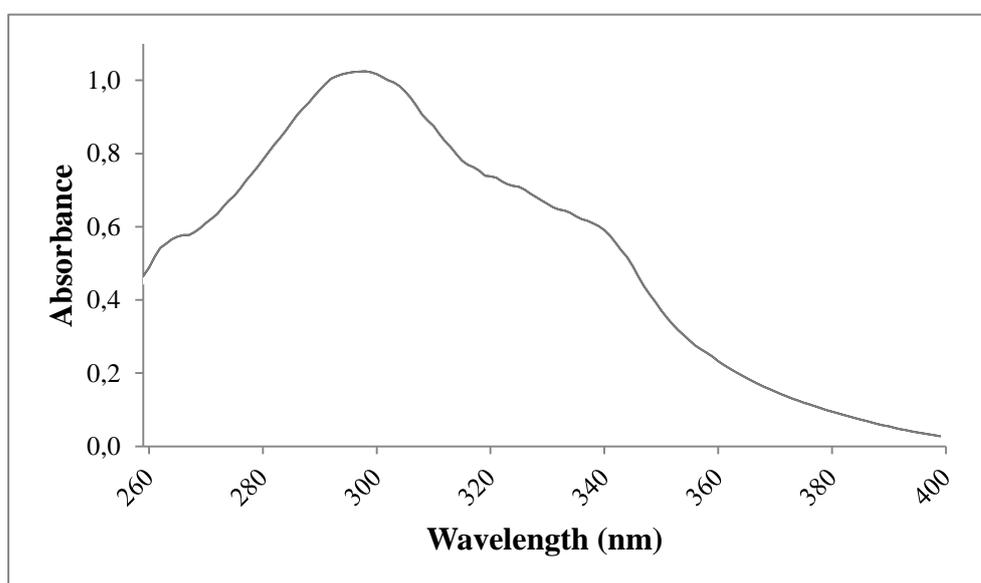
Figure 18. Absorbance profile curve of INHHQ in 100% DMSO between 260 and 400 nm.

After 30 h in 10% DMSO, the absorbance, measured between 250 and 400 nm, decreased (Figure 19). The two INHHQ major bands decreased by 10.2% and 8.9% at 330 and 290 nm, respectively, indicating a good INHHQ stability in such conditions, which is similar to *in vivo* tests condition.
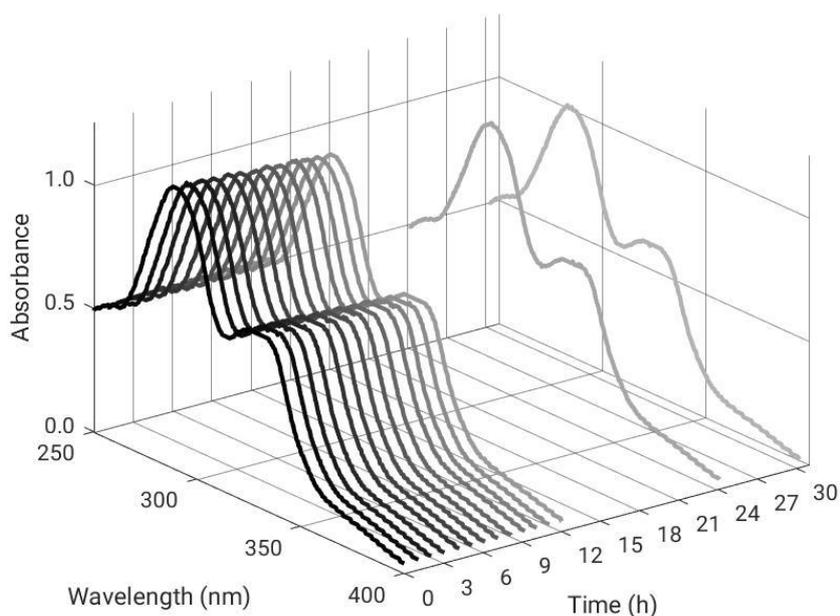
Figure 19. Absorbance profile curves of INHHQ in 10% DMSO over 30 h between 250 and 400 nm.

When dissolved in 1.0% DMSO, the absorbance of INHHQ slightly decreased after 30 h, measuring at the two major bands, 330 nm (3.6%) and 290 nm (3.4%), indicating a good INHHQ stability in 1.0% DMSO, which is similar to *in vitro* cells tests condition.

The minor decreasing absorbance in 1.0% DMSO when compared with 10% DMSO is unexpected, since it is believed that in a higher proportion of water the equilibrium should be shifted to the INHHQ hydrolysis direction. The result suggest that INHHQ, in 1.0% DMSO condition, undergoes hydrolysis and reach the equilibrium already at the time considered as t=0, and after that it remains almost constant over time.

5.2.2.
HPCIH

After 30 h at 100% DMSO, the absorbance profiles data for HPCIH were obtained for each time. In Figure 20 is presented the absorbance profile of the compound, showing one major band in 301 nm. The absorbance decreasing after 30 h for this band was 1.2%: this indicates a good HPCIH stability in 100% DMSO.
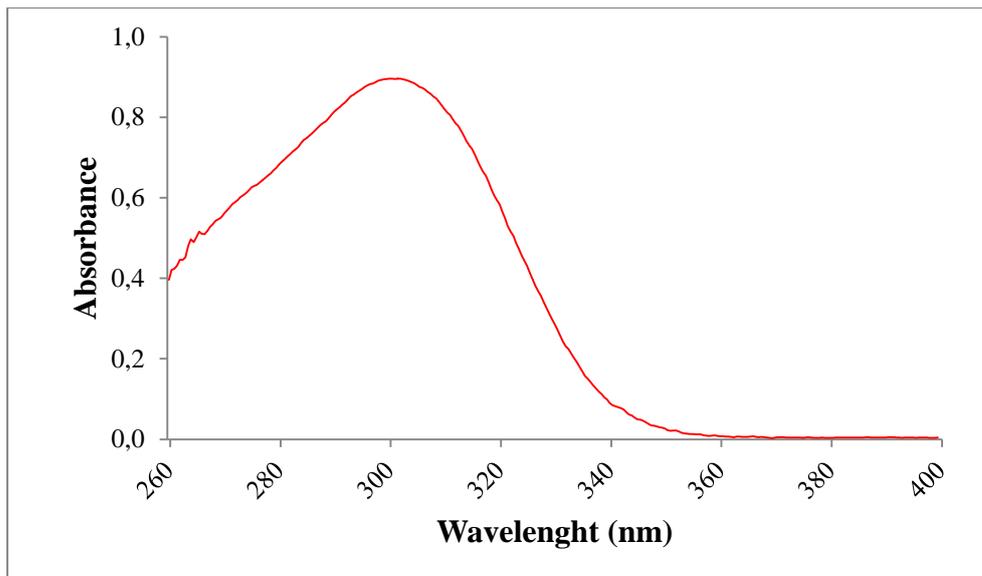
Figure 20. Absorbance profile curve of HPCIH in 100% DMSO between 260 and 400 nm

After 30 h at 10% DMSO, the absorbance, measured between 250 and 400 nm, decreased 31.5% for the maior HPCIH band in 301 nm. In Figure 21 are presented all absorbance profiles curves, showing that HPCIH hydrolyses in 10% DMSO condition occurred during the first few hours, and then stability is reached.
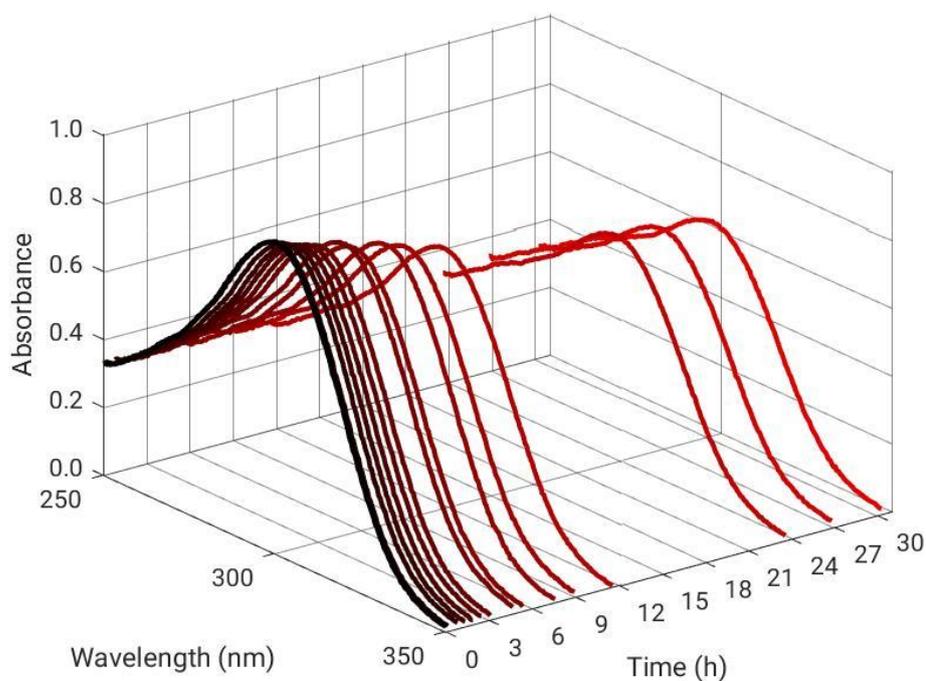

Figure 21. Absorbance profile curves of HPCIH in 10% DMSO over 30 h between 250 and 400 nm.

After 30 h in 1.0% DMSO, the absorbance decrease after 30 h for the HPCIH major band was 19.3%.

The minor decreasing absorbance in 1.0% DMSO when compared with 10% DMSO, similarly to INHHQ profile (see section: 5.2.1), could suggest that in 1.0% DMSO condition, the compound undergoes hydrolysis and reach the equilibrium already at the time considered as t=0, and after that it remains almost constant over time.

5.2.3.
H2QBS

The absorbance for H2QBS was measured during 30 h in 100% DMSO. The profile curves between 270 and 620 nm is resported in Figure 22 as black curve. This absorbance profile of the compound showed a unique band in 398 nm. The absorbance decrease after 30 h for this band was 0.2% suggesting high compound stability in this condition. In the same figure is reported the H2QBS profile curves in 10% DMSO (green curve in Figure 22). In this condition is observed the appearance of a second band in 466 nm. The two H2QBS major bands in this condition result in a slight variation after 30 h, 0.6 and 2.7% for 398 and 466 nm, respectively, showing a high stability of the compound in this form in the 10% DMSO condition, as reported in Figure 23. The appearance of the second band in 466 nm is probably due to the hydrolysis of the compound. This hydrolysis is not reconductible to the H2QBS precursors, namely 8HQ and sulfanilic acid, whose profile is showed in Figure 22 (blue and red curves, respectively). The variation of 398 nm intensity band, at the same concentration of the compound in two different solutions, namely 100 and 10% DMSO in water, was calculated as a 30.9% decrease, suggesting that about 70% of the inicial H2QBS concentration is preserved in 10% DMSO.

When dissolved in 1.0% DMSO, the absorbance of H2QBS shows a different pattern: for the 398 nm band the absorbance after 30 h showed an increase of 47.43%; for the 466 nm bands the absorbance showed of 8.3%, suggesting an inversion in the pattern observed in 10% DMSO condition.
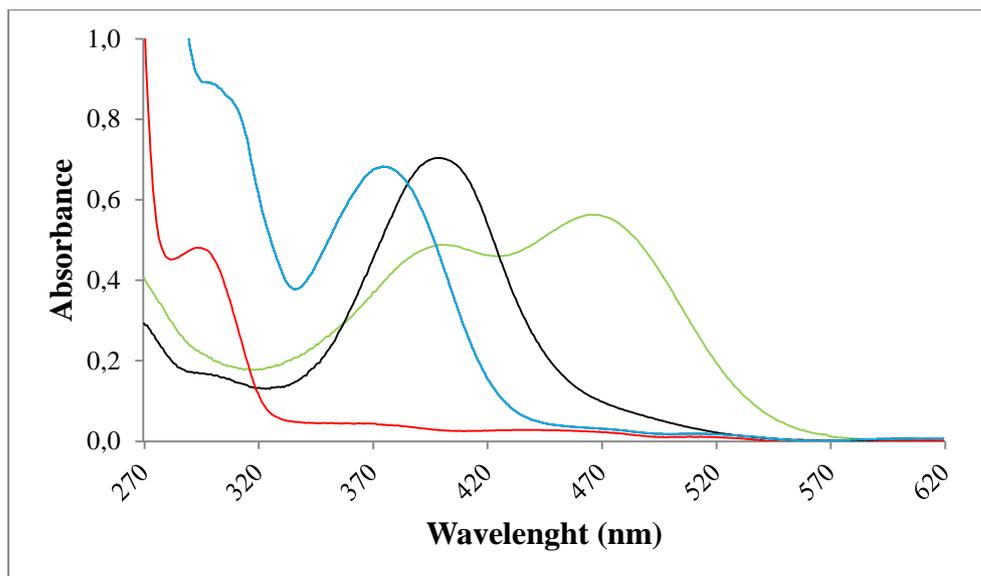
Figure 22. Absorbance profile curves of H2QBS and its precursors between 270 and 620 nm. Black curve represents H2QBS profile in 100% DMSO condition; grren curve represents H2QBS profile in 10% DMSO condition; blue and red curve represents 8HQ and sulfanilic acid in 100% DMSO condition, respectively.
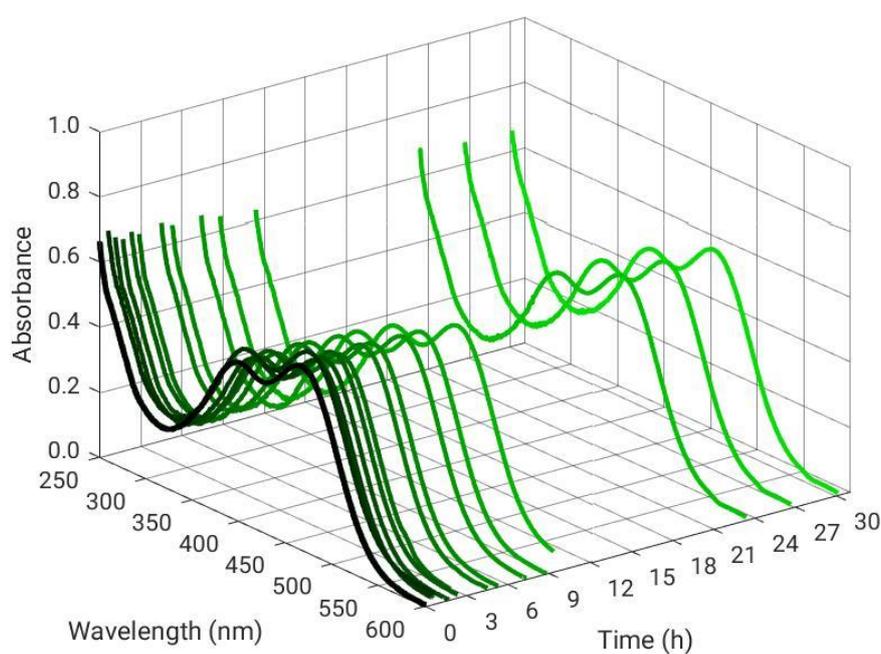
Figure 23. Absorbance profile curves of H2QBS in 10% DMSO over 30 h between 250 and 600 nm.

5.2.4.
INHOVA

After 30 h in 100% DMSO, the absorbance profiles data for INHOVA were obtained for each time. In Figure 24 is presented the absorbance profile of

the compound, showing one maior band at 302 nm. The absorbance decreasing after 30 h for this band was 3.9%: this indicates a good INHOVA stability in 100% DMSO.
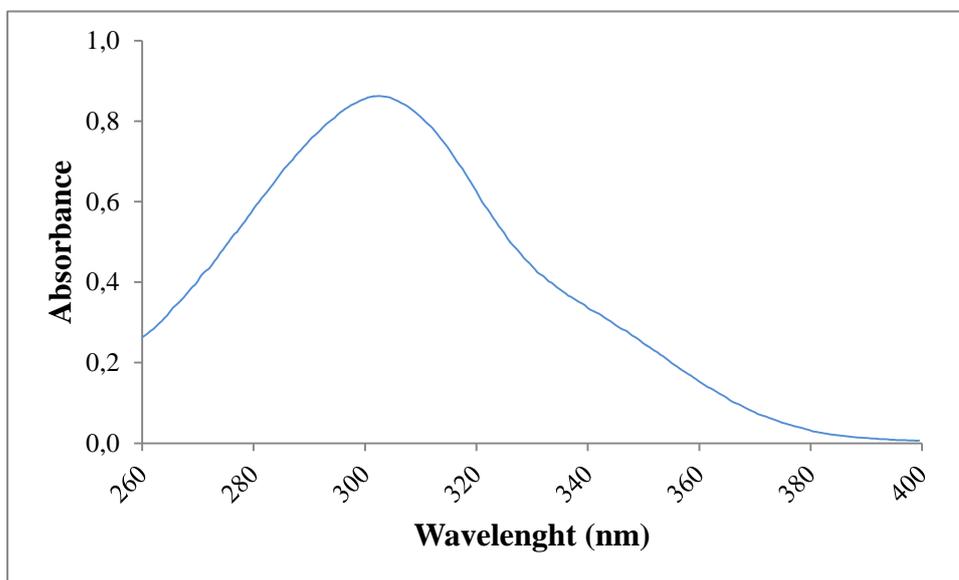
Figure 24. Absorbance profile curve of INHOVA in 100% DMSO between 260 and 400 nm.

After 30 h in 10% DMSO, the absorbance, measured between 250 and 400 nm, showed the appearance of a second band in 268 nm. During 30 h the two bands showed opposite behavior over time. While the band signal at 302 nm decays, the one at 268 nm increases, obtaining an isosbestic point at 272 nm (Figure 25): this indicates the presence of only two absorbent species in equilibrium (Atkins & Shriver, 2006a). This wavelength of absorbance at 268 nm coincides with the *o*-HVa major band absorbance (Figure 25, black curve), suggesting hydrolysis of INHOVA to its precursor, *o*-HVa. The tridimensional profile of INHOVA in 10% DMSO condition is reported in Appendix 1.
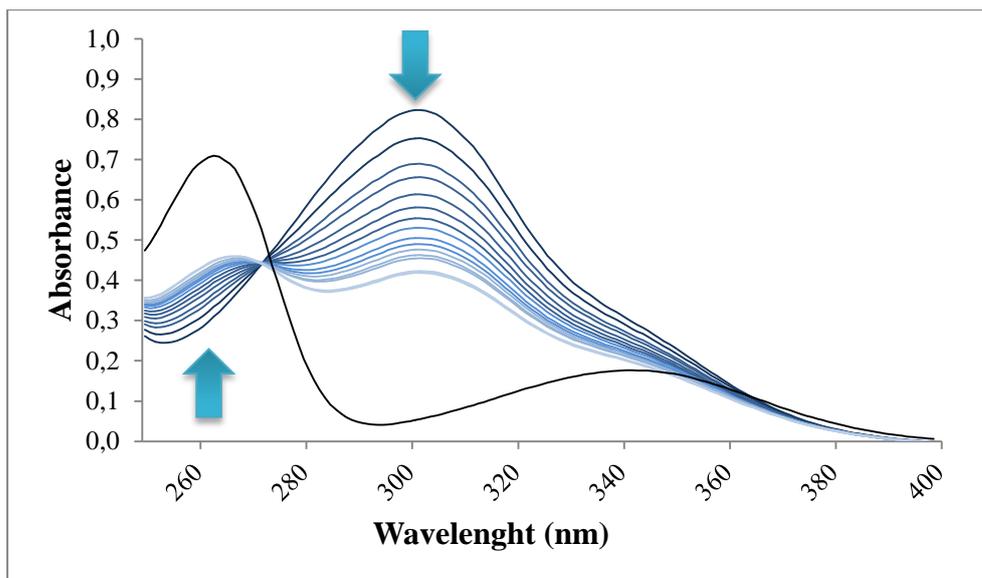
Figure 25. Absorbance profile curves of INHOVA in 10% DMSO over 30 h between 250 and 400 nm. In black is reported the *o*-HVa absorvance profile curve in the same condition. The blue arrows indicate the temporal sampling ordering.

In Figure 26 it is presented the absorbance tracking curve in 30 hours of the two INHOVA major bands in this condition, 302 nm and 268 nm. The absorbance after 30 h for the band at 302 nm showed a total decrease of 49.1%, suggesting the progressive INHOVA hydrolyses, while the absorbance for the band at 268 nm showed a total increase of 24.0%, suggesting the progressive formation of the *o*-HVa. The equilibrium for the hydrolysis / formation reactions is acheaved after about 16h (dashed line in Figure 26). This result indicates that INHOVA does not have the required stability characteristics for the proposed *in vivo* tests conditions.
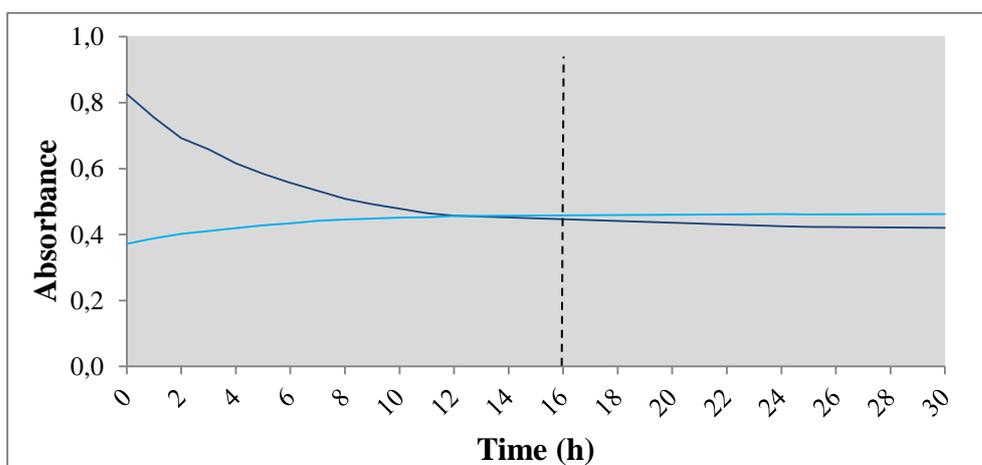
Figure 26. Absorbance tracking curve of INHOVA major bands in 10% DMSO over 30 h. 302 nm is presented in dark blue and 268 nm in light blue. The dashed line indicates the the reaction equilibrium achievement.

After 30 h in 1.0% DMSO, the absorbance profiles data for INHOVA were obtained for each time. The absorbance after 30 h for the 302 nm band showed a decrease 8.2%. Similarly to the other hydrazones, INHOVA, in 1.0% DMSO condition, undergoes hydrolysis and reach the equilibrium already at the time considered as t=0, and after that it remains almost constant over time.

5.3.
In vitro assays

Based on stability studies, only three of the four compounds, namely, INHHQ, HPCIH and H2QBS, continued to be analyzed *in vitro* in order to evaluate their ability to disrupt biometal-Aβ_{1-40} interactions in solution.

The tests were performed through 1D and 2D NMR spectroscopy on different Aβ-Cu^{2+}-MPAC and Aβ-Zn^{2+}-MPAC systems. Results concerning the ligand INHHQ were previously published by the research group of Prof. Rey (Hauser-Davis *et al.*, 2015), and it was used as a model to perform the analyses with HPCIH and H2QBS. Even so, the results obtained for INHHQ are reported below to simplify the comparisons with the other compounds.

Cell studies were also performed for the three compounds in order to assess the cytotoxicity of each one, and to evaluate the capacity of the hydrazonic ligands INHHQ and HPCIH to affect APP pathway.

5.3.1.
Aβ_{1-40} monomers and potential MPACs interaction evaluation

First of all, ^{1}H NMR spectra were obtained for Aβ_{1-40}, both in the absence and in the presence of each potential MPAC, in order to verify if direct interaction between the peptide monomers and the compounds tested exist.

The 8.4-6.2 ppm range was analyzed for Aβ in presence of the potential MPACs to detect the Aβ ^{1}H NMR profile changes. If the changes include vanishing of any of the original signals in the Aβ-free ^{1}H NMR profile, than it is possible to conclude that interaction between Aβ and the compound has occurred. Otherwise, if the Aβ-MPAC ^{1}H NMR profile shows no disappearance of existing signal, but instead the appearance of new compound-specific signals, this behavior suggests that the resulting profile is indeed the superposition of two distinct profiles, one related to Aβ and the other related to the MPAC.

As indicated before, ^{1}H NMR results concerning the Aβ$_{1-40}$-INHHQ system were previously published by our research group, showing no direct interaction between the peptide and the compound (Figure 27) (Hauser-Davis *et al.*, 2015). It is possible to note that the peptide ^{1}H NMR spectrum, in black, coincides with the ^{1}H NMR spectrum of a 1:1 Aβ:INHHQ mixture, in red, with exception of two peaks, at around 7.75 and 7.42 ppm. These are the NMR signals of the ligand, demonstrating the lack of interaction between Aβ, in its soluble monomeric form, and INHHQ (Hauser-Davis *et al.*, 2015).
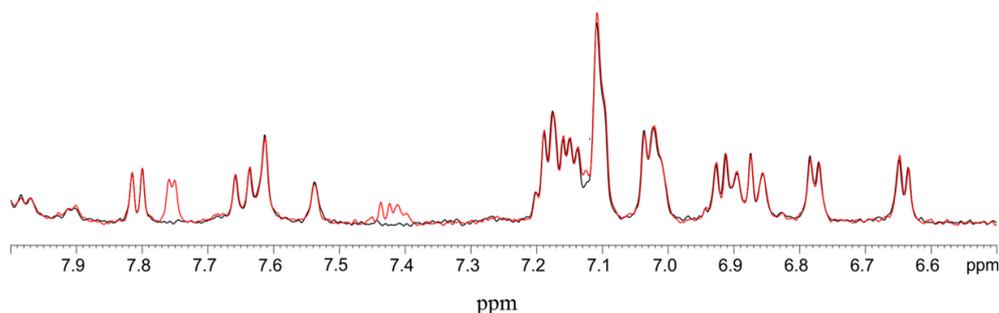
Figure 27. ^{1}H NMR spectra of Aβ (black) and 1:1 Aβ:INHHQ (red). Adapted from Hauser-Davis *et al.*, 2015.

Figure 28 shows that the only differences between the ^{1}H NMR spectrum of Aβ, in black, and that of a 1:1 Aβ:HPCIH mixture, in red, are the characteristic signals of HPCIH, demonstrating the lack of interaction between Aβ monomers and HPCIH.
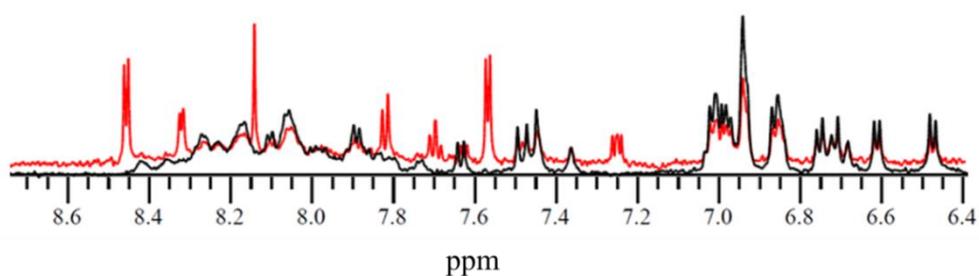
Figure 28. ^{1}H NMR spectra of Aβ (black) and 1:1 Aβ:HPCIH (red).

In Figure 29, it is possible to note that the peptide ^{1}H NMR spectrum, in black, coincides with the ^{1}H NMR spectrum of a 1:1 Aβ:H2QBS mixture, in green, with the addition of the characteristic signals of the ligand. Therefore, there is no interaction between Aβ monomers and H2QBS.
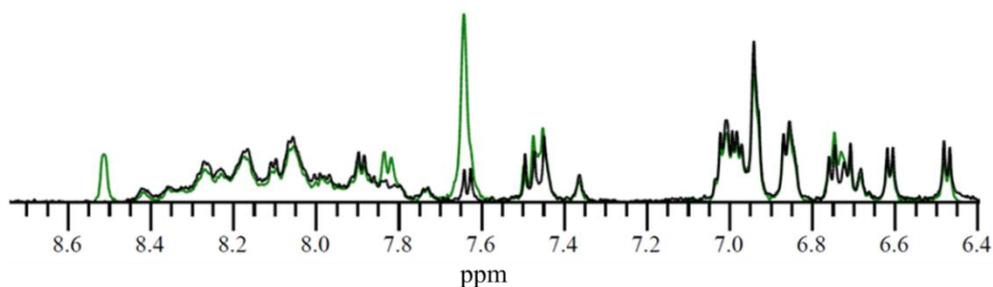
Figure 29. ^{1}H NMR spectra of Aβ (black) and 1:1 Aβ:H2QBS (green).

5.3.2.
Evaluation of potential MPACs capacity to distrupt biometal-Aβ$_{1-40}$ interactions

^{1}H x ^{15}N HSQC contour plots for each Aβ-Cu^{2+}-MPAC and Aβ-Zn^{2+}-MPAC system were obtained to verify the real potential of INHHQ, HPCIH and H2QBS to disrupt biometal-Aβ$_{1-40}$ interactions in solution. Once again, results concerning INHHQ were previously published by our research group (Hauser-Davis *et al.*, 2015), and this compound was used as a model to perform the analyses with HPCIH and H2QBS. The INHHQ results are reported below to simplify the comparisons with the other compounds.

5.3.2.1.
Aβ-Cu-MPAC systems

Figure 30 reports the free peptide bidimensional contour plot profile (in black), and the change in that profile observed when one equivalent of Cu^{2+} is added (in blue). As previously reported (Mekmouche *et al.*, 2005; Hauser-Davis *et al.*, 2015), the spectral changes due to the divalent metals' addition into Aβ samples were centered on histidine residues (His6, His13, and His14), indicating their direct involvement as metal coordinating sites. This causes peak broadenings and losses in signals intensities. ^{1}H x ^{15}N HSQC contour maps of Aβ-Cu^{2+}/Zn^{2+} also show disappearance of the correlation signals related to amino acid residues three-dimensionally close to the histidines, such as those of glutamic acid, glutamine and lysine in positions 11, 15 and 16, respectively, and the intensity decrease of several spots, such as those of tyrosine, glutamic acid and arginine in positions 10, 3 and 5, correspondingly. For these reasons, Figure 30 only shows the bidimensional contour plot of the peptide portion affected by Cu addition.

These are the residues which interact, directly and indirectly, with physiological metal ions. To this solution containing $A\beta_{1-40}:Cu^{2+}$ in the proportion 1:1, were added, in the different experiments described below, increasing concentrations of each MPAC, until the maximum signal recovery was reached.
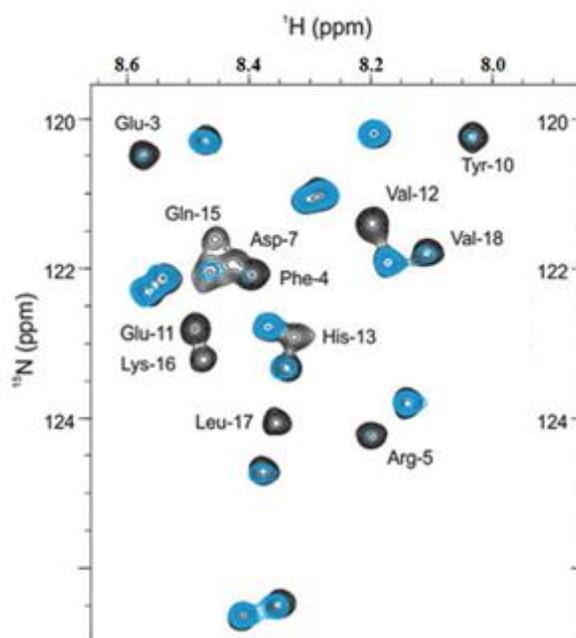
Figure 30. Bidimensional contour plots profile for the $A\beta_{1-40}$-Cu system in ^{1}H x ^{15}N HSQC NMR analysis. $A\beta$ (black) and $A\beta$ with 1 eq of Cu^{2+} (blue). Adapted from Hauser-Davis *et al.*, 2015.

5.3.2.1.1.
$A\beta_{1-40}$-Cu^{2+}-INHHQ system

Figure 31A shows the free peptide bidimensional contour plot profile (in black), and the profile changes when one equivalent of Cu^{2+} was added (in blue). Whereas in Figure 31B it is plotted the obtained profile of the system when five equivalents of INHHQ were added to the solution (grey), evidencing the complete overlap of this plot with the free $A\beta$ one (black) (Hauser-Davis *et al.*, 2015).
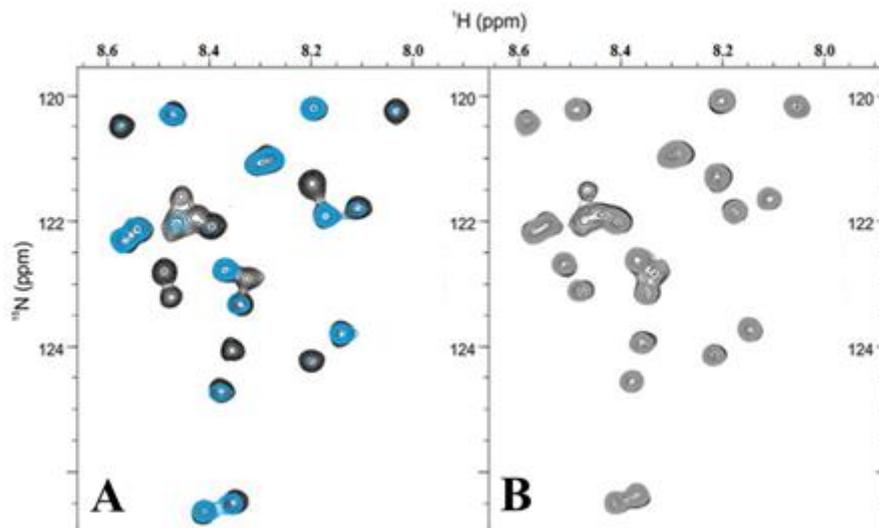
Figure 31. Bidimensional contour plot profile of $A\beta_{1-40}$-Cu^{2+}-INHHQ system in the ^{1}H x ^{15}N HSQC NMR analysis. A) $A\beta$-free profile (black), and the profile of $A\beta$-Cu^{2+} (1:1) (blue). B) $A\beta$-free profile (black), and the profile of $A\beta$-Cu^{2+}-INHHQ (1:1:5) (grey). Adapted from Hauser-Davis *et al.*, 2015.

The recovery profile derived from the treatment of HSQC data is reported as the I/I_0 intensity ratio for each $A\beta$ residue by means of bar graphs. I_0 is the NMR signal intensity of each residue correlation in the absence of metals, which is considered as the 100% intensity level, whereas I is the NMR signal intensity of each residue correlation in the analyzed system during the titrations. Signal recovery may, in some cases, present a value higher than one. This is due to the changes on the bidimensional contour plots shape, which is affected by DMSO increasing in the solution.

In Figure 32 it is shown the I/I_0 intensity ratio profiles for each $A\beta$ residue: blue bars stand for the $A\beta$-Cu^{2+} system without INHHQ; light brown bars, for the $A\beta$-Cu^{2+}-INHHQ system in the 1:1:1 ratio; dark grey bars, for the $A\beta$-Cu^{2+}-INHHQ system in the 1:1:3 ratio; grey bars, for the $A\beta$-Cu^{2+}-INHHQ system in the 1:1:5 ratio and, finally, black bars for the $A\beta$-Cu^{2+}-INHHQ system in the 1:1:10 ratio.
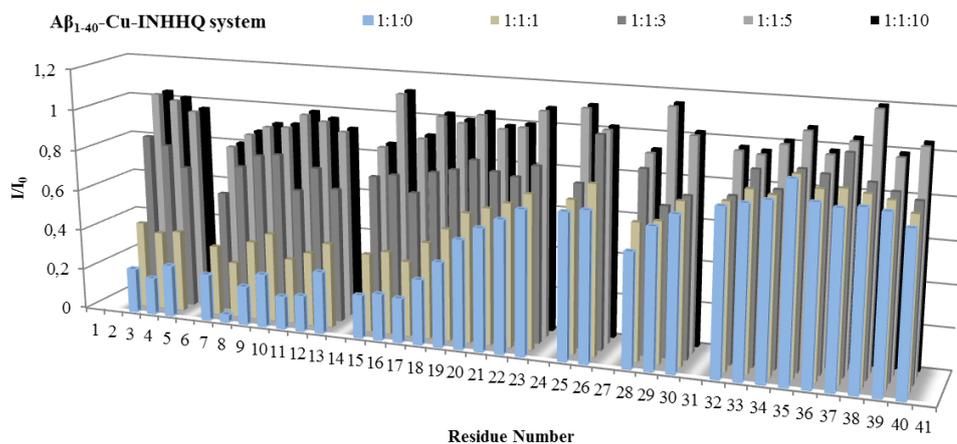
Figure 32. I/I_0 intensity profiles for the Aβ residues in $Aβ_{1-40}$-Cu^{2+}-INHHQ system. Aβ-Cu without INHHQ (blue bars), Aβ-Cu-INHHQ system in with 1, 3, 5 and 10 INHHQ equivalents (soft brown, dark grey, grey and black bars, respectively). Adapted from Hauser-Davis *et al.*, 2015.

The addition of one and three INHHQ equivalents to the system showed a little recovery of the signal (light brown and dark grey bars, respectively), which demonstrate that INHHQ does not work as a traditional, strong chelating agent. Chelating ligands such as EDTA lead to a complete signal intensity recovery with the addition of only one equivalent (Hauser-Davis *et al.*, 2015). Instead of this, five equivalents of INHHQ were necessary to obtain the highest possible recovery (grey bars), which, for some residues, does not represent the complete recovery of the signal. The experiment was continued by adding ten INHHQ equivalents, showing no changes in the intensities ratio profile (black bars). This results suggest that INHHQ could be considered a good candidate for further studies, due to its MPAC-like profile, different from that of a common chelator.

5.3.2.1.2.
$Aβ_{1-40}$-Cu^{2+}-HPCIH system

Figure 33A shows the free peptide bidimensional contour plot profile (black), and the profile changes when one equivalent of Cu^{2+} was added to it (blue). On the other hand, in Figure 33B, it is reported the obtained profile for the system when five equivalents of HPCIH were added to the solution (red), showing an almost complete signal overlap with the contour plot of free Aβ (black).
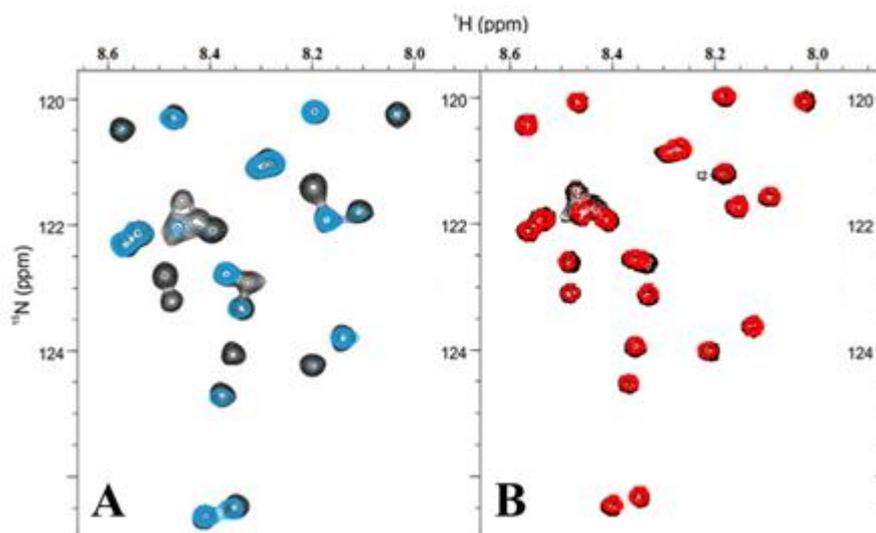
Figure 33. Bidimensional contour plot profile of Aβ$_{1-40}$-Cu^{2+}-HPCIH system in the ^{1}H x ^{15}N HSQC NMR analysis. A) Aβ-free profile (black), and the profile of Aβ-Cu^{2+} (1:1) (blue). B) Aβ-free profile (black), and the profile of Aβ-Cu^{2+}-HPCIH (1:1:5) (red).

In Figure 34 it is shown the I/I$_0$ intensity ratio profiles for each Aβ residue: blue bars stand for the Aβ-Cu^{2+} system without HPCIH; pink bars, for the Aβ-Cu^{2+}-HPCIH system in the 1:1:1 ratio; dark red bars, for the Aβ-Cu^{2+}-HPCIH system in the 1:1:3 ratio; red bars, for the Aβ-Cu^{2+}-HPCIH system in the 1:1:5 ratio and, finally, black bars for the Aβ-Cu^{2+}-HPCIH system in the 1:1:10 ratio.
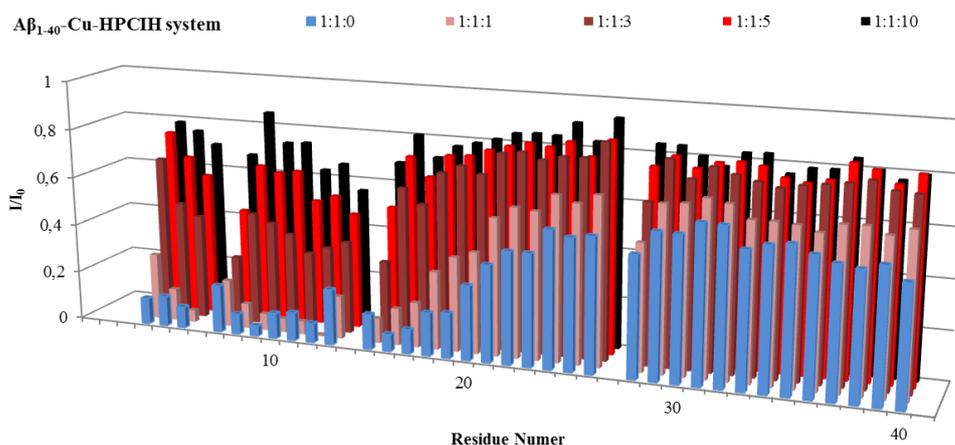
Figure 34. I/I$_0$ intensity profiles for the Aβ residues in Aβ$_{1-40}$-Cu^{2+}-HPCIH system. Aβ-Cu without HPCIH (blue bars), Aβ-Cu-HPCIH system in with 1, 3, 5 and 10 HPCIH equivalents (pink, dark red, red and black bars respectively).

Similarly to the INHHQ system (see section 5.3.2.1.1), the addition of one and three HPCIH equivalents to the system (pink and dark red bars, respectively) showed a low recovery of the total signal, which demonstrates that HPCIH does

not work as a strong chelating agent. Also, in this case, as well as in INHHQ experiments, five ligand equivalents were necessary to obtain the highest possible signal recovery (red bars), which, in this case, does not represent a recovery of 100%. The experiment was followed by the addition of ten equivalents of HPICH, showing no significant changes in the residues profile (black bars), suggesting that five equivalents could be considered already as the resulted in the maximum signal recovery possible with this MPAC.

5.3.2.1.3.
$A\beta_{1-40}$-Cu^{2+}-H2QBS system

Figure 33A shows the free peptide bidimensional contour plot profile (black), and the profile changes when one equivalent of Cu^{2+} was added to it (blue). On the other hand, in Figure 33B, it is reported the obtained profile for the system when three equivalents of H2QBS were added to the solution (green), showing a complete signal overlap with the contour plot of free $A\beta$ (black).
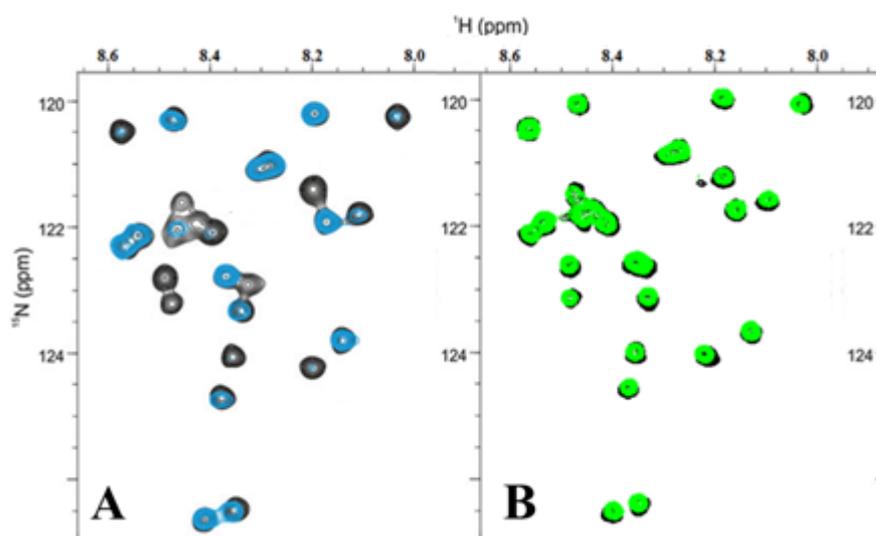
Figure 35. Bidimensional contour plot profile of $A\beta_{1-40}$-Cu^{2+}-H2QBS system in the ^{1}H x ^{15}N HSQC NMR analysis. A) $A\beta$-free profile (black), and the profile of $A\beta$-Cu^{2+} (1:1) (blue). B) $A\beta$-free profile (black), and the profile of $A\beta$-Cu^{2+}-H2QBS (1:1:3) (green).

In Figure 36 it is shown the I/I_0 intensity ratio profiles for each $A\beta$ residue: blue bars represent the $A\beta$-Cu^{2+} system without H2QBS; dark green bars, the $A\beta$-Cu^{2+}-H2QBS system in the 1:1:1 ratio; green bars, the $A\beta$-Cu^{2+}-H2QBS system in the 1:1:3 ratio and, finally, black bars denote the $A\beta$-Cu^{2+}-H2QBS system in the 1:1:5 ratio.
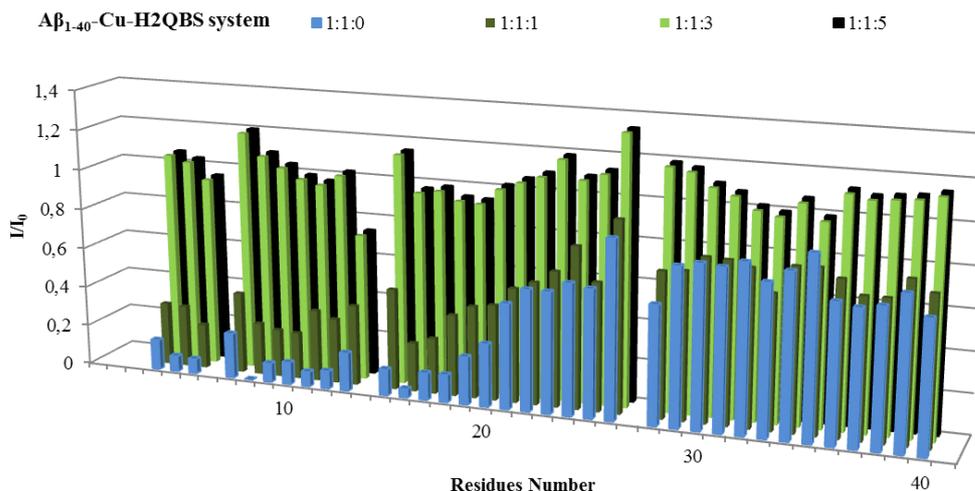
Figure 36 I/I$_0$ intensity profiles for the Aβ residues in Aβ$_{1-40}$-Cu^{2+}-H2QBS system. Aβ-Cu without H2QBS (blue bars), Aβ-Cu-H2QBS system in with 1, 3 and 5 H2QBS equivalents (dark green, green and black bars respectively).

Similarly to the former two systems (see sections 5.3.2.1.1 and 5.3.2.1.2), the addition of one H2QBS equivalent to the system showed a low recovery of the total signal (dark green bars). However, different from the former cases, three equivalents of H2QBS are already enough to obtain the maximum signal recovery (green bars), and the addition of two more equivalents (black bars) does not change the recovery profile. These results point to H2QBS as possessing a higher affinity for Cu^{2+} ions than INHHQ and HPCIH in Aβ$_{1-40}$-Cu^{2+}-MPAC system.

Figure 37 summarizes the different profiles for the three ligands, *i.e.*, INHHQ, HPCIH and H2QBS, compared with a strong chelant, EDTA, displayed as the signal recovery average, obtained as the mean of the intensity signal recovery of each evaluated amino acid, in function of the number of equivalents of each compound. The profiles for the three compounds are very different from EDTA profile, where one equivalent of the compound is enough to obtain the full signal recovery for all the residues. The results suggest that H2QBS has strongest affinity for copper than the other two compounds. Also, a more similar profile between INHHQ and HPCIH, than between INHHQ and H2QBS, is observed, suggesting that, for this sistem, in metal complexation, INHHQ acts similarly to HPCIH, probably with the involvement of the hydrazonic moiety, and with the phenol group not taking part in coordination.
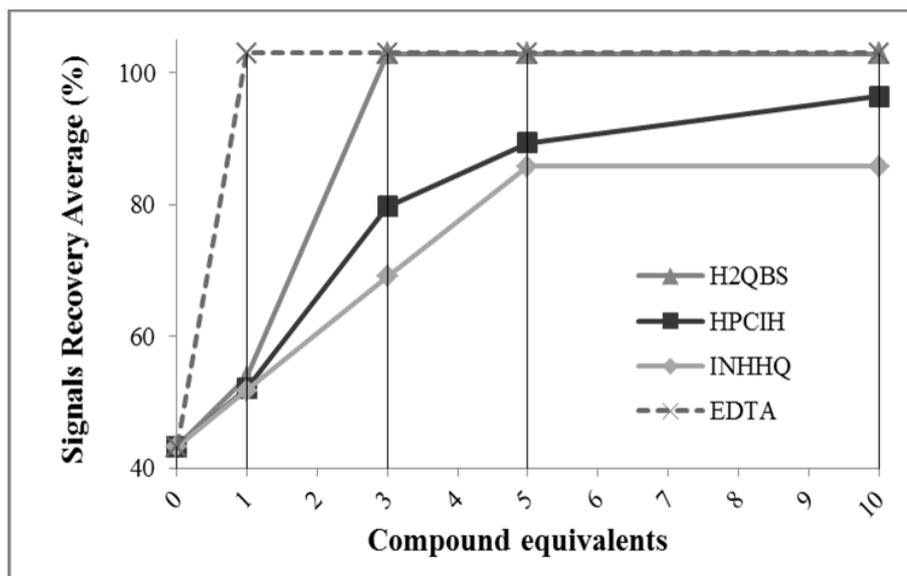
Figure 37. INHHQ, HPCIH, H2QBS and EDTA NMR signal recovery profiles in $A\beta_{1-40}$-Cu^{2+}-MPAC systems.

5.3.2.2.
Aβ-Zn^{2+}-MPAC systems

For the Aβ-Zn^{2+}-MPAC system, only the most promising hydrazonic compounds, namely, INHHQ and HPCIH, were tested, confirming the same recovery pattern observed in the Aβ-Cu^{2+}-MPAC systems.

^{1}H x ^{15}N HSQC NMR for $A\beta_{1-40}$-Zn^{2+}-INHHQ system was previously published by our research group showing, once again, that INHHQ does not work as strong chelating agent (Hauser-Davis *et al.*, 2015). Similarly to the $A\beta_{1-40}$-Cu^{2+}-INHHQ system (see 5.3.2.1.1), five equivalents of INHHQ were necessary to obtain the highest possible recovery (Hauser-Davis *et al.*, 2015). More details in

Appendix **2**.

Similarly to Aβ-Cu^{2+}-HPCIH system (see section 5.3.2.1.2), the addition of five equivalent shows the maximum recovery achieved in this system, and the addition of 10 equivalents showed no difference at all. More detail in Appendix 3.

These results suggest that the compounds interfere with metal-protein interactions by a mechanism that probably involves metal sequestration, since there is no direct interaction between Aβ$_{1-40}$ and the compounds (see section: 5.3.1). These results are not unexpected, due to the dissociation constant (K_d) value for Aβ$_{1-40}$-Zn^{2+} referred as about 10^5 L mol^{-1} (Tõugu *et al.*, 2008), which are about the same order of magnitude of the K_d for INHHQ-Zn^{2+} (about 5.2 10^5 L mol^{-1})(De Freitas, 2014), and the K_d for HPCIH-Zn^{2+} (about 1.4 10^5 L mol^{-1}) (Cukierman, 2016).

More specific, the obtained data for the two systems, Aβ$_{1-40}$-Cu^{2+}/Zn^{2+}-MPAC, for INHHQ and HPCIH, suggest that both are a good candidate for further studies, due to their profile, more similar to MPAC than a chelating agent.

5.3.3.
Cell studies

Cell studies were performed in order to evaluate the cytotoxicity of INHHQ, HPCIH and H2QBS, in three different cells lines. The most promising compounds were also evaluated for their potential capacity to affect APP pathway, by proteomic analyses of exposed SW APP mutant HEK 293 cells line.

5.3.3.1.
Cytotoxicity

5.3.3.1.1.
SH-SY5Y

The cytotoxicity test results in vitality profile data were obtained as percentage of vitality in function of each compound concentration. All the data are reported in Figure 38, where statistical differences are marked with symbol (*). This cell line did not show high sensitivity to DMSO, showing always no significant differences between the control group and the group treated with the vehicle.

For SH-SY5Y cell line results show that three compounds seem to have similar behavior and all the tolerance and the toxic doses were defined in 100 and 250 μmol L^{-1} respectively, for all the copounds. No impoving dose where observed for these cells line among the tested doses.

The IC$_{50}$ are calculed in 695, 569 and 504 μmol L^{-1} for INHHQ, HPCIH and H2QBS, respectively, suggesting that H2QBS is the most toxic compound for this cells line.
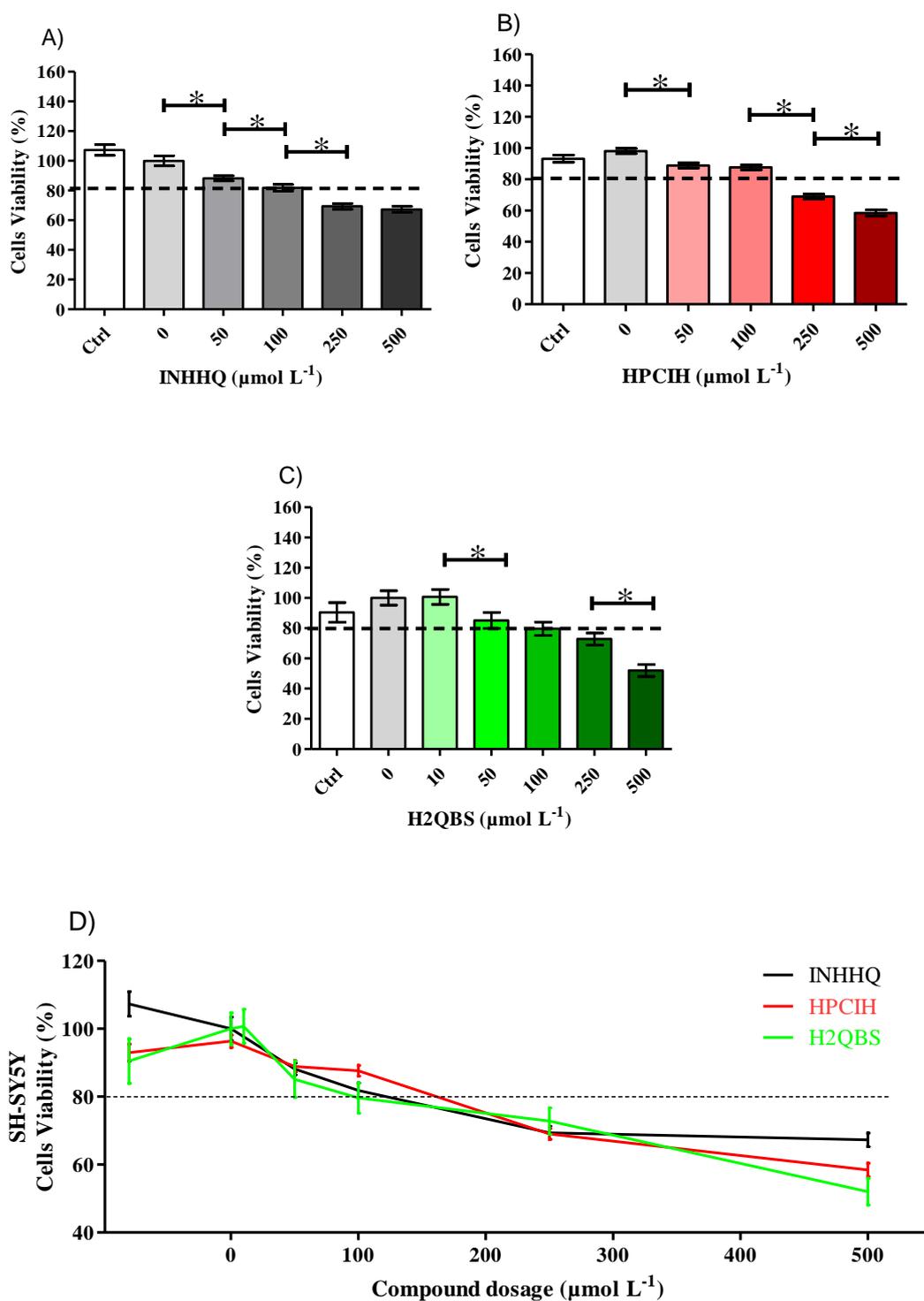
Figure 38. Cytotoxicity in SH-SY5Y cells line. A) cells viability for increasing concentration of INHHQ; B) cells viability for increasing concentration of HPCIH; C) cells viability for increasing concentration of H2QBS and D) cells viability curves for increasing concentration of each compound. All data where reported as mean and error bars. The dashed line indicates the value of 80% (*p<0.05).

5.3.3.1.2.
SW APP HEK 293

The cytotoxicity test results in vitality profile data were obtained as percentage of vitality in function of each compound concentration for SW APP HEK 293 cells line. All the data are reported in Figure 39, where statistical differences are marked with symbol (*). This cell line show high sensitivity to DMSO, resulting always in significant difference between the control group and the group treated with the vehicle.

The improving, tolerance and toxic doses INHHQ experiments was fixed in 10, 100 and 250 µmol L^{-1} in 1% DMSO respectively; for HPCIH experiment were fixed in 100, 10 and 250 µmol L^{-1} in 1% DMSO respectively; for H2QBS experiments, the tolerance and toxic doses were fixed in 50 and 250 µmol L^{-1} in 1% DMSO respectively, improving dose was no observed among this compound tested doses in this cells line.

The IC_{50} are calculated in 698, 481 and 1384 µmol L^{-1} for INHHQ, HPCIH and H2QBS, respectively.
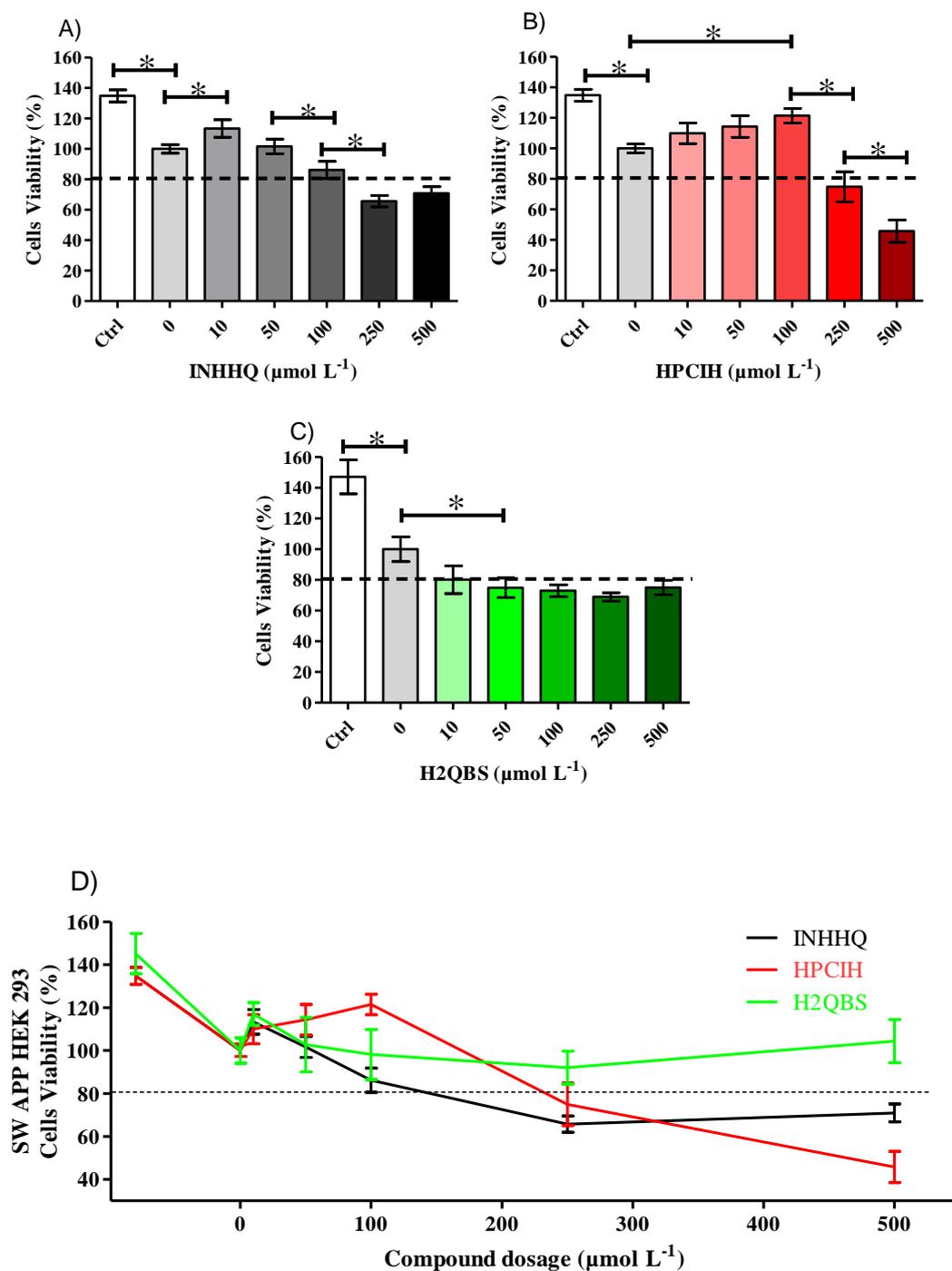
Figure 39. Cytotoxicity in SW APP HEK 293 cells line. A) cells viability for increasing concentration of INHHQ; B) cells viability for increasing concentration of HPCIH; C) cells viability for increasing concentration of H2QBS and D) cells viability curves for increasing concentration of each compound. All data where reported as mean and error bars. The dashed line indicates the value of 80% (*p<0.05).

5.3.3.1.3.
HEK 293

The cytotoxicity test results in vitality profile data were obtained as percentage of vitality in function of each compound concentration for SW APP HEK 293 cells line. All the data are reported in Figure 40, where statistical differences are marked with symbol (*). This cell line show high sensitivity to DMSO, resulting always in significant difference between the control group and the group treated with the vehicle. This similarity between HEK 293 and SW APP HEK 293 is expected, since the basic difference between the two cells lines is the APP overexpression, which is not involved in the DMSO toxicity mechanisms.

The improving dose was not observed among the tested doses in this cells line for the three compounds. The toxicity profiles of INHHQ and H2QBS result to be similar, with tolerated and toxic doses fived in 10 and 50 μmol L^{-1} in 1% DMSO respectively; for HPCIH experiment were fixed in 100 and 250 μmol L^{-1} in 1% DMSO respectively.

The IC$_{50}$ are calculated in 537, 797 and 589 μmol L^{-1} for INHHQ, HPCIH and H2QBS, respectively. In this scenario, INHHQ and H2QBS show very similar trend, with INHHQ showing higher toxicity than HPCIH. Recall that two most toxic compounds for this line share the hydroxyl quinolinic portion

These results, together with the cytotoxicity results for SW APP HEK 293 cells lines, suggest that INHHQ toxicity is related to APP SW expression. The only difference between the two cells line is the presence of mutated APP, which is normal in HEK 293 cells line (see section 2.3.2.1). Apparently, the lack of overexpression of APP increases INHHQ toxicity, suggesting some synergic effect between the compound and the overexpressed APP pathway. These effects are evaluated by proteomic studies (see section: 5.3.3.2).
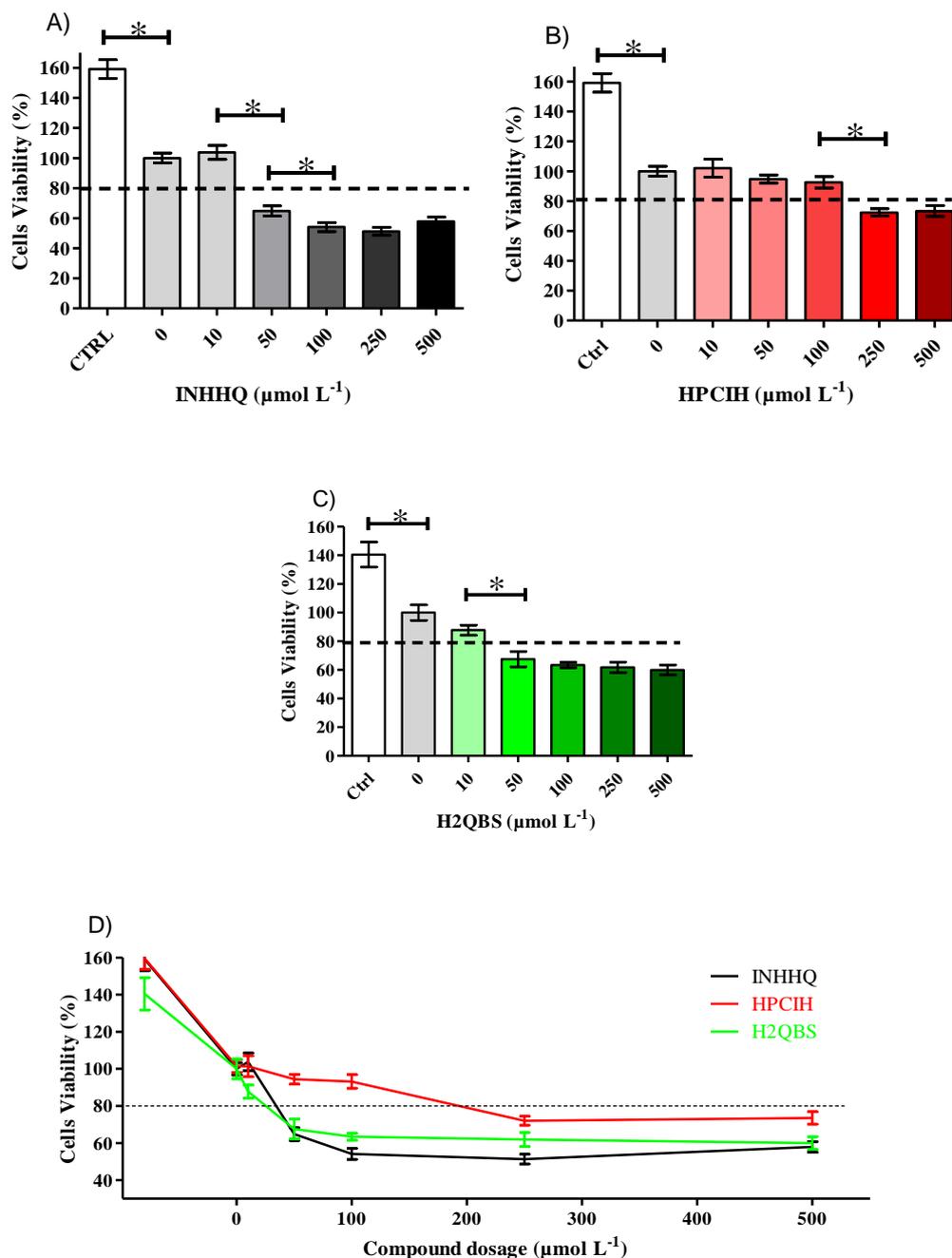
Figure 40. Cytotoxicity in HEK 293 cells line. A) cells viability for increasing concentration of INHHQ; B) cells viability for increasing concentration of HPCIH; C) cells viability for increasing concentration of H2QBS and D) cells viability curves for increasing concentration of each compound. All data where reported as mean and error bars. The dashed line indicates the value of 80% (*$p < 0.05$).

In Table 2 all the cytotoxicity results presented above are summarized. Table rows stand for each of the four relevant cytotoxic parameters (corresponding to the improving, tolerated, toxic and IC$_{50}$ doses) for all the compounds. Table columns stand for the cell lines. The cases in which the dosages were not found are marked as "not observed". Data shown in bold

represent the most toxic value for each parameter. As it can be seen, H2QBS is the compound that has more toxic parameters, globally, and it seems to be is the most toxic for all parameters related to SW APP HEK 293 cells line, the one that express APP mutation. This result, suggests its inadequacy for proteomic studies, at least until its mechanism of action be studied in more details. INHHQ and HPCIH have the lower toxicity for SW APP HEK 293 cells line, and their cytotoxicity appears to be APP mutation-related, since the two compounds have different cytotoxicity profile for HEK 293 cells line. They seem to be the best candidates to have their potential to interfere with the APP processing pathway evaluated by proteomic screening.

Table 2. Cytotoxicity results for the three compounds in the three cell lines.

		SH-SY5Y	SW APP HEK 293	HEK 293
Improving dose (μmol L^{-1})	INHHQ	not observed	10	not observed
	HPCIH	not observed	100	not observed
	H2QBS	not observed	**not observed**	not observed
Tolerated dose (μmol L^{-1})	INHHQ	100	100	**10**
	HPCIH	100	250	100
	H2QBS	100	**50**	**10**
Toxic dose (μmol L^{-1})	INHHQ	250	**250**	**50**
	HPCIH	250	500	250
	H2QBS	250	not observed	**50**
IC$_{50}$ (μmol L^{-1})	INHHQ	695	698	**537**
	HPCIH	569	**481**	797
	H2QBS	**504**	1384	589

5.3.3.2.
Proteomic screening

Since INHHQ and HPCIH do not directly interact with Aβ (see section: 5.3.1) and their cytotoxicity appear to be APP mutation-related (see section: 5.3.3.1), proteomic screening experiments were performed in order to evaluate their ability to interfere with the APP processing pathway, responsible for Aβ production (see section: 1.1.2.2). The intracellular levels of APP, BACE-1, Aβ and α and β CTF portions (Figure 3) were determined in SW APP HEK 293 cells line, which express SW APP (see section: 2.3.2.1), through SDS-PAGE and western blot experiments. The cells were exposed, over 24 h to the compounds in independent triplicate experiments. Three doses for each compound were used, namely improving, tolerated and the toxic concentrations, according to previous experiments (see section: 5.3.3.1.2). All the data were normalized to the value related to cells treated only with vehicle (complete medium with 1% DMSO, without the compound), in order to evaluate the statistic variations depending exclusively on the compounds presence and not on DMSO exposure.

Figure 41 shows the APP full length normalized concentration as a function of the compounds doses. It is possible to note that, in INHHQ exposure exepriments, full-length APP concentration shows significant statistic difference comparing to 0 µmol L^{-1} INHHQ only when 500 µmol L^{-1} of compound are added to the medium, marked in Figure 41A with the symbol (*). This difference results in increase of APP concentration, which may suggest increase of its synthesis or decrease of APP digestion. However, as previously seen, this concentration of INHHQ is already considered toxic to this cell line, so the intrinsic compound toxicity may have indirectly affected the APP processing mechanism. No statistical differences were detected for HPCIH exposure experiments (Figure 41B).
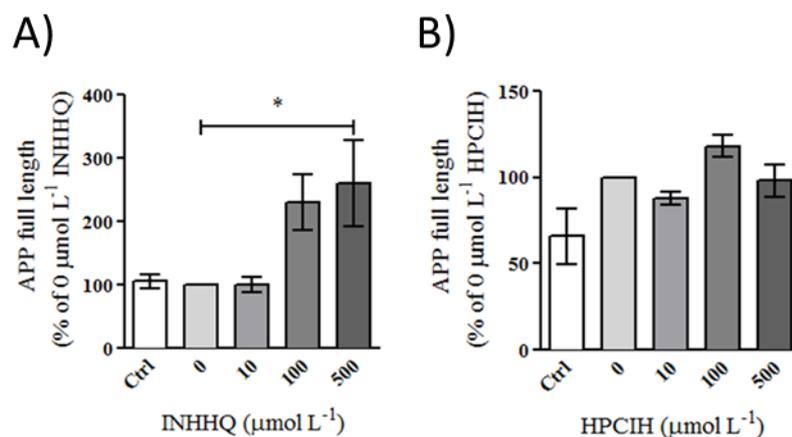
Figure 41. Levels of APP full length in SW APP HEK 293 cells line after exposure. A) INHHQ and B) HPCIH exposure triplicates, respectively. Graph of means ± standard deviation of all condition, (*p<0.05).

Figure 42 shows the amyloidogenic secretase BACE-1 normalized concentration as a function of the compounds doses. It is possible to note thatit is possible to note that BACE-1 concentration shows no significant statistic difference with 0 μmol L^{-1} when the compounds are added to the medium, until the toxic concentration is reached. These data suggest that the compounds do not affect significatively BACE-1 expression, neither in toxic condition.
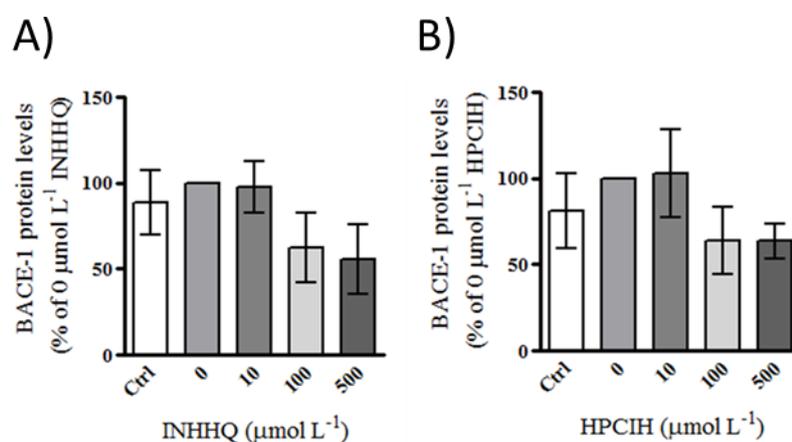
Figure 42. Levels of BACE-1 in SW APP HEK 293 cells line after exposure. A) INHHQ and B) HPCIH exposure triplicates, respectively. Graph of means ± standard deviation of all condition, (*p<0.05).

Figure 43 shows the Aβ intracellular oligomers normalized concentration as a function of the compounds doses. It is possible to note that Aβ intracellular oligomers concentration shows no significant statistic difference with 0 μmol L^{-1} when the compounds are added to the medium, until the toxic concentration is reached. These data suggest that the compound does not affect the capacity of the cell to secrete Aβ intracellular oligomers, neither in toxic condition.
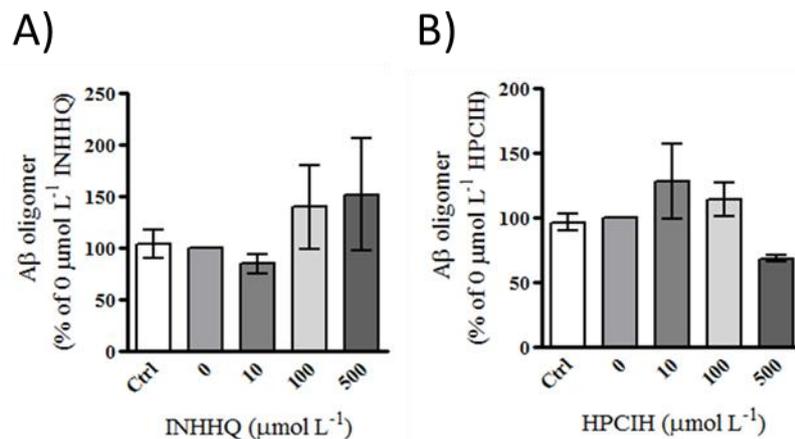
Figure 43. Levels of Aβ intracellular oligomers in SW APP HEK 293 cells line after exposure. A) INHHQ and B) HPCIH exposure triplicates, respectively. Graph of means ± standard deviation of all condition, (*p<0.05).

Figure 44 shows the α-CTF portion normalized concentration as a function of the compounds doses. It is possible to note that the α-CTF portion concentration shows no significant statistic difference with 0 μmol L^{-1} when the compounds are added to the medium, until the toxic concentration is reached. These data suggest that the compounds do not affect the non-amyloidogenic APP pathway on the α-CTF production step.
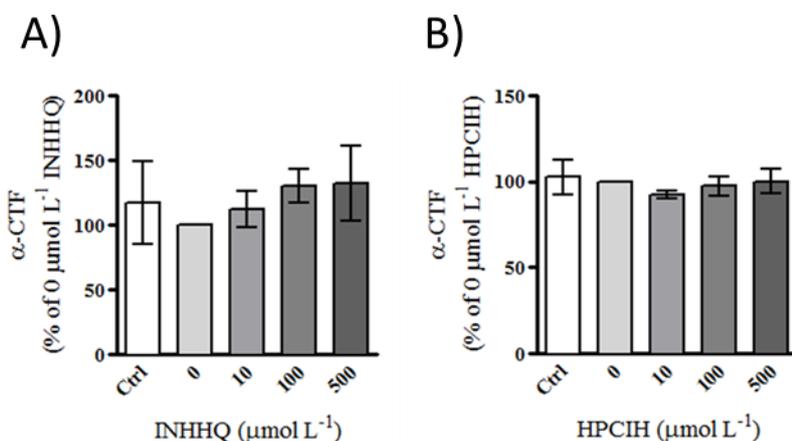
Figure 44. Levels of α-CTF portion in in SW APP HEK 293 cells line after exposure. A) INHHQ and B) HPCIH exposure triplicates, respectively. Graph of means ± standard deviation of all condition, (*p<0.05).

Figure 45 shows the β-CTF portion normalized concentration as a function of the compounds doses. Itis possible to note that β-CTF portion concentration shows significant statistic difference with 0 μmol L^{-1} INHHQ starting when 100 μmol L^{-1} of INHHQ are added to the medium, marked in Figure 45A with the symbol (*).

Also in HPCIH exposure the β-CTF portion concentration shows significant statistic difference with 0 µmol L^{-1} HPCIH when 500 µmol L^{-1} of HPCIH are added to the medium, this difference is marked in Figure 45B with the symbol (*).

These difference results in decrease of β-CTF portion concentration, which, along with other results, suggest that INHHQ and HPCIH, , could affect the activity of γ secretases, which are the responsible enzymes for β-CTF portion cleavage.

This class of enzymes is modulated by physiological metals (Hou *et al.*, 2015; Gerber *et al.*, 2017). However, as previously seen, the 100 µmol L^{-1} concentration of INHHQ correspond to the tolerance limit of this cell line and the 500 µmol L^{-1} concentration of HPCIH is toxic to this cell line (see section: 5.3.3.1.2), so the intrinsic compound cytoxicity may have indirectly affected the APP processing mechanism in this step., as well as in APP full length first digestion in INHHQ case.
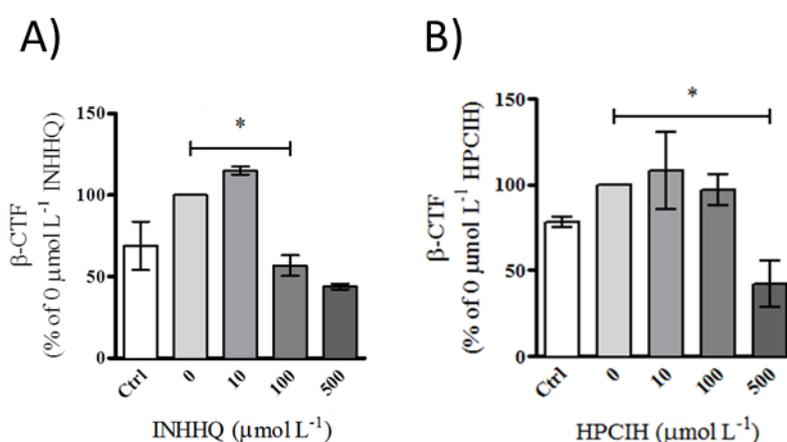

Figure 45. Levels of β-CTF portion in SW APP HEK 293 cells line after exposure. A) INHHQ and B) HPCIH exposure triplicates, respectively. Graph of means ± standard deviation of all condition, (*p<0.05).

The results presented herein suggest that INHHQ and HPCIH possess intracellular activity; however, the potential interaction of the compounds with secretases still needs further investigations.

5.4.
In vivo studies

In vivo studies were performed in order to assess the acute toxicity in healthy rats, by IP overdose injection, and to evaluate behavioral changes, such as

anxiety, fear and memory patterns, in healthy and AD model mice (effectiveness studies) with the IP injection of an innocuous dose of the most promising compound, *i.e.*, INHHQ.

5.4.1.
Acute toxicity assays

Adult male Wistar rats injected intraperitoneally with 200 mg kg^{-1} of each one of the three compounds, namely, INHHQ, HPCIH and H2QBS, showed no lethality and no behavioral changes within 72 h of observation between injection and sacrifice. In order to better establish the acute toxicity of the MPACs, some biochemical parameters were analyzed. Since most of data reported in here did not present a parametric distribution, all the data were treated as non-parametric, in order to allow comparing them.

The animals were weighted prior to IP injection, in order to calculate the volume of compound to be injected. The distribution of the weight of the animals showed not statistical difference among all the groups (Figure 46).
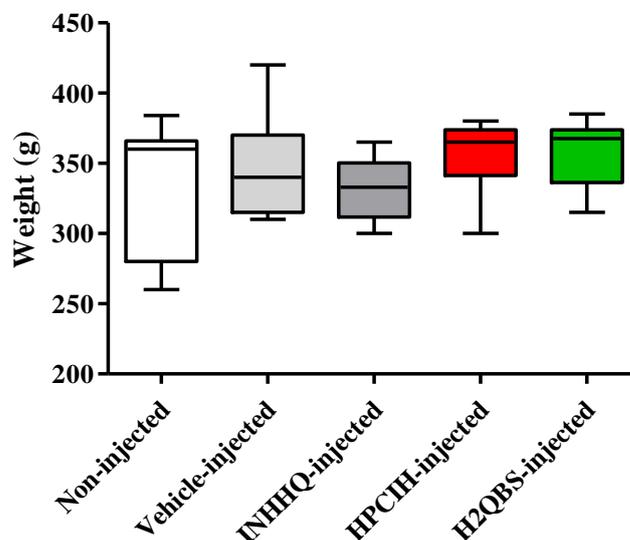
Figure 46. Whiskers Graph distribution of rats weight.

As no lethality was observed in any of the group over 72 h, the animals were sacrificed after this interval. Subsequently, the brain, liver, kidneys and heart, were removed from the animals, showed no significant macroscopic abnormalities in terms of morphology.

The test for organs weight showed statistical difference between the liver weight medians of the vehicle-injected and INHHQ-injected animals (Figure 47B) and between the heart weight medians of the vehicle-injected and INHHQ-injected (Figure 47D) rats. No statistical differences were detected between the brain and kidneys weight medians (Figure 47A and Figure 47C).
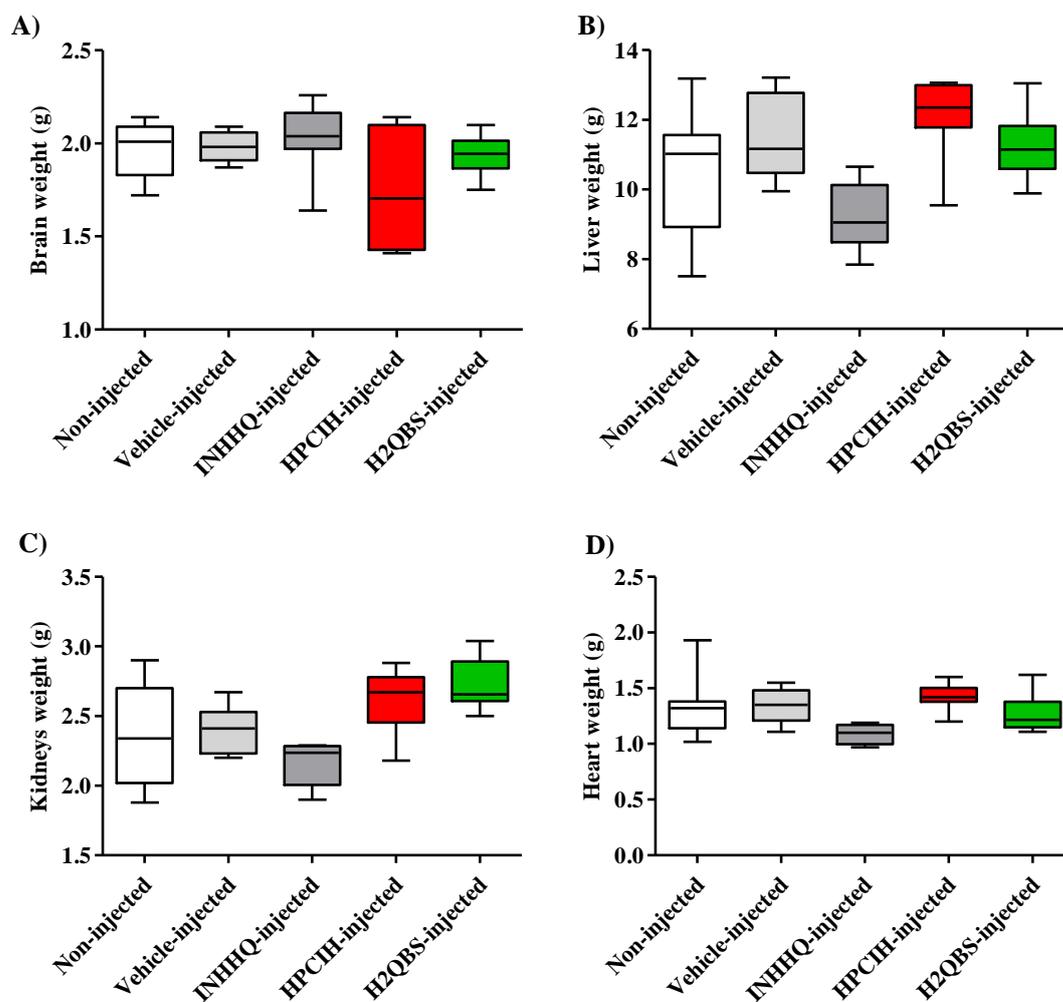
Figure 47. Whiskers Graph distribution of organs weight. A) Brain; B) Liver, C) Kidneys and D) Heart.

5.4.1.1.
Oxidative stress evaluation

GSH levels were determined as an oxidative stress parameter in brain and liver, immediately after the sacrifice, in order to reduce the oxidation of this tripeptide.

Figure 48 shows the GSH levels for each group of injection in brain and liver. GSH quantification results showed no statistical differences in brain (Figure 48A); however, a statistically relevant difference between the liver GSH levels medians of vehicle-injected and HPCIH-injected animals was observed (Figure 48B).
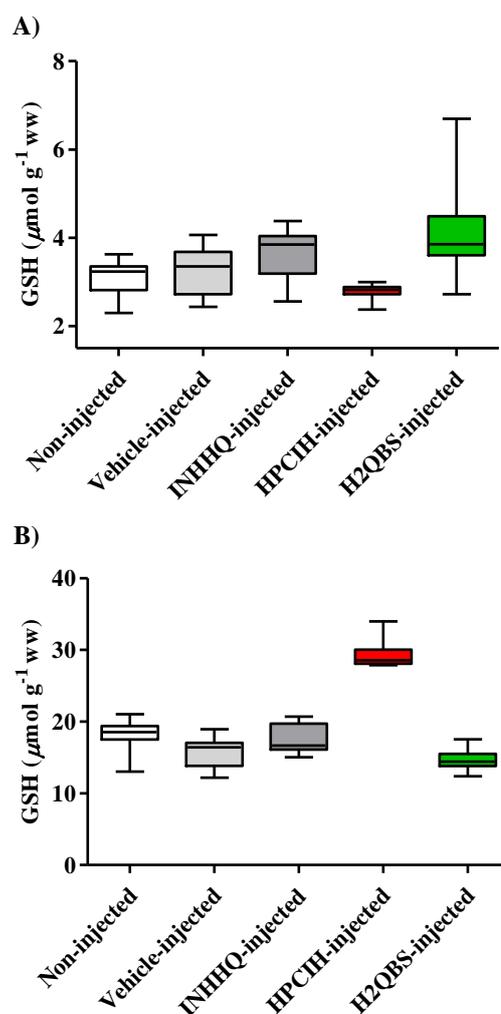
Figure 48. Whiskers Graph distribution of GSH levels. A) Brain; B) Liver. (ww= wet weight of the organ).

5.4.1.2.
Metals quantification

The objective of employing MPACs is the redistribution of the physiological metals that are poorly distributed in most amyloidogenic diseases (see section 1.4.6). For this proposal, concentrations of the physiological metals copper, iron and zinc were evaluated in the organs removed, by ICP-MS, after lyophilization.

5.4.1.2.1.
Copper

Figure 49 shows Cu levels for each group of injection in different organs. The test for Cu concentration levels showed a small statistical difference between the brain medians of non-injected and INHHQ-injected animals and between the vehicle-injected and H2QBS-injected groups (Figure 49A). Differences were also detected between liver Cu concentration medians of the vehicle-injected and H2QBS-injected animals (Figure 49B). In heart, Cu concentration levels, also showed a statistically relevant difference between medians of non-injected and HPCIH- and H2QBS-injected, as well as between vehicle-injected and H2QBS-injected groups (Figure 49D). No statistical differences were detected in the kidneys' Cu levels (Figure 49C).

The homeostatic regulation of this metal is made in the liver, which appears to be affected especially in the condition of H2QBS overdose, which make it the most toxic compound concerning these parameters, and suggests a higher affinity for Cu than those of INHHQ and HPCIH, as observed in HSQC experiments (Linder *et al.*, 1998).
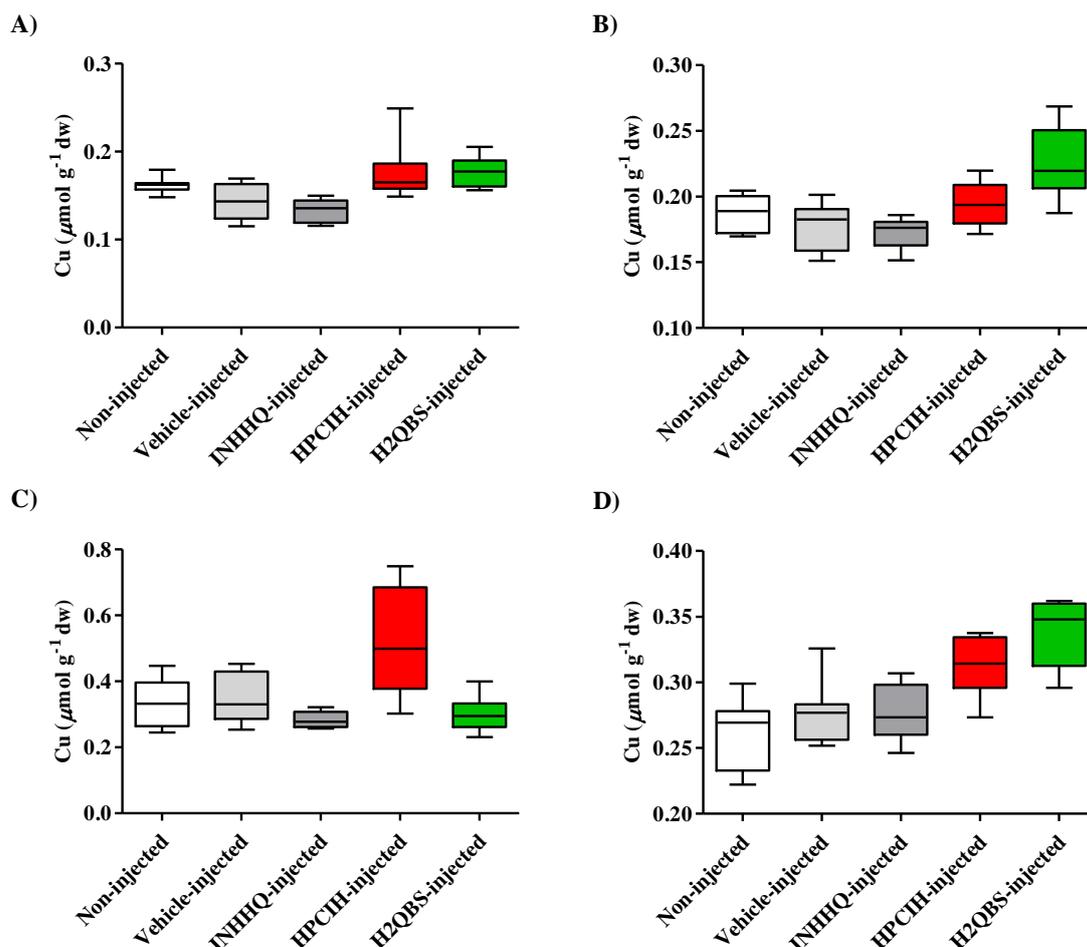
Figure 49. Whiskers Graph distribution of Cu levels. A) Brain; B) Liver, C) Kidneys and D) Heart. (dw= dry weight of the organ).

5.4.1.2.2.
Iron

Figure 50 shows Fe levels for each group of injection in different organs. The test for Fe concentration showed significant statistical differences between the brain medians of non-injected and H2QBS-injected animals, and between the vehicle-injected and INHHQ and H2QBS-injected groups (Figure 50A). Differences were detected between the liver Fe concentration medians of non-injected and vehicle and H2QBS-injected and both non-injected and vehicle-injected groups (Figure 50B). No statistical differences were detected in kidneys and hearth Fe levels (Figure 50C and 72D).

The results for this parameter confirm the hepatotoxicity of DMSO (Mathew *et al.*, 1980), due to statistical significant differences between non-

injected and vehicle-injected groups. The most remarkable result of this analysis is the capacity of H2QBS, at least when present at high doses, to displace Fe from liver to brain, even in a healthy condition, *i.e.*, in conditions where metal homeostasis is not unbalanced, suggesting that, as stated above, it does not seem appropriate as an MPAC.
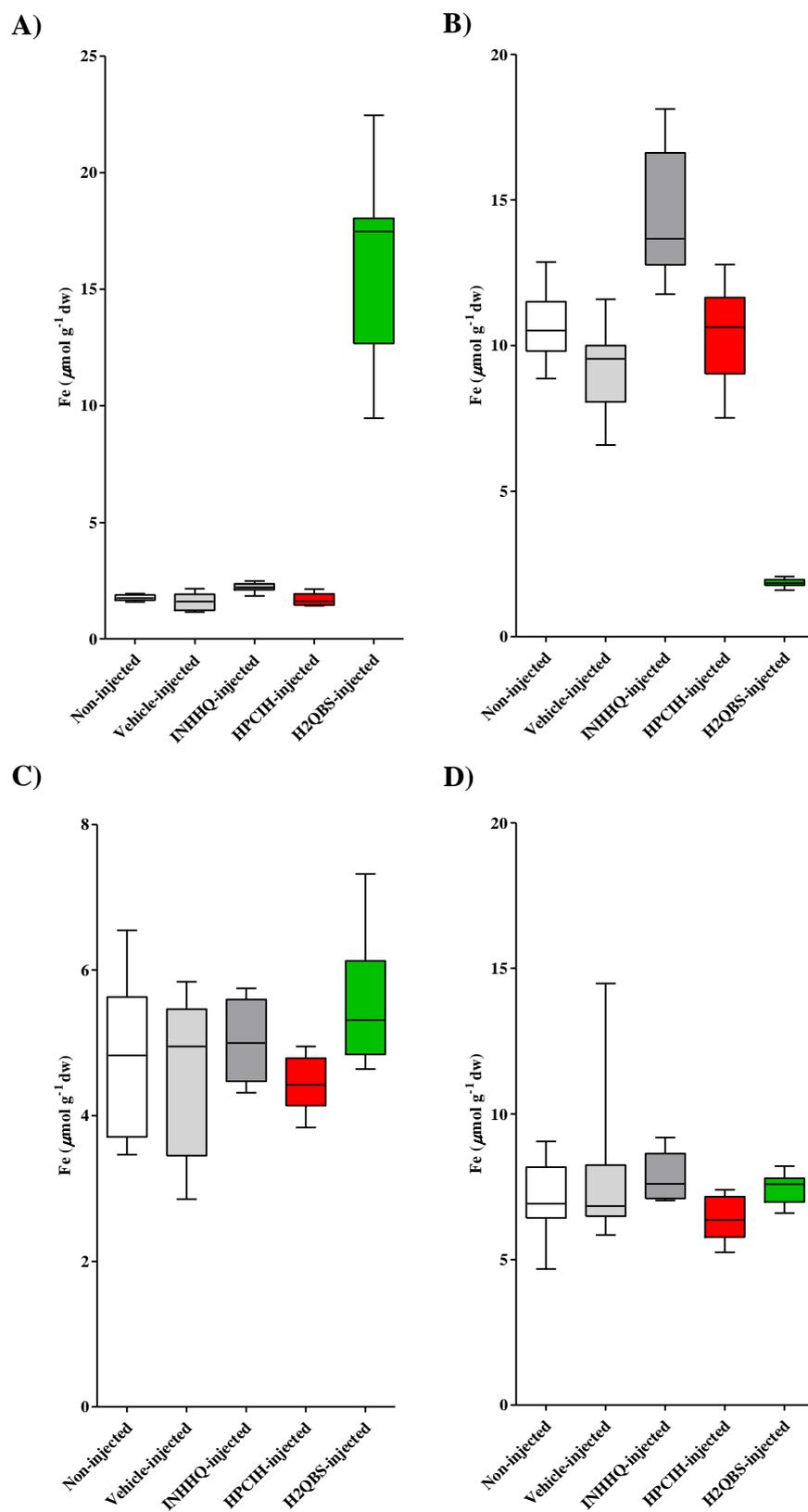
Figure 50. Whiskers Graph distribution of Fe levels. A) Brain; B) Liver, C) Kidneys and D) Heart. (dw= dry weight of the organ).

5.4.1.2.3.
Zinc

Figure 51 shows Zn levels for the each group of injection in different organs. The test for Zn concentration showed statistical differences between brain and liver medians of H2QBS-injected and both non-injected and vehicle-injected groups, as well as between the vehicle-injected and INHHQ-injected animals (Figure 51A and Figure 51B). Differences were also detected in kidneys between the INHHQ-injected and both non-injected and vehicle-injected groups (Figure 51C). Heart Zn concentration levels medians of the vehicle-injected and INHHQ-injected animals showed a small significant difference as well (Figure 51D).

A)

B)

C)

D)
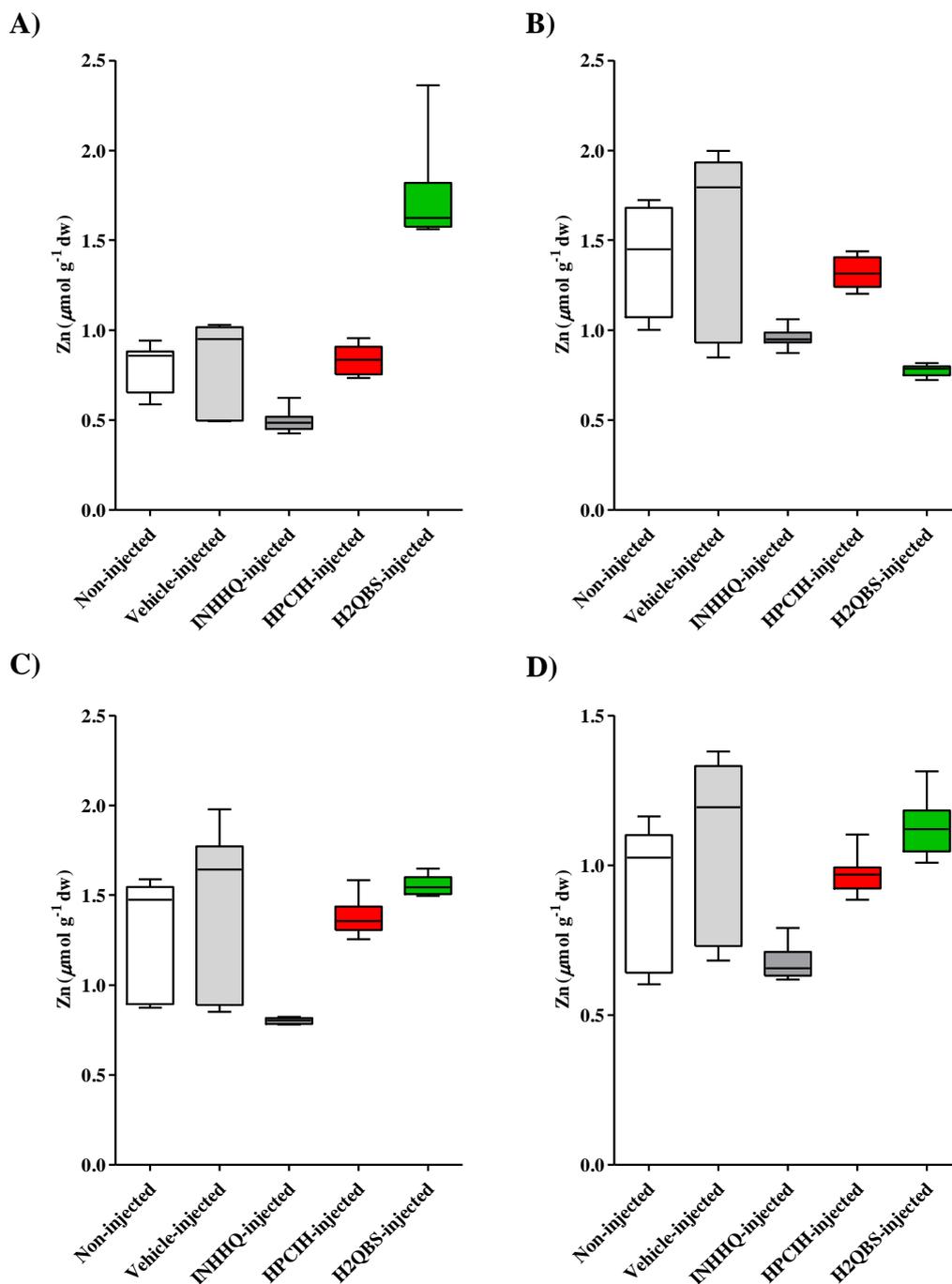
Figure 51. Whiskers Graph distribution of Zn levels. A) Brain; B) Liver, C) Kidneys and D) Heart. (dw= dry weight of the organ).

Table 3 summarizes all the parameters analyzed for acute toxicity, reporting all significant statistic differences discussed above. It becomes clear that H2QBS is the compound that most appears in the table, and the observation of the magnitude of the differences for each parameters, especially for zinc and iron

brain concentrations, suggests that it possesses a high capacity to displace metals in rats, when high doses of the compound are applied. This result, together with the ^{1}H x ^{15}N HSQC results derived from the Aβ-Cu^{2+}-H2QBS system, strongly suggests its inadequacy as a "Metal-Protein Attenuating Compound", until its mechanism of action be studied in more details. For this reason it was decided not go further with this compound investigation for this thesis work.

Table 3. Summary of data which presented statistical difference between medians (Kruskal-Wallis test, CI=95%).

V stand for vehicle injected and C stand for non-injected.

	Brain	Liver	Kidneys	Heart
Organ weight		V-INHHQ		V-INHHQ
GSH levels		V-HPCIH		
[Cu]	C-INHHQ V-H2QBS	V-H2QBS		C-HPCIH C-H2QBS V-H2QBS
[Fe]	C-H2QBS V-INHHQ V-H2QBS	C-V C-H2QBS V-H2QBS		
[Zn]	C-H2QBS V-H2QBS	C-H2QBS V-H2QBS	C-INHHQ V-INHHQ	V-INHHQ

5.4.2.
Effectiveness studies

Effectiveness studies were performed in order to evaluate the ability of the most promising compound, INHHQ, to affect the behavior in animal models. For this purpose anxiety and memory were evaluated in mice.

5.4.2.1.
Anxiety

Anxiety is a strong symptom in AD affected people. In order to evaluate INHHQ effect on anxiety, elevated plus maze assay was performed with mice.

The experiment was performed using a control group and three different concentrations of the drug, 1, 10 and 25 mg kg^{-1} (n=10 for each group). The control group is composed by vehicle-injected mice.

5.4.2.1.1.
Effect of INHHQ on elevated plus maze labyrinth

Figure 52 illustrates the effect of the treatment with the doses of 0, 1 and 10 mg kg^{-1} of INHHQ, 1 h (Figure 52A) and 4 h (Figure 52B) after the injection. The data are reported as percentage of time and entries in the open and closed arms in EPM model. The ANOVA test did not detect significant differences between groups. Therefore, data suggest that INHHQ treatment does not alter the fear / anxiety-related defensive responses observed in EPM model.
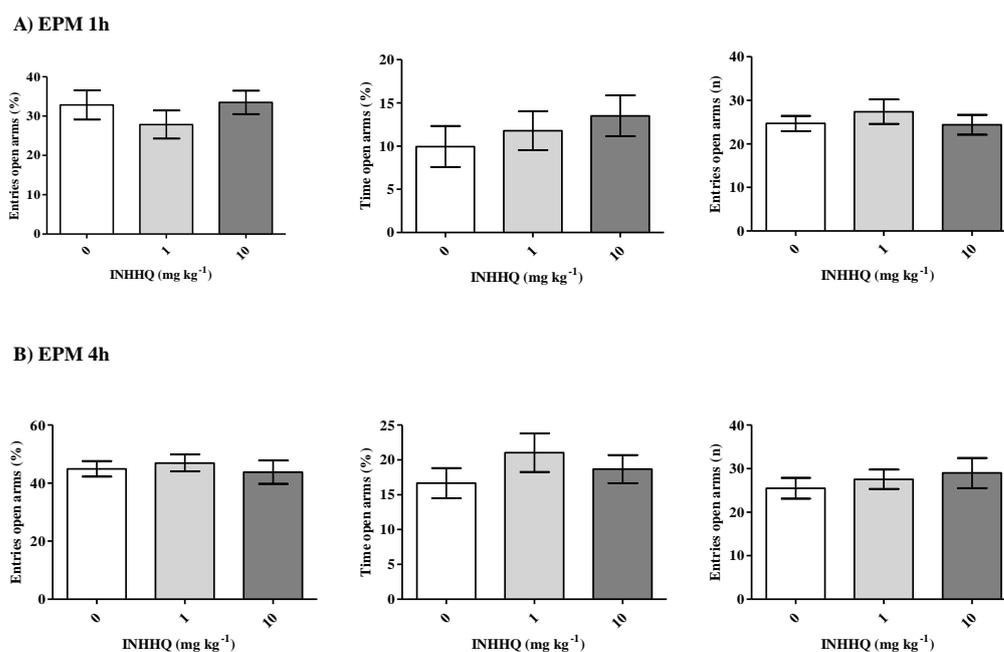
Figure 52. Effects of treatment with doses of 0, 1 and 10 mg kg^{-1} of INHHQ. (A) 1h and (B) 4 h after the injection.

5.4.2.1.2.
Evaluation of INHHQ effect on mice defensive response in open field

As observed in Figure 53, treatment with three INHHQ doses, namely, 0, 1 and 10 mg kg^{-1}, injected 1 and 4 h before the test, was not able to significantly change the percentage of time spent in center and the covered distance in OF model, showing no alteration in fear behavior of the animal INHHQ-related. As in

EPM model, treatment with these doses of drug did not alter the indexes of emotionality and locomotive activity in the OF model, suggesting no fear / anxiety alteration drug-related.

A) Open Field 1h
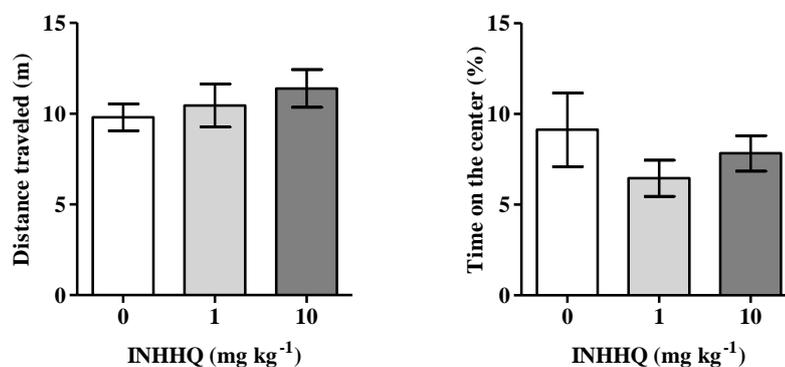
B) Open Field 4h
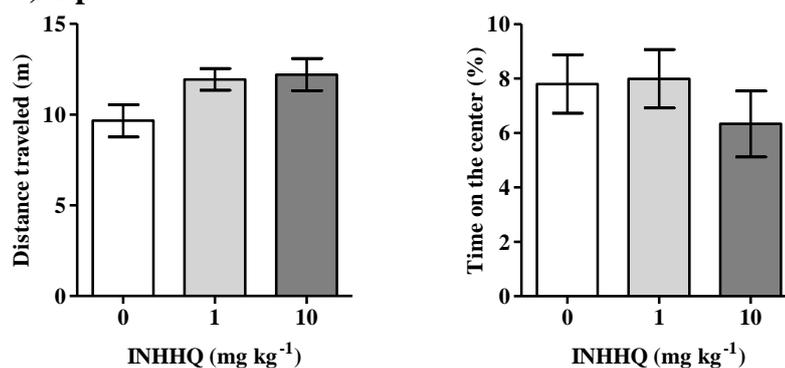
Figure 53. Covered distance and time in the center after 0, 1 and 10 mg kg^{-1} of INHHQ injection. A) 1h and (B) 4 h after the injection.

5.4.2.2.
Memory

Memory is the strongest symptom in AD affected people. In order to evaluate INHHQ effect on memory, NOR tests was performed with healthy and AD model mice.

5.4.2.2.1.
Evaluation of the effect of INHHQ on the object recognition test

Novel object recognition (NOR) experiment in healthy mice was performed using, as control group, vehicle-injected mice, and three different concentrations of the drug, namely, 1, 10 and 25 mg kg^{-1} (n=10 for each group).

Figure 54 shows animals behavior in object recognition task, at injection different time and different INHHQ doses. F stand for familiar object and N stand for novel object, dashed line indicates in all graphs the 50% of exploration time. Figure 54A shows the effect of INHHQ (1, 10 and 25 mg kg^{-1}), injected 1 h before the test, into the object recognition model. During the test phase, the object recognition paradigm, the animals treated with the 1 mg kg^{-1} dose of INHHQ, as well as the control animals, presented increase in the time of exploration of the new object in relation to the familiar object. However, animals treated with 10 and 25 mg kg^{-1} did not show differences in the time of exploration between the familiar object and the new object. Therefore, the results described above suggest that the doses of 10 and 25 mg kg^{-1} of INHHQ induce impairment in the acquisition of the object recognition memory when treated 1 h before the test.

Figure 54B and Figure 54C shows the effect of INHHQ (1, 10 and 25 mg kg^{-1}), injected 4 and 24 h prior to the test in the object recognition model, respectively. During the test phase in the object recognition paradigm, all animals, regardless of doses received from INHHQ, as well as control animals, presented an increase in the time of exploration of the new object in relation to the familiar object. Therefore, the different doses of INHHQ were not able to induce impairment in the acquisition of the object recognition memory when administered 4 or 24 h before the test.

A) NOR 1h

B) NOR 4h

C) NOR 24h
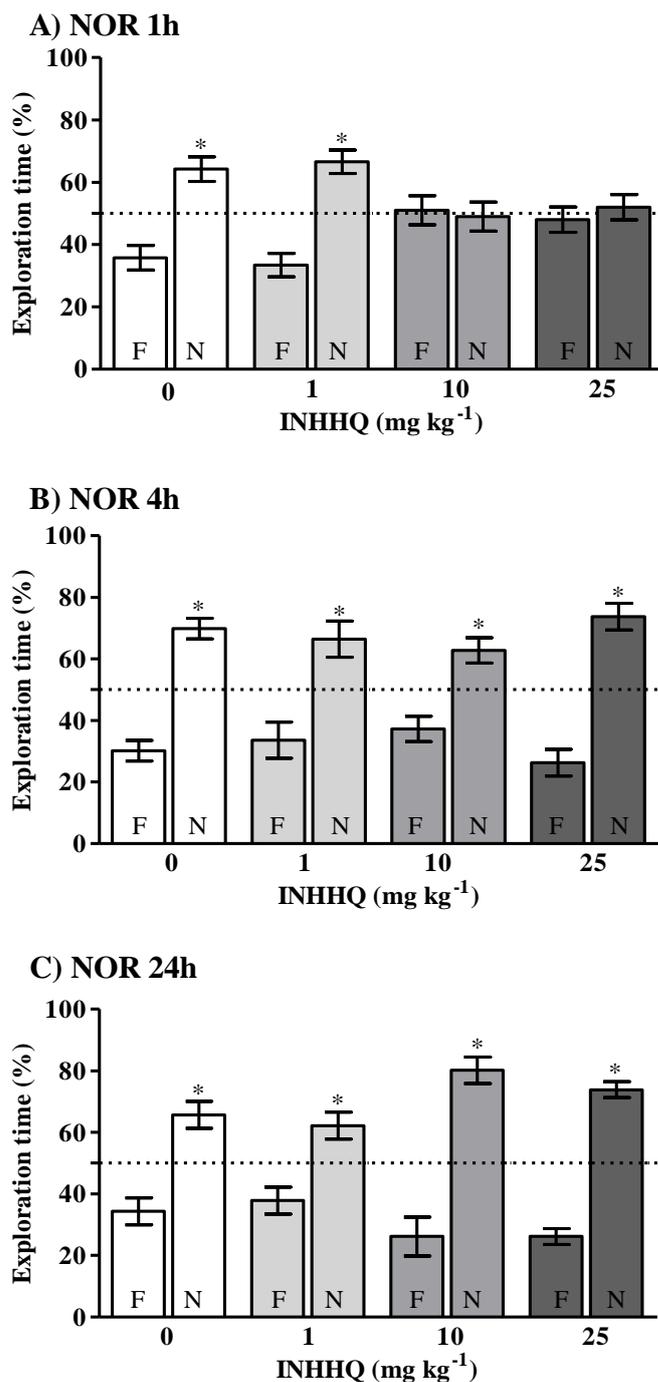
Figure 54. INHHQ effects in NOR test. Doses of 1, 10 and 25 mg kg^{-1}, injected (A) 1 h, (B) 4 h and (C) 24 h before the NOR. The dashed line indicates the value of 50%. F = familiar object, N = novel object.

5.4.2.2.2.
The effect of INHHQ on the AD animal model

In view of the obtained results for EPM, OF and NOR test in healty mice, and in order to evaluate the effect of INHHQ on AD animal model, the dose of 1 mg kg^{-1} was selected. This dose was not able to induce cognitive impairment in

the animals (section 5.4.2.2.1). The AD memory loss symptom is obtained by AβOs i.c.v. injection.

The experiment was performed with four animal groups (n=10 for each group):

1) Injected IP with vehicle (10% DMSO in saline solution) 1 h prior to i.c.v. injection with vehicle (saline solution);

2) Injected IP with 1 mg kg^{-1} of INHHQ in 10% DMSO in saline solution 1 h prior to i.c.v. injection with vehicle (saline solution);

3) Injected IP with vehicle (10% DMSO in saline solution) 1 h prior to i.c.v. injection with AβOs in saline solution;

4) Injected IP with 1 mg kg^{-1} of INHHQ in 10% DMSO in saline solution 1 h prior to i.c.v. injection with AβOs in saline solution.

The first group represents control mice. The second group represents healthy mice exposed to INHHQ. The third group represents AD mice without INHHQ treatment. The fourth group represents AD mice treated whit INHHQ.

Figure 55 illustrates the behavior of each group, with the NOR task performed in different times. In Figure 55A are reported the data for the NOR test performed 24h after the treatments. During the test phase, animals receiving vehicle IP and AβOs i.c.v. presented cognitive impairment, since, as expected, there was no significant difference between the exploration time of familiar (F) and novel (N) object. However, treatment with INHHQ 1 mg kg^{-1} was able to prevent the cognitive impairment induced by the injection of AβOs, as showed by the lasts two bars in Figure 55A. Animals, injected whit AβOs, which received the INHHQ dose spent more time exploring the new object than the familiar one. This same exploration profile suggests recognition learning was observed in animals receiving i.c.v. vehicle, pretreated or not with INHHQ 1 mg kg^{-1}, confirming that the short-term memory loss was AβOs-related.

Twenty four hours after the experimental task (48 hs after the treatment), the test was repeated without a new training, in order to evaluate long-term memory. As seen in Figure 55B, animals injected with i.c.v. vehicle, regardless of pretreatment, showed normal long-term memory. However, as in short-term memory test (Figure 55A), animals pretreated with vehicle IP and injected with AβOs showed a cognitive impairment in the object recognition task assessed 24 h

after training, as expected, confirming that the long-term memory loss was AβOs-related. This loss was prevented with the pre-treatment with INHHQ, as showed by the lasts two bars in Figure 55B.

Seven days after the first training, a second training was performed, and the object recognition task was repeated (Figure 55C). Once again, a cognitive impairment was observed in animals pretreated with vehicle IP and AβOs i.c.v. Similar to the results described above, pretreatment with 1mg kg^{-1} dose of INHHQ continued to prevent short-term memory impairment induced by i.c.v. AβOs injection 9 days after the treatment, as showed by the lasts two bars in Figure 55C.

This result strongly suggest a preventive activity of low INHHQ dose, 1 mg kg^{-1}, in the AD model for this memory task, for short- and long-term memory, confirming the great potential of INHHQ as a disease-modifying drug for the treatment of AD, and suggesting that other compounds, such as HPCIH, can also constitute a good candidate for further *in vivo* investigations.

A) NOR 24 h

B) NOR 48 h

C) NOR 7 days
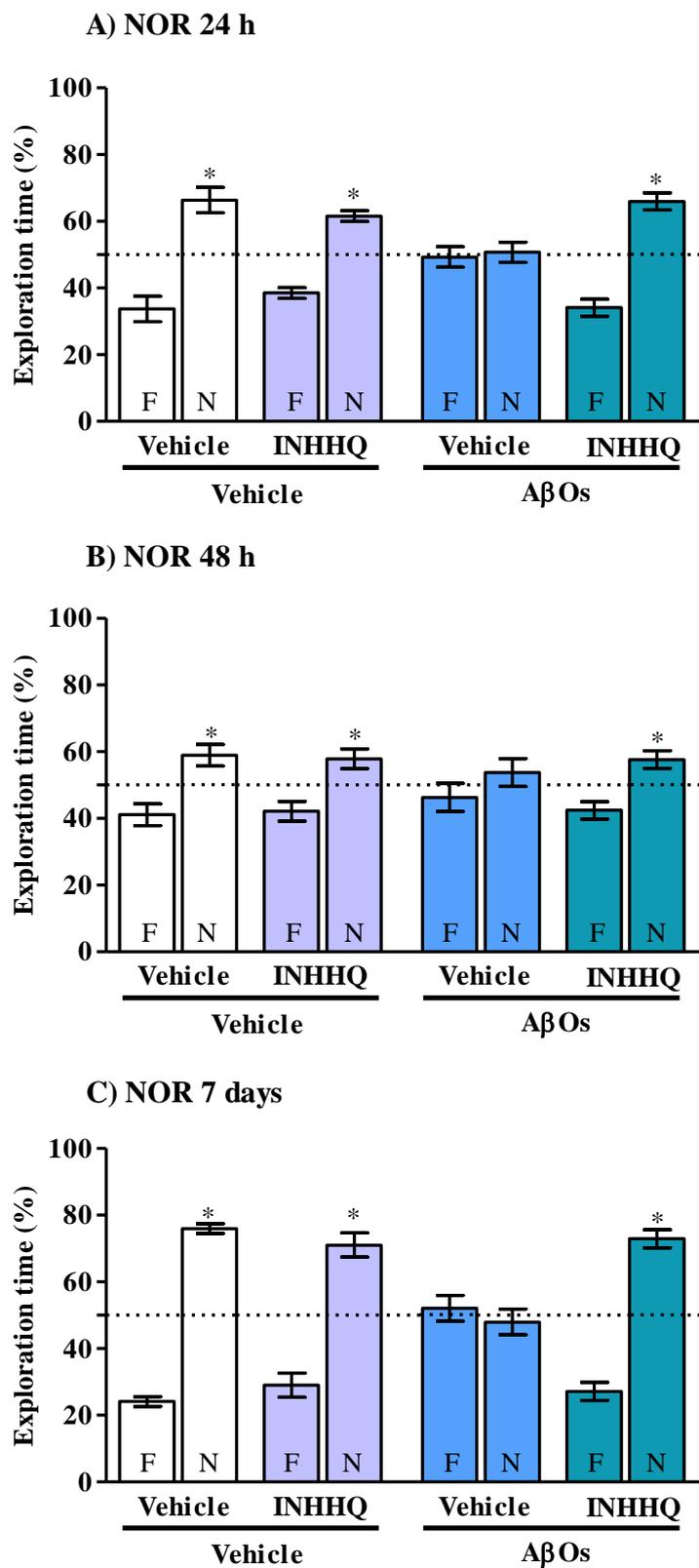
Figure 55. Graphs of INHHQ effects in NOR test in AD model. IP and i.c.v. injection (A) 24 h, (B) 48 hs and (C) 7 days before the NOR test. The dashed line indicates the value of 50%. F = familiar object, N = novel object.

6.
Conclusions

AD is the major cause of dementia worldwide. The disease mechanisms are not totally understood and, up to the present, there is no cure for this pathology. From a biological point of view, it is well-known that the AD typical cellular chain of events involves Aβ peptide. Despite the fact that aggregation of the Aβ peptide is one of the most important characteristics of AD pathogenesis, the exact role of the extracellular plaques composed by this peptide is not fully understood. In fact, the hypothesis that Aβ neurotoxicity is better explained by its soluble oligomers is becoming well accepted. In the last decade, a set of different evidences have shown to support the direct link between biometals and Aβ oligomerization and toxicity. Based on this hypothesis, the use of MPACs seems to be the best choice to avoid the oligomerization of Aβ mediated by physiological metals.

The current MPACs scenario counts on different classes of molecules; the most representative being the class of 8-hydroxyquinoline derivatives. Amongst the four compounds studied in the present work, three, namely, INHHQ, HPCIH and INHOVA, are aroylhydrazones and two contain an 8-hydroxyquinoline moiety, namely INHHQ and H2QBS. INHHQ is, therefore, a hybrid compound.

Assays showed a high stability of the compounds at 100% DMSO solution, and a suitable durability pattern in 10% and 1.0% DMSO solution, with the exception of INHOVA, which is very sensitive to hydrolysis.

In vitro NMR studies showed no direct interaction between INHHQ, HPCIH or H2QBS with monomers of the Aβ peptide. ^{1}H x ^{15}N HSQC NMR experiments point to a similar metal-sequestering profile for INHHQ and HPCIH: both compounds must be present with a concentration five times higher than that of Aβ to efficiently compete with it for metals, as expected for a MPAC. H2QBS, on the other hand, showed a higher capacity for the removal of Cu^{2+} and Zn^{2+} ions from Aβ.

INHHQ and HPCIH possess the lower cytotoxicity for the SW APP HEK 293 cell line, and it appears to be APP mutation-related, since both compounds show different cytotoxicity profiles for the HEK 293 cell line, which express non-mutated APP form.

In vivo acute toxicity tests, performed through IP injection of 200 mg kg^{-1} of each compound in healthy male Wistar rats, indicated no lethality for all the three compounds tested, and the analysis of biological concentration of GSH, Cu, Fe and Zn in brain, liver, kidneys and heart were evaluated. The results suggested that H2QBS present high capacity to displace biometals in rats, when high doses are administered. This compound was excluded for further studies in this work.

INHHQ and HPCIH were then evaluated for their potential capacity to affect the APP pathway, by means of proteomic analyses in exposed APP-mutated cells. Results suggested a possible influence of both compounds in the activity of γ-secretases, which are copper-dependent enzymes. INHHQ also showed the capacity to interfere with the APP synthesis / digestion ratio, confirming its strong intracellular activity. These results point to INHHQ as the most promising MPAC among the compounds considered.

In vivo effectiveness studies, performed in Swiss mice, confirmed that INHHQ single-dose treatment does not alter the fear / anxiety-related defensive responses. Doses higher than 1 mg kg^{-1} induce temporary cognitive impairment in healthy mice. Finally, using a well-established murine model of AD, it has been concluded that a single-dose of 1 mg kg^{-1} INHHQ is able to prevent both short- and long-term memory impairments induced by the i.c.v. infusion of Aβ oligomers, and this effect persist for, at least, one week after compound administration.

The results presented in this thesis indicate that INHHQ, which was the subject of both national and regional patent applications in Brazil, the United States and the European Union, under the protocol numbers BR 10 2013 033006 0, US 15/106,181 and EP14872636.7, is a very promising "Metal-Protein Attenuating Compound" for the bioinorganic management of Alzheimer's disease. Another hydrazone examined in this work, HPCIH, is also of interest and will be the issue of future investigations.

7.
Future perspectives

During the development of the present work, several points were raised that can be suggested as a continuation of this study.

Firstly, INHHQ and HPCIH showed high potential capacity to affect APP pathway, specifically suggesting possible interaction of both compounds with γ-secretases. This finding must be studied in more details, by *in vitro* evaluation of secretase activity in presence of the different doses of the two MPACs.

Secondly, the preliminary effectiveness experiment in AD mice model for INHHQ should be confirmed repeating the experience in triplicate. Also, as HPCIH showed to be a potencial candidate, the same tests should be performed for HPCIH.

8. References

ADELMAN, A. Selegiline and vitamin E in Alzheimer's disease. **J Fam Pract,** v. 45, n. 2, p. 98-100, Aug 1997. ISSN 0094-3509.

ADLARD, P. A. *et al.* Metal ionophore treatment restores dendritic spine density and synaptic protein levels in a mouse model of Alzheimer's disease. **PLoS One,** v. 6, n. 3, p. e17669, 2011. ISSN 1932-6203.

_____. Cognitive loss in zinc transporter-3 knock-out mice: a phenocopy for the synaptic and memory deficits of Alzheimer's disease? **J Neurosci,** v. 30, n. 5, p. 1631-6, Feb 2010. ISSN 1529-2401.

AKTER, K. *et al.* Diabetes mellitus and Alzheimer's disease: shared pathology and treatment? **Br J Clin Pharmacol,** v. 71, n. 3, p. 365-76, Mar 2011. ISSN 1365-2125.

ALMEIDA, S. S.; TONKISS, J.; GALLER, J. R. Prenatal protein malnutrition affects exploratory behavior of female rats in the elevated plus-maze test. **Physiol Behav,** v. 60, n. 2, p. 675-80, Aug 1996. ISSN 0031-9384.

ALZHEIMER, A. *et al.* An English translation of Alzheimer's 1907 paper, "Uber eine eigenartige Erkankung der Hirnrinde". **Clin Anat,** v. 8, n. 6, p. 429-31, 1995. ISSN 0897-3806.

ANAND, P.; SINGH, B. A review on cholinesterase inhibitors for Alzheimer's disease. **Arch Pharm Res,** v. 36, n. 4, p. 375-99, Apr 2013. ISSN 0253-6269.

ANSELONI, V. Z.; BRANDÃO, M. L. Ethopharmacological analysis of behaviour of rats using variations of the elevated plus-maze. **Behav Pharmacol,** v. 8, n. 6-7, p. 533-40, Nov 1997. ISSN 0955-8810.

ATKINS, P. W.; SHRIVER, D. F. I. C. **Shriver & Atkins inorganic chemistry**. 4th ed. / Peter Atkins ... [*et al.*]. Oxford: Oxford University Press, 2006a. ISBN 9780199264636.

_____. **Shriver & Atkins inorganic chemistry**. 4th ed. / Peter Atkins ... [*et al.*]. Oxford: Oxford University Press, 2006b. ISBN 9780199264636.

ATWOOD, C. S. *et al.* Role of free radicals and metal ions in the pathogenesis of Alzheimer's disease. **Met Ions Biol Syst,** v. 36, p. 309-64, 1999. ISSN 0161-5149.

_____. Dramatic aggregation of Alzheimer abeta by Cu(II) is induced by conditions representing physiological acidosis. **J Biol Chem,** v. 273, n. 21, p. 12817-26, May 1998. ISSN 0021-9258.

AULD, D. S. *et al.* Alzheimer's disease and the basal forebrain cholinergic system: relations to beta-amyloid peptides, cognition, and treatment strategies. **Prog Neurobiol,** v. 68, n. 3, p. 209-45, Oct 2002. ISSN 0301-0082.

AUSTIN, C. P. *et al.* The knockout mouse project. **Nat Genet,** v. 36, n. 9, p. 921-4, Sep 2004. ISSN 1061-4036.

BARNES, D. E.; YAFFE, K. Vitamin E and donepezil for the treatment of mild cognitive impairment. **N Engl J Med,** v. 353, n. 9, p. 951-2; author reply 951-2, Sep 2005. ISSN 1533-4406.

BARNETT, S. A. **The rat : a study in behavior**. Revised ed. Chicago ; London: University of Chicago Press, 1975. ISBN 0226037401 : ¹12.00.

BARNHAM, K. J.; BUSH, A. I. Metals in Alzheimer's and Parkinson's diseases. **Curr Opin Chem Biol,** v. 12, n. 2, p. 222-8, Apr 2008. ISSN 1367-5931.

BARNHAM, K. J.; MASTERS, C. L.; BUSH, A. I. Neurodegenerative diseases and oxidative stress. **Nat Rev Drug Discov,** v. 3, n. 3, p. 205-14, Mar 2004. ISSN 1474-1776.

BARREIROS, A. L. B. S.; DAVID, J. M.; DAVID, J. P. Estresse oxidativo: relação entre geração de espécies reativas e defesa do organismo. **Química Nova,** v. 29, p. 113-123, 2006. ISSN 0100-4042.

BARTUS, R. T. *et al.* The cholinergic hypothesis of geriatric memory dysfunction. **Science,** v. 217, n. 4558, p. 408-14, Jul 1982. ISSN 0036-8075.

BASHA, M. R. *et al.* The fetal basis of amyloidogenesis: exposure to lead and latent overexpression of amyloid precursor protein and beta-amyloid in the aging brain. **J Neurosci,** v. 25, n. 4, p. 823-9, Jan 2005. ISSN 1529-2401.

BATES, K. *et al.* Aging, cortical injury and Alzheimer's disease-like pathology in the guinea pig brain. **Neurobiol Aging,** v. 35, n. 6, p. 1345-51, Jun 2014. ISSN 1558-1497.

BECKER, E.; RICHARDSON, D. R. Development of novel aroylhydrazone ligands for iron chelation therapy: 2-pyridylcarboxaldehyde isonicotinoyl hydrazone analogs. **J Lab Clin Med,** v. 134, n. 5, p. 510-21, Nov 1999. ISSN 0022-2143.

BEDSE, G. *et al.* Aberrant insulin signaling in Alzheimer's disease: current knowledge. **Front Neurosci,** v. 9, p. 204, 2015. ISSN 1662-4548.

BEKRIS, L. M. *et al.* Genetics of Alzheimer disease. **J Geriatr Psychiatry Neurol,** v. 23, n. 4, p. 213-27, Dec 2010. ISSN 0891-9887.

BENILOVA, I.; KARRAN, E.; DE STROOPER, B. The toxic Aβ oligomer and Alzheimer's disease: an emperor in need of clothes. **Nat Neurosci,** v. 15, n. 3, p. 349-57, Jan 2012. ISSN 1546-1726.

BENNETT, B. M. *et al.* Cognitive deficits in rats after forebrain cholinergic depletion are reversed by a novel NO mimetic nitrate ester. **Neuropsychopharmacology,** v. 32, n. 3, p. 505-13, Mar 2007. ISSN 0893-133X.

BEYDOUN, M. A. *et al.* Association of adiposity status and changes in early to mid-adulthood with incidence of Alzheimer's disease. **Am J Epidemiol,** v. 168, n. 10, p. 1179-89, Nov 2008. ISSN 1476-6256.

BEYREUTHER, K.; MULTHAUP, G.; MASTERS, C. L. Alzheimer's disease: genesis of amyloid. **Ciba Found Symp,** v. 199, p. 119-27; discussion 127-31, 1996. ISSN 0300-5208.

BIEDLER, J. L.; HELSON, L.; SPENGLER, B. A. Morphology and growth, tumorigenicity, and cytogenetics of human neuroblastoma cells in continuous culture. **Cancer Res,** v. 33, n. 11, p. 2643-52, Nov 1973. ISSN 0008-5472.

BIESCHKE, J. *et al.* Small-molecule conversion of toxic oligomers to nontoxic β-sheet-rich amyloid fibrils. **Nat Chem Biol,** v. 8, n. 1, p. 93-101, Jan 2012. ISSN 1552-4469.

BLANCHARD, D. C.; GRIEBEL, G.; BLANCHARD, R. J. The Mouse Defense Test Battery: pharmacological and behavioral assays for anxiety and panic. **Eur J Pharmacol,** v. 463, n. 1-3, p. 97-116, Feb 2003. ISSN 0014-2999.

BLANQUET, V. *et al.* The beta amyloid protein (AD-AP) cDNA hybridizes in normal and Alzheimer individuals near the interface of 21q21 and q22.1. **Ann Genet,** v. 30, n. 2, p. 68-9, 1987. ISSN 0003-3995.

BODENHAUSEN, G.; RUBEN, D. J. Natural abundance nitrogen-15 NMR by enhanced heteronuclear spectroscopy. v. 69, n. 1, p. 185-189, 1980.

BOLIN, C. M. *et al.* Exposure to lead and the developmental origin of oxidative DNA damage in the aging brain. **FASEB J,** v. 20, n. 6, p. 788-90, Apr 2006. ISSN 1530-6860.

BRAAK, H.; BRAAK, E. Neuropathological stageing of Alzheimer-related changes. **Acta Neuropathol,** v. 82, n. 4, p. 239-59, 1991. ISSN 0001-6322.

BRITO-MOREIRA, J. *et al.* Aβ oligomers induce glutamate release from hippocampal neurons. **Curr Alzheimer Res,** v. 8, n. 5, p. 552-62, Aug 2011. ISSN 1875-5828.

BUCCAFUSCO, J. J. *et al.* Long-lasting cognitive improvement with nicotinic receptor agonists: mechanisms of pharmacokinetic-pharmacodynamic discordance. **Trends Pharmacol Sci,** v. 26, n. 7, p. 352-60, Jul 2005. ISSN 0165-6147.

BURNETTE, W. N. "Western blotting": electrophoretic transfer of proteins from sodium dodecyl sulfate--polyacrylamide gels to unmodified nitrocellulose and radiographic detection with antibody and radioiodinated protein A. **Anal Biochem,** v. 112, n. 2, p. 195-203, Apr 1981. ISSN 0003-2697.

BUSH, A. I. The metallobiology of Alzheimer's disease. **Trends Neurosci,** v. 26, n. 4, p. 207-14, Apr 2003. ISSN 0166-2236.

_____. The metal theory of Alzheimer's disease. **J Alzheimers Dis,** v. 33 Suppl 1, p. S277-81, 2013. ISSN 1875-8908.

BUSH, A. I. *et al.* Rapid induction of Alzheimer A beta amyloid formation by zinc. **Science,** v. 265, n. 5177, p. 1464-7, Sep 1994. ISSN 0036-8075.

BUTTERFIELD, D. A.; DI DOMENICO, F.; BARONE, E. Elevated risk of type 2 diabetes for development of Alzheimer disease: a key role for oxidative stress in brain. **Biochim Biophys Acta,** v. 1842, n. 9, p. 1693-706, Sep 2014. ISSN 0006-3002.

CAI, X. D.; GOLDE, T. E.; YOUNKIN, S. G. Release of excess amyloid beta protein from a mutant amyloid beta protein precursor. **Science,** v. 259, n. 5094, p. 514-6, Jan 1993. ISSN 0036-8075.

CAMMAROTA, M. *et al.* Relationship between short- and long-term memory and short- and long-term extinction. **Neurobiol Learn Mem,** v. 84, n. 1, p. 25-32, Jul 2005. ISSN 1074-7427.

CAMPBELL, A. *et al.* Chronic exposure to aluminum in drinking water increases inflammatory parameters selectively in the brain. **J Neurosci Res,** v. 75, n. 4, p. 565-72, Feb 2004. ISSN 0360-4012.

CARDARELLI, R.; KERTESZ, A.; KNEBL, J. A. Frontotemporal dementia: a review for primary care physicians. **Am Fam Physician,** v. 82, n. 11, p. 1372-7, Dec 2010. ISSN 1532-0650.

CHANG, T. P.; RANGAN, C. Iron poisoning: a literature-based review of epidemiology, diagnosis, and management. **Pediatr Emerg Care,** v. 27, n. 10, p. 978-85, Oct 2011. ISSN 1535-1815.

CHAPPELL, J. *et al.* A re-examination of the role of basal forebrain cholinergic neurons in spatial working memory. **Neuropharmacology,** v. 37, n. 4-5, p. 481-7, 1998 Apr-May 1998. ISSN 0028-3908.

CHARTIER-HARLIN, M. C. *et al.* Early-onset Alzheimer's disease caused by mutations at codon 717 of the beta-amyloid precursor protein gene. **Nature,** v. 353, n. 6347, p. 844-6, Oct 1991. ISSN 0028-0836.

CHASAPIS, C. T. *et al.* Zinc and human health: an update. **Arch Toxicol,** v. 86, n. 4, p. 521-34, Apr 2012. ISSN 1432-0738.

CHEN, H. X. *et al.* Preparation of coordination polymers with 8-hydroxyquinoline azo benzensulfonic acid as a planar multidentate ligand and the study of their photochemical and photo-stability properties. **Dalton Trans,** v. 42, n. 14, p. 4831-9, Apr 2013. ISSN 1477-9234.

CHEN, S. Y. *et al.* Design, synthesis, and biological evaluation of curcumin analogues as multifunctional agents for the treatment of Alzheimer's disease. **Bioorg Med Chem,** v. 19, n. 18, p. 5596-604, Sep 2011. ISSN 1464-3391.

CHERNY, R. A. *et al.* Treatment with a copper-zinc chelator markedly and rapidly inhibits beta-amyloid accumulation in Alzheimer's disease transgenic mice. **Neuron,** v. 30, n. 3, p. 665-76, Jun 2001. ISSN 0896-6273.

_____. Aqueous dissolution of Alzheimer's disease Abeta amyloid deposits by biometal depletion. **J Biol Chem,** v. 274, n. 33, p. 23223-8, Aug 1999. ISSN 0021-9258.

CHRISTIE, J. E. *et al.* Physostigmine and arecoline: effects of intravenous infusions in Alzheimer presenile dementia. **Br J Psychiatry,** v. 138, p. 46-50, Jan 1981. ISSN 0007-1250.

CLAIRE M. ARMSTRONG *et al.* Structural Variations and Formation Constants of First-Row Transition Metal Complexes of Biologically Active Aroylhydrazones. **European Journal Of Inorganic Chemistry,** v. 2003, n. 6, p. 1145-1156, 2003.

CRAFT, S.; WATSON, G. S. Insulin and neurodegenerative disease: shared and specific mechanisms. **Lancet Neurol,** v. 3, n. 3, p. 169-78, Mar 2004. ISSN 1474-4422.

CRAPPER, D. R.; KRISHNAN, S. S.; DALTON, A. J. Brain aluminum distribution in Alzheimer's disease and experimental neurofibrillary degeneration. **Science,** v. 180, n. 4085, p. 511-3, May 1973. ISSN 0036-8075.

CROOK, R. *et al.* A variant of Alzheimer's disease with spastic paraparesis and unusual plaques due to deletion of exon 9 of presenilin 1. **Nat Med,** v. 4, n. 4, p. 452-5, Apr 1998. ISSN 1078-8956.

CRUZ, A. P.; FREI, F.; GRAEFF, F. G. Ethopharmacological analysis of rat behavior on the elevated plus-maze. **Pharmacol Biochem Behav,** v. 49, n. 1, p. 171-6, Sep 1994. ISSN 0091-3057.

CUKIERMAN, D. S. **LIGANTES AROILHIDRAZÔNICOS: Uma nova classe de promissores MPACs na terapia da doença de Alzheimer**. 2016. (Bachelor). Departamento de Química PUC-Rio, PUC-Rio

CUKIERMAN, D. S. *et al.* **A moderate metal-binding hydrazone meets the criteria for a bioinorganic approach towards Parkinson's disease: Therapeutic potential, blood-brain barrier crossing evaluation and preliminary toxicological studies**. Journal of Inorganic Biochemistry 2017.

CULLIS, J. O. Diagnosis and management of anaemia of chronic disease: current status. **Br J Haematol,** v. 154, n. 3, p. 289-300, Aug 2011. ISSN 1365-2141.

CUNNINGHAM, E. L.; PASSMORE, A. P. Drug development in dementia. **Maturitas,** v. 76, n. 3, p. 260-6, Nov 2013. ISSN 1873-4111.

D'HOOGE, R.; DE DEYN, P. P. Applications of the Morris water maze in the study of learning and memory. **Brain Res Brain Res Rev,** v. 36, n. 1, p. 60-90, Aug 2001.

DAMASCENO, D. C. *et al.* Oxidative stress and diabetes in pregnant rats. **Anim Reprod Sci,** v. 72, n. 3-4, p. 235-44, Aug 2002. ISSN 0378-4320.

DANSCHER, G. *et al.* Increased amount of zinc in the hippocampus and amygdala of Alzheimer's diseased brains: a proton-induced X-ray emission spectroscopic analysis of cryostat sections from autopsy material. **J Neurosci Methods,** v. 76, n. 1, p. 53-9, Sep 1997. ISSN 0165-0270.

DANYSZ, W. *et al.* Neuroprotective and symptomatological action of memantine relevant for Alzheimer's disease--a unified glutamatergic hypothesis on the mechanism of action. **Neurotox Res,** v. 2, n. 2-3, p. 85-97, 2000. ISSN 1029-8428.

DAVIES, P.; MALONEY, A. J. Selective loss of central cholinergic neurons in Alzheimer's disease. **Lancet,** v. 2, n. 8000, p. 1403, Dec 1976. ISSN 0140-6736.

DE FALCO, A. *et al.* DOENÇA DE ALZHEIMER: HIPÓTESES ETIOLÓGICAS E PERSPECTIVAS DE TRATAMENTO. **Química Nova,** v. 39, p. 63-80, 2016. ISSN 0100-4042.

DE FELICE, F. G. *et al.* Protection of synapses against Alzheimer's-linked toxins: insulin signaling prevents the pathogenic binding of Abeta oligomers. **Proc Natl Acad Sci U S A,** v. 106, n. 6, p. 1971-6, Feb 2009. ISSN 1091-6490.

DE FREITAS, L. V. **Ligantes derivados da isoniazida e sua coordenação aos íons cobre(II) e zinco(II): potenciais Compostos Atenuantes da Interação Metal-Proteína (MPACs) na terapia da Doença de Alzheimer** 2014. (Doctor). Departamento de Química da PUC-Rio, PUC-Rio

DE FREITAS, L. V. *et al.* Structural and vibrational study of 8-hydroxyquinoline-2-carboxaldehyde isonicotinoyl hydrazone--a potential metal-protein attenuating compound (MPAC) for the treatment of Alzheimer's disease. **Spectrochim Acta A Mol Biomol Spectrosc,** v. 116, p. 41-8, Dec 2013. ISSN 1873-3557.

DE LA MONTE, S. M. Contributions of brain insulin resistance and deficiency in amyloid-related neurodegeneration in Alzheimer's disease. **Drugs,** v. 72, n. 1, p. 49-66, Jan 2012a. ISSN 0012-6667.

_____. Triangulated mal-signaling in Alzheimer's disease: roles of neurotoxic ceramides, ER stress, and insulin resistance reviewed. **J Alzheimers Dis,** v. 30 Suppl 2, p. S231-49, 2012b. ISSN 1875-8908.

DE LA MONTE, S. M. *et al.* Insulin resistance and neurodegeneration: roles of obesity, type 2 diabetes mellitus and non-alcoholic steatohepatitis. **Curr Opin Investig Drugs,** v. 10, n. 10, p. 1049-60, Oct 2009. ISSN 2040-3429.

_____. Therapeutic rescue of neurodegeneration in experimental type 3 diabetes: relevance to Alzheimer's disease. **J Alzheimers Dis,** v. 10, n. 1, p. 89-109, Sep 2006. ISSN 1387-2877.

DEIBEL, M. A.; EHMANN, W. D.; MARKESBERY, W. R. Copper, iron, and zinc imbalances in severely degenerated brain regions in Alzheimer's disease: possible relation to oxidative stress. **J Neurol Sci,** v. 143, n. 1-2, p. 137-42, Nov 1996. ISSN 0022-510X.

DEUTSCH, J. A. The cholinergic synapse and the site of memory. **Science,** v. 174, n. 4011, p. 788-94, Nov 1971. ISSN 0036-8075.

DORAISWAMY, P. M.; FINEFROCK, A. E. Metals in our minds: therapeutic implications for neurodegenerative disorders. **Lancet Neurol,** v. 3, n. 7, p. 431-4, Jul 2004. ISSN 1474-4422.

DRACHMAN, D. A.; LEAVITT, J. Human memory and the cholinergic system. A relationship to aging? **Arch Neurol,** v. 30, n. 2, p. 113-21, Feb 1974. ISSN 0003-9942.

DRACHMAN, D. A.; SAHAKIAN, B. J. Memory and cognitive function in the elderly. A preliminary trial of physostigmine. **Arch Neurol,** v. 37, n. 10, p. 674-5, Oct 1980. ISSN 0003-9942.

DRAKESMITH, H.; PRENTICE, A. M. Hepcidin and the iron-infection axis. **Science,** v. 338, n. 6108, p. 768-72, Nov 2012. ISSN 1095-9203.

DRINGENBERG, H. C. Alzheimer's disease: more than a 'cholinergic disorder' - evidence that cholinergic-monoaminergic interactions contribute to EEG slowing and dementia. **Behav Brain Res,** v. 115, n. 2, p. 235-49, Nov 2000. ISSN 0166-4328.

DUNNETT, S. B.; EVERITT, B. J.; ROBBINS, T. W. The basal forebrain-cortical cholinergic system: interpreting the functional consequences of excitotoxic lesions. **Trends Neurosci,** v. 14, n. 11, p. 494-501, Nov 1991. ISSN 0166-2236.

DWORETZKY, B. A. The neurology of memory. **Semin Speech Lang,** v. 22, n. 2, p. 95-105, 2001. ISSN 0734-0478.

DYSKEN, M. W. *et al.* Effect of vitamin E and memantine on functional decline in Alzheimer disease: the TEAM-AD VA cooperative randomized trial. **JAMA,** v. 311, n. 1, p. 33-44, Jan 2014. ISSN 1538-3598.

EL-HAWASH, S. A.; ABDEL WAHAB, A. E.; EL-DEMELLAWY, M. A. Cyanoacetic acid hydrazones of 3-(and 4-)acetylpyridine and some derived ring systems as potential antitumor and anti-HCV agents. **Arch Pharm (Weinheim),** v. 339, n. 1, p. 14-23, Jan 2006. ISSN 0365-6233.

ELLMAN, G. L. Tissue sulfhydryl groups. **Arch Biochem Biophys,** v. 82, n. 1, p. 70-7, May 1959. ISSN 0003-9861.

ELLUL, J. *et al.* The effects of commonly prescribed drugs in patients with Alzheimer's disease on the rate of deterioration. **J Neurol Neurosurg Psychiatry,** v. 78, n. 3, p. 233-9, Mar 2007. ISSN 1468-330X.

ENNACEUR, A.; DELACOUR, J. A new one-trial test for neurobiological studies of memory in rats. 1: Behavioral data. **Behav Brain Res,** v. 31, n. 1, p. 47-59, Nov 1988. ISSN 0166-4328.

EVANS, J. R. Antioxidant vitamin and mineral supplements for slowing the progression of age-related macular degeneration. **Cochrane Database Syst Rev**, n. 2, p. CD000254, 2006. ISSN 1469-493X.

FANSELOW, M. S.; LEDOUX, J. E. Why we think plasticity underlying Pavlovian fear conditioning occurs in the basolateral amygdala. **Neuron,** v. 23, n. 2, p. 229-32, Jun 1999. ISSN 0896-6273.

FERREIRA, S. T. *et al.* Inflammation, defective insulin signaling, and neuronal dysfunction in Alzheimer's disease. **Alzheimers Dement,** v. 10, n. 1 Suppl, p. S76-83, Feb 2014. ISSN 1552-5279.

FERREIRA, S. T.; KLEIN, W. L. The Aβ oligomer hypothesis for synapse failure and memory loss in Alzheimer's disease. **Neurobiol Learn Mem,** v. 96, n. 4, p. 529-43, Nov 2011. ISSN 1095-9564.

FERREIRA, S. T.; VIEIRA, M. N.; DE FELICE, F. G. Soluble protein oligomers as emerging toxins in Alzheimer's and other amyloid diseases. **IUBMB Life,** v. 59, n. 4-5, p. 332-45, 2007 Apr-May 2007. ISSN 1521-6543.

FIGUEIREDO, C. P. *et al.* Memantine rescues transient cognitive impairment caused by high-molecular-weight aβ oligomers but not the persistent impairment induced by low-molecular-weight oligomers. **J Neurosci,** v. 33, n. 23, p. 9626-34, Jun 2013. ISSN 1529-2401.

FINEFROCK, A. E.; BUSH, A. I.; DORAISWAMY, P. M. Current status of metals as therapeutic targets in Alzheimer's disease. **J Am Geriatr Soc,** v. 51, n. 8, p. 1143-8, Aug 2003. ISSN 0002-8614.

FRIEDLICH, A. L. *et al.* Neuronal zinc exchange with the blood vessel wall promotes cerebral amyloid angiopathy in an animal model of Alzheimer's disease. **J Neurosci,** v. 24, n. 13, p. 3453-9, Mar 2004. ISSN 1529-2401.

FRISARDI, V. *et al.* Aluminum in the diet and Alzheimer's disease: from current epidemiology to possible disease-modifying treatment. **J Alzheimers Dis,** v. 20, n. 1, p. 17-30, 2010. ISSN 1875-8908.

GENTSCH, C. *et al.* Different reaction patterns in individually and socially reared rats during exposures to novel environments. **Behav Brain Res,** v. 4, n. 1, p. 45-54, Jan 1982. ISSN 0166-4328.

GERBER, H. *et al.* Zinc and Copper Differentially Modulate Amyloid Precursor Protein Processing by γ-Secretase and Amyloid-β Peptide Production. **J Biol Chem,** v. 292, n. 9, p. 3751-3767, Mar 2017. ISSN 1083-351X.

GIACCONE, G. *et al.* Down patients: extracellular preamyloid deposits precede neuritic degeneration and senile plaques. **Neurosci Lett,** v. 97, n. 1-2, p. 232-8, Feb 1989. ISSN 0304-3940.

GIOVANNINI, M. G. *et al.* Beta-amyloid-induced inflammation and cholinergic hypofunction in the rat brain in vivo: involvement of the p38MAPK pathway. **Neurobiol Dis,** v. 11, n. 2, p. 257-74, Nov 2002. ISSN 0969-9961.

GOATE, A. *et al.* Segregation of a missense mutation in the amyloid precursor protein gene with familial Alzheimer's disease. **Nature,** v. 349, n. 6311, p. 704-6, Feb 1991. ISSN 0028-0836.

GONZÁLEZ-BARÓ, A. C. *et al.* **Spectroscopic and theoretical study of the o-vanillin hydrazone of the mycobactericidal drug isoniazid**. Journal of Molecular Structure. 1007**:** 95–101 p. 2012a.

_____. **Spectroscopic and theoretical study of the o-vanillin hydrazone of the mycobactericidal drug isoniazid** Journal of Molecular Structure. 1007**:** 95–101 p. 2012b.

GONZÁLEZ-CASTAÑEDA, R. E. *et al.* Neural restrictive silencer factor and choline acetyltransferase expression in cerebral tissue of Alzheimer's Disease patients: A pilot study. **Genet Mol Biol,** v. 36, n. 1, p. 28-36, Mar 2013. ISSN 1415-4757.

GOODMAN, L. S. *et al.* **Goodman & Gilman's the pharmacological basis of therapeutics**. 9th. New York: McGraw-Hill, Health Professions Division, 1996. xxi, 1905 p. ISBN 9780070262669 (hardcover alk. paper) 0070262667 (hardcover alk. paper).

GRAEFF, F. G.; DEL-BEN, C. M. Neurobiology of panic disorder: from animal models to brain neuroimaging. **Neurosci Biobehav Rev,** v. 32, n. 7, p. 1326-35, Sep 2008. ISSN 0149-7634.

GRAHAM, F. L. *et al.* Characteristics of a human cell line transformed by DNA from human adenovirus type 5. **J Gen Virol,** v. 36, n. 1, p. 59-74, Jul 1977. ISSN 0022-1317.

GREEN, A. *et al.* Muscarinic and nicotinic receptor modulation of object and spatial n-back working memory in humans. **Pharmacol Biochem Behav,** v. 81, n. 3, p. 575-84, Jul 2005. ISSN 0091-3057.

GREEN, M. R.; SAMBROOK, J. **Molecular cloning : a laboratory manual**. 4th ed. / Michael R. Green, Joseph Sambrook. Cold Spring Harbor, N.Y.: Cold Spring Harbor Laboratory Press, 2012.

GRIEBEL, G. *et al.* Some critical determinants of the behaviour of rats in the elevated plus-maze. **Behav Processes,** v. 29, n. 1-2, p. 37-47, Apr 1993. ISSN 0376-6357.

GROSSEN, N. E.; KELLEY, M. J. Species-specific behavior and acquisition of avoidance behavior in rats. **J Comp Physiol Psychol,** v. 81, n. 2, p. 307-10, Nov 1972. ISSN 0021-9940.

GROUP, A.-R. E. D. S. R. A randomized, placebo-controlled, clinical trial of high-dose supplementation with vitamins C and E, beta carotene, and zinc for age-related macular degeneration and vision loss: AREDS report no. 8. **Arch Ophthalmol,** v. 119, n. 10, p. 1417-36, Oct 2001. ISSN 0003-9950.

GUIMARAES, H. C. *et al.* Apathy Is not Associated with Performance in Brief Executive Tests in Patients with Mild Cognitive Impairment and Mild Alzheimer's Disease. **Curr Alzheimer Res,** v. 11, n. 8, p. 792-8, 2014. ISSN 1875-5828.

HAASS, C. *et al.* Mutations associated with a locus for familial Alzheimer's disease result in alternative processing of amyloid beta-protein precursor. **J Biol Chem,** v. 269, n. 26, p. 17741-8, Jul 1994. ISSN 0021-9258.

_____. Amyloid beta-peptide is produced by cultured cells during normal metabolism. **Nature,** v. 359, n. 6393, p. 322-5, Sep 1992. ISSN 0028-0836.

HABIG, W. H.; PABST, M. J.; JAKOBY, W. B. Glutathione S-transferases. The first enzymatic step in mercapturic acid formation. **J Biol Chem,** v. 249, n. 22, p. 7130-9, Nov 1974. ISSN 0021-9258.

HALEY, B. E. **The relationship of the toxic effects of mercury to exacerbation**

of the medical condition classified as Alzheimer's disease. Medical Veritas. 4**:** 1510–1524 p. 2007.

HANDLEY, S. L.; MITHANI, S. Effects of alpha-adrenoceptor agonists and antagonists in a maze-exploration model of 'fear'-motivated behaviour. **Naunyn Schmiedebergs Arch Pharmacol,** v. 327, n. 1, p. 1-5, Aug 1984. ISSN 0028-1298.

HASSELMO, M. E. The role of acetylcholine in learning and memory. **Curr Opin Neurobiol,** v. 16, n. 6, p. 710-5, Dec 2006. ISSN 0959-4388.

HAUSER-DAVIS, R. A. *et al.* Disruption of zinc and copper interactions with Aβ(1-40) by a non-toxic, isoniazid-derived, hydrazone: a novel biometal homeostasis restoring agent in Alzheimer's disease therapy? **Metallomics,** v. 7, p. 743-747, April 01 2015. ISSN 1756-591X.

HAYES, J. D.; PULFORD, D. J. The glutathione S-transferase supergene family: regulation of GST and the contribution of the isoenzymes to cancer chemoprotection and drug resistance. **Crit Rev Biochem Mol Biol,** v. 30, n. 6, p. 445-600, 1995. ISSN 1040-9238.

HENDRIKS, L. *et al.* Presenile dementia and cerebral haemorrhage linked to a mutation at codon 692 of the beta-amyloid precursor protein gene. **Nat Genet,** v. 1, n. 3, p. 218-21, Jun 1992. ISSN 1061-4036.

HOERNKE, M.; KOKSCH, B.; BREZESINSKI, G. Influence of the hydrophobic interface and transition metal ions on the conformation of amyloidogenic model peptides. **Biophys Chem,** v. 150, n. 1-3, p. 64-72, Aug 2010. ISSN 1873-4200.

HOGG, S. A review of the validity and variability of the elevated plus-maze as an animal model of anxiety. **Pharmacol Biochem Behav,** v. 54, n. 1, p. 21-30, May 1996. ISSN 0091-3057.

HOOPER, P. L. *et al.* Zinc lowers high-density lipoprotein-cholesterol levels. **JAMA,** v. 244, n. 17, p. 1960-1, 1980 Oct 24-31 1980. ISSN 0098-7484.

HOU, P. *et al.* Role of copper and the copper-related protein CUTA in mediating APP processing and Aβ generation. **Neurobiol Aging,** v. 36, n. 3, p. 1310-5, Mar 2015. ISSN 1558-1497.

HOYER, S. The brain insulin signal transduction system and sporadic (type II) Alzheimer disease: an update. **J Neural Transm (Vienna),** v. 109, n. 3, p. 341-60, Mar 2002. ISSN 0300-9564.

HUANG, X. *et al.* Zinc-induced Alzheimer's Abeta1-40 aggregation is mediated by conformational factors. **J Biol Chem,** v. 272, n. 42, p. 26464-70, Oct 1997. ISSN 0021-9258.

IKEDA, M. *et al.* Diagnostic significance of skin immunolabelling with antibody against native cerebral amyloid in Alzheimer's disease. **Neurosci Lett,** v. 150, n. 2, p. 159-61, Feb 1993. ISSN 0304-3940.

IMHOF, J. T. *et al.* Influence of gender and age on performance of rats in the elevated plus maze apparatus. **Behav Brain Res,** v. 56, n. 2, p. 177-80, Sep 1993. ISSN 0166-4328.

IWATSUBO, T. *et al.* Amyloid beta protein (A beta) deposition: A beta 42(43) precedes A beta 40 in Down syndrome. **Ann Neurol,** v. 37, n. 3, p. 294-9, Mar 1995. ISSN 0364-5134.

IZQUIERDO, I. **The art of forgetting**. Cham: Springer, 2015. x, 64 pages ISBN 9783319067155 (alk. paper).

IZQUIERDO, I. *et al.* Mechanisms for memory types differ. **Nature,** v. 393, n. 6686, p. 635-6, Jun 1998. ISSN 0028-0836.

JACKREL, M. E.; SHORTER, J. Reversing deleterious protein aggregation with re-engineered protein disaggregases. **Cell Cycle,** v. 13, n. 9, p. 1379-83, May 2014. ISSN 1551-4005.

JARRETT, J. T.; BERGER, E. P.; LANSBURY, P. T. The carboxy terminus of the beta amyloid protein is critical for the seeding of amyloid formation: implications for the pathogenesis of Alzheimer's disease. **Biochemistry,** v. 32, n. 18, p. 4693-7, May 1993. ISSN 0006-2960.

JARVIS, K. E.; GRAY, A. L.; HOUK, R. S. **Handbook of inductively coupled plasma mass spectrometry**. Woking: Viridian, 2003. ISBN 0954489101 (pbk.).

JENKINS, E. C. *et al.* Fine mapping of an Alzheimer disease-associated gene encoding beta-amyloid protein. **Biochem Biophys Res Commun,** v. 151, n. 1, p. 1-8, Feb 1988. ISSN 0006-291X.

JOACHIM, C. L.; MORI, H.; SELKOE, D. J. Amyloid beta-protein deposition in tissues other than brain in Alzheimer's disease. **Nature,** v. 341, n. 6239, p. 226-30, Sep 1989. ISSN 0028-0836.

JOHNSTON, A. L.; FILE, S. E. Sex differences in animal tests of anxiety. **Physiol Behav,** v. 49, n. 2, p. 245-50, Feb 1991. ISSN 0031-9384.

JUROWSKI, K. *et al.* Biological consequences of zinc deficiency in the pathomechanisms of selected diseases. **J Biol Inorg Chem,** v. 19, n. 7, p. 1069-79, Oct 2014. ISSN 1432-1327.

KAJAL, A. *et al.* Therapeutic potential of hydrazones as anti-inflammatory agents. **Int J Med Chem,** v. 2014, p. 761030, 2014. ISSN 2090-2069.

KAR, S. *et al.* Interactions between beta-amyloid and central cholinergic neurons: implications for Alzheimer's disease. **J Psychiatry Neurosci,** v. 29, n. 6, p. 427-41, Nov 2004. ISSN 1180-4882.

KAUFFMAN, G. B.; LINDLEY, E. V. J. A classic in coordination chemistry: A resolution experiment for the inorganic laboratory. **J. Chem. Educ.,** v. 51, n. 6, p. 424, 1974.

KAWAHARA, M.; KATO-NEGISHI, M. Link between Aluminum and the Pathogenesis of Alzheimer's Disease: The Integration of the Aluminum and Amyloid Cascade Hypotheses. **Int J Alzheimers Dis,** v. 2011, p. 276393, Mar 2011. ISSN 2090-0252.

KAWAS, C. H. Clinical practice. Early Alzheimer's disease. **N Engl J Med,** v. 349, n. 11, p. 1056-63, Sep 2003. ISSN 1533-4406.

KESSING, L. V.; HARHOFF, M.; ANDERSEN, P. K. Treatment with antidepressants in patients with dementia--a nationwide register-based study. **Int Psychogeriatr,** v. 19, n. 5, p. 902-13, Oct 2007. ISSN 1041-6102.

KLAASSEN, C. D.; CASARETT, L. J.; DOULL, J. **Casarett and Doull's toxicology : the basic science of poisons**. 7th ed. United States: New York : McGraw-Hill Education, c2013., 2008.

KLATZO, I.; WISNIEWSKI, H.; STREICHER, E. EXPERIMENTAL PRODUCTION OF NEUROFIBRILLARY DEGENERATION. I. LIGHT MICROSCOPIC OBSERVATIONS. **J Neuropathol Exp Neurol,** v. 24, p. 187-99, Apr 1965. ISSN 0022-3069.

KLEIN, W. L. Synaptotoxic amyloid-β oligomers: a molecular basis for the cause, diagnosis, and treatment of Alzheimer's disease? **J Alzheimers Dis,** v. 33 Suppl 1, p. S49-65, 2013. ISSN 1875-8908.

KNOBLOCH, M. *et al.* Abeta oligomer-mediated long-term potentiation impairment involves protein phosphatase 1-dependent mechanisms. **J Neurosci,** v. 27, n. 29, p. 7648-53, Jul 2007. ISSN 1529-2401.

KOFFIE, R. M.; HYMAN, B. T.; SPIRES-JONES, T. L. Alzheimer's disease: synapses gone cold. **Mol Neurodegener,** v. 6, n. 1, p. 63, 2011. ISSN 1750-1326.

KONG, Y.; WU, J.; YUAN, L. MicroRNA Expression Analysis of Adult-Onset Drosophila Alzheimer's Disease Model. **Curr Alzheimer Res,** v. 11, n. 9, p. 882-91, 2014. ISSN 1875-5828.

KOSTOVA, I.; SASO, L. Advances in research of Schiff-base metal complexes as potent antioxidants. **Curr Med Chem,** v. 20, n. 36, p. 4609-32, 2013. ISSN 1875-533X.

KÁSA, P.; RAKONCZAY, Z.; GULYA, K. The cholinergic system in Alzheimer's disease. **Prog Neurobiol,** v. 52, n. 6, p. 511-35, Aug 1997. ISSN 0301-0082.

LA DEDA, M. *et al.* Investigations on the electronic effects of the peripheral 4'-group on 5-(4'-substituted)phenylazo-8-hydroxyquinoline ligands: zinc and aluminium complexes. **Dalton Trans**, n. 16, p. 2424-31, Aug 2004. ISSN 1477-9226.

LACOR, P. N. *et al.* Synaptic targeting by Alzheimer's-related amyloid beta oligomers. **J Neurosci,** v. 24, n. 45, p. 10191-200, Nov 2004. ISSN 1529-2401.

LAMBERT, M. P. *et al.* Diffusible, nonfibrillar ligands derived from Abeta1-42 are potent central nervous system neurotoxins. **Proc Natl Acad Sci U S A,** v. 95, n. 11, p. 6448-53, May 1998. ISSN 0027-8424.

LAURSEN, S. E.; BELKNAP, J. K. Intracerebroventricular injections in mice. Some methodological refinements. **J Pharmacol Methods,** v. 16, n. 4, p. 355-7, Dec 1986. ISSN 0160-5402.

LEAL, M. F. C. *et al.* Especiação de cobre e zinco em urina: importância dos metais em doenças neurodegenerativas. **Química Nova,** v. 35, p. 1985-1990, 2012. ISSN 0100-4042.

LEDO, J. H. *et al.* Amyloid-β oligomers link depressive-like behavior and cognitive deficits in mice. **Mol Psychiatry,** v. 18, n. 10, p. 1053-4, Oct 2013. ISSN 1476-5578.

LEI, P. *et al.* Tau deficiency induces parkinsonism with dementia by impairing APP-mediated iron export. **Nat Med,** v. 18, n. 2, p. 291-5, Feb 2012. ISSN 1546-170X.

LEONG, C. C.; SYED, N. I.; LORSCHEIDER, F. L. Retrograde degeneration of neurite membrane structural integrity of nerve growth cones following in vitro exposure to mercury. **Neuroreport,** v. 12, n. 4, p. 733-7, Mar 2001. ISSN 0959-4965.

LESTER-COLL, N. *et al.* Intracerebral streptozotocin model of type 3 diabetes: relevance to sporadic Alzheimer's disease. **J Alzheimers Dis,** v. 9, n. 1, p. 13-33, Mar 2006. ISSN 1387-2877.

LEVI, R. *et al.* Immuno-detection of aluminium and aluminium induced conformational changes in calmodulin--implications in Alzheimer's

disease. **Mol Cell Biochem,** v. 189, n. 1-2, p. 41-6, Dec 1998. ISSN 0300-8177.

LEVINE, H. *et al.* Clioquinol and other hydroxyquinoline derivatives inhibit Aβ(1–42) oligomer assembly. **Neuroscience Letters,** v. 465, n. 1, p. 99-103, 2009.

LEVY, E. *et al.* Mutation of the Alzheimer's disease amyloid gene in hereditary cerebral hemorrhage, Dutch type. **Science,** v. 248, n. 4959, p. 1124-6, Jun 1990. ISSN 0036-8075.

LEWIS, M. R.; KOKAN, L. Zinc gluconate: acute ingestion. **J Toxicol Clin Toxicol,** v. 36, n. 1-2, p. 99-101, 1998. ISSN 0731-3810.

LINDER, M. C. *et al.* Copper transport. **Am J Clin Nutr,** v. 67, n. 5 Suppl, p. 965S-971S, May 1998. ISSN 0002-9165.

LISTER, R. G. Ethologically-based animal models of anxiety disorders. **Pharmacol Ther,** v. 46, n. 3, p. 321-40, 1990. ISSN 0163-7258.

LIU, J.; KLAASSEN, C. D. Absorption and distribution of cadmium in metallothionein-I transgenic mice. **Fundam Appl Toxicol,** v. 29, n. 2, p. 294-300, Feb 1996. ISSN 0272-0590.

LOURENCO, M. V. *et al.* TNF-α mediates PKR-dependent memory impairment and brain IRS-1 inhibition induced by Alzheimer's β-amyloid oligomers in mice and monkeys. **Cell Metab,** v. 18, n. 6, p. 831-43, Dec 2013. ISSN 1932-7420.

LOURENCO, M. V.; FERREIRA, S. T.; DE FELICE, F. G. Neuronal stress signaling and eIF2α phosphorylation as molecular links between Alzheimer's disease and diabetes. **Prog Neurobiol,** v. 129, p. 37-57, Jun 2015. ISSN 1873-5118.

LOVELL, M. A. *et al.* Copper, iron and zinc in Alzheimer's disease senile plaques. **J Neurol Sci,** v. 158, n. 1, p. 47-52, Jun 1998. ISSN 0022-510X.

LUE, L. F. *et al.* Soluble amyloid beta peptide concentration as a predictor of synaptic change in Alzheimer's disease. **Am J Pathol,** v. 155, n. 3, p. 853-62, Sep 1999. ISSN 0002-9440.

LYKETSOS, C. G. *et al.* Mental and behavioral disturbances in dementia: findings from the Cache County Study on Memory in Aging. **Am J Psychiatry,** v. 157, n. 5, p. 708-14, May 2000. ISSN 0002-953X.

MAGAI, C. *et al.* A controlled clinical trial of sertraline in the treatment of depression in nursing home patients with late-stage Alzheimer's disease. **Am J Geriatr Psychiatry,** v. 8, n. 1, p. 66-74, 2000. ISSN 1064-7481.

MAISONNETTE, S.; MORATO, S.; BRANDÃO, M. L. Role of resocialization and of 5-HT1A receptor activation on the anxiogenic effects induced by isolation in the elevated plus-maze test. **Physiol Behav,** v. 54, n. 4, p. 753-8, Oct 1993. ISSN 0031-9384.

MANCINO, A. M. *et al.* Effects of clioquinol on metal-triggered amyloid-beta aggregation revisited. **Inorg Chem,** v. 48, n. 20, p. 9596-8, Oct 2009. ISSN 1520-510X.

MARIEN, M. R.; COLPAERT, F. C.; ROSENQUIST, A. C. Noradrenergic mechanisms in neurodegenerative diseases: a theory. **Brain Res Brain Res Rev,** v. 45, n. 1, p. 38-78, Apr 2004.

MARINO, T. *et al.* On the metal ion (Zn(2+), Cu(2+)) coordination with beta-amyloid peptide: DFT computational study. **Interdiscip Sci,** v. 2, n. 1, p. 57-69, Mar 2010. ISSN 1913-2751.

MARIOTTINI, G. L. *et al.* **Introduzione alle colture cellulari**. II edition. Tecniche nuove, 2010.

MARTYN, C. N. *et al.* Geographical relation between Alzheimer's disease and aluminum in drinking water. **Lancet,** v. 1, n. 8629, p. 59-62, Jan 1989. ISSN 0140-6736.

MATHEW, T. *et al.* Hepatotoxicity of dimethylformamide and dimethylsulfoxide at and above the levels used in some aflatoxin studies. **Lab Invest,** v. 42, n. 2, p. 257-62, Feb 1980. ISSN 0023-6837.

MATTSON, M. P. *et al.* beta-Amyloid precursor protein metabolites and loss of neuronal Ca2+ homeostasis in Alzheimer's disease. **Trends Neurosci,** v. 16, n. 10, p. 409-14, Oct 1993. ISSN 0166-2236.

MAURER, K.; VOLK, S.; GERBALDO, H. **Auguste D and Alzheimer's disease**. The Lancet. 349**:** 1546-1549 p. 1997.

MAYEUX, R.; STERN, Y. Epidemiology of Alzheimer disease. **Cold Spring Harb Perspect Med,** v. 2, n. 8, 2012. ISSN 2157-1422.

MCKHANN, G. *et al.* Clinical diagnosis of Alzheimer's disease: report of the NINCDS-ADRDA Work Group under the auspices of Department of Health and Human Services Task Force on Alzheimer's Disease. **Neurology,** v. 34, n. 7, p. 939-44, Jul 1984. ISSN 0028-3878.

MEHAN, S. *et al.* **Dementia – A Complete Literature Review on Various Mechanisms Involves in Pathogenesis and an Intracerebroventricular Streptozotocin Induced Alzheimer's Disease**. Inflammatory Diseases - Immunopathology, Clinical and Pharmacological Bases 2012.

MEKMOUCHE, Y. *et al.* Characterization of the ZnII binding to the peptide amyloid-beta1-16 linked to Alzheimer's disease. **Chembiochem,** v. 6, n. 9, p. 1663-71, Sep 2005. ISSN 1439-4227.

MELOV, S. '…and C is for Clioquinol' – the AβCs of Alzheimer's disease. **Trend in Neurosciences,** v. 25, n. 3, p. 121-123, 2002.

MICHAELSON, D. M. APOE ε4: The most prevalent yet understudied risk factor for Alzheimer's disease. **Alzheimers Dement,** v. 10, n. 6, p. 861-868, Nov 2014. ISSN 1552-5279.

MIURA, T. *et al.* Metal binding modes of Alzheimer's amyloid beta-peptide in insoluble aggregates and soluble complexes. **Biochemistry,** v. 39, n. 23, p. 7024-31, Jun 2000. ISSN 0006-2960.

MOLINO, I. *et al.* Efficacy of memantine, donepezil, or their association in moderate-severe Alzheimer's disease: a review of clinical trials. **ScientificWorldJournal,** v. 2013, p. 925702, 2013. ISSN 1537-744X.

MONAMY, V. **Animal Experimentation: A Guide to the Issues**. Cambridge University Press, 2009. ISBN 9780511801808.

MONTGOMERY, K. C. The relation between fear induced by novel stimulation and exploratory behavior. **J Comp Physiol Psychol,** v. 48, n. 4, p. 254-60, Aug 1955. ISSN 0021-9940.

MONTGOMERY, K. C.; MONKMAN, J. A. The relation between fear and exploratory behavior. **J Comp Physiol Psychol,** v. 48, n. 2, p. 132-6, Apr 1955. ISSN 0021-9940.

MORATO, S.; BRANDÃO, M. L. Transporting rats to the test situation on a cart can modify rat exploratory behavior in the elevated plus-maze. **Psychobiology,** v. 24, n. 3, p. 247-252, 1996. ISSN 0889-6313.

MORRIS, J. K.; BURNS, J. M. Insulin: an emerging treatment for Alzheimer's disease dementia? **Curr Neurol Neurosci Rep,** v. 12, n. 5, p. 520-7, Oct 2012. ISSN 1534-6293.

MOSES, S. N.; COLE, C.; RYAN, J. D. Relational memory for object identity and spatial location in rats with lesions of perirhinal cortex, amygdala and hippocampus. **Brain Res Bull,** v. 65, n. 6, p. 501-12, May 2005. ISSN 0361-9230.

MOSS, S. *et al.* Design of the Acoustic Electric Feedthrough Demonstrator Mk II. **Materials Forum,** v. 33, p. 187--200, 2009.

MUIR, J. L. *et al.* Excitotoxic lesions of basal forebrain cholinergic neurons: effects on learning, memory and attention. **Behav Brain Res,** v. 57, n. 2, p. 123-31, Nov 1993. ISSN 0166-4328.

MULLAN, M. *et al.* A pathogenic mutation for probable Alzheimer's disease in the APP gene at the N-terminus of beta-amyloid. **Nat Genet,** v. 1, n. 5, p. 345-7, Aug 1992. ISSN 1061-4036.

MURRELL, J. *et al.* A mutation in the amyloid precursor protein associated with hereditary Alzheimer's disease. **Science,** v. 254, n. 5028, p. 97-9, Oct 1991. ISSN 0036-8075.

MUTHURAJU, S. *et al.* Acetylcholinesterase inhibitors enhance cognitive functions in rats following hypobaric hypoxia. **Behav Brain Res,** v. 203, n. 1, p. 1-14, Oct 2009. ISSN 1872-7549.

NAIR, S. *et al.* Genome-wide analysis of Saccharomyces cerevisiae identifies cellular processes affecting intracellular aggregation of Alzheimer's amyloid-β42: importance of lipid homeostasis. **Mol Biol Cell,** v. 25, n. 15, p. 2235-49, Aug 2014. ISSN 1939-4586.

NAKAMOTO, K. **Infrared and Raman spectra of inorganic and coordination compounds**. 6th ed. Hoboken, N.J.: Wiley ; [Oxford : Wiley-Blackwell, distributor], 2009. ISBN 9780471744924 (set) : ¹103.00

NESSE, R. M. Proximate and evolutionary studies of anxiety, stress and depression: synergy at the interface. **Neurosci Biobehav Rev,** v. 23, n. 7, p. 895-903, Nov 1999. ISSN 0149-7634.

NG, S. *et al.* Mercury, APOE, and children's neurodevelopment. **Neurotoxicology,** v. 37, p. 85-92, Jul 2013. ISSN 1872-9711.

NIE, Q.; DU, X. G.; GENG, M. Y. Small molecule inhibitors of amyloid β peptide aggregation as a potential therapeutic strategy for Alzheimer's disease. **Acta Pharmacol Sin,** v. 32, n. 5, p. 545-51, May 2011. ISSN 1745-7254.

NINFA, A. J.; BALLOU, D. P.; BENORE, M. **Fundamental laboratory approaches for biochemistry and biotechnology**. 2nd ed. / Alexander J. Ninfa, David P. Ballou, Marilee Benore. Hoboken, N.J.: Wiley ; Chichester, 2010. ISBN 9780470087664 (pbk.) : ¹50.50
0470087668 (pbk.) : ¹50.50.

NYTH, A. L.; GOTTFRIES, C. G. The clinical efficacy of citalopram in treatment of emotional disturbances in dementia disorders. A Nordic multicentre study. **Br J Psychiatry,** v. 157, p. 894-901, Dec 1990. ISSN 0007-1250.

O' NEILL, C. PI3-kinase/Akt/mTOR signaling: impaired on/off switches in aging, cognitive decline and Alzheimer's disease. **Exp Gerontol,** v. 48, n. 7, p. 647-53, Jul 2013. ISSN 1873-6815.

OGA, E. F. Spectrophotometric determination of isoniazid in pure and pharmaceutical Formulations using vanillin. **International Journal of Pharmacy and Pharmaceutical Sciences,** v. Vol 2, Suppl 1,, p. 55-58, 2010.

OTT, A. *et al.* Diabetes mellitus and the risk of dementia: The Rotterdam Study. **Neurology,** v. 53, n. 9, p. 1937-42, Dec 1999. ISSN 0028-3878.

PARIKH, V. *et al.* Interactions between Aβ oligomers and presynaptic cholinergic signaling: Age-dependent effects on attentional capacities. **Behav Brain Res,** v. 274, p. 30-42, Nov 2014. ISSN 1872-7549.

PARK, C. R. *et al.* Intracerebroventricular insulin enhances memory in a passive-avoidance task. **Physiol Behav,** v. 68, n. 4, p. 509-14, Feb 2000. ISSN 0031-9384.

PELLOW, S. Anxiolytic and anxiogenic drug effects in a novel test of anxiety: are exploratory models of anxiety in rodents valid? **Methods Find Exp Clin Pharmacol,** v. 8, n. 9, p. 557-65, Sep 1986. ISSN 0379-0355.

PELLOW, S. *et al.* Validation of open:closed arm entries in an elevated plus-maze as a measure of anxiety in the rat. **J Neurosci Methods,** v. 14, n. 3, p. 149-67, Aug 1985. ISSN 0165-0270.

PENDERGRASS, J. C. *et al.* Mercury vapor inhalation inhibits binding of GTP to tubulin in rat brain: similarity to a molecular lesion in Alzheimer diseased brain. **Neurotoxicology,** v. 18, n. 2, p. 315-24, 1997. ISSN 0161-813X.

PEREZ, F. P. *et al.* Late-onset Alzheimer's disease, heating up and foxed by several proteins: pathomolecular effects of the aging process. **J Alzheimers Dis,** v. 40, n. 1, p. 1-17, 2014. ISSN 1875-8908.

PERRY, E. K. *et al.* Neurotransmitter enzyme abnormalities in senile dementia. Choline acetyltransferase and glutamic acid decarboxylase activities in necropsy brain tissue. **J Neurol Sci,** v. 34, n. 2, p. 247-65, Nov 1977. ISSN 0022-510X.

PERRY, G. *et al.* The role of iron and copper in the aetiology of neurodegenerative disorders: therapeutic implications. **CNS Drugs,** v. 16, n. 5, p. 339-52, 2002. ISSN 1172-7047.

PLUM, L. M.; RINK, L.; HAASE, H. The essential toxin: impact of zinc on human health. **Int J Environ Res Public Health,** v. 7, n. 4, p. 1342-65, Apr 2010. ISSN 1660-4601.

POWER, A. E.; VAZDARJANOVA, A.; MCGAUGH, J. L. Muscarinic cholinergic influences in memory consolidation. **Neurobiol Learn Mem,** v. 80, n. 3, p. 178-93, Nov 2003. ISSN 1074-7427.

PUZZO, D. *et al.* Picomolar amyloid-beta positively modulates synaptic plasticity and memory in hippocampus. **J Neurosci,** v. 28, n. 53, p. 14537-45, Dec 2008. ISSN 1529-2401.

REGER, M. A. *et al.* Intranasal insulin improves cognition and modulates beta-amyloid in early AD. **Neurology,** v. 70, n. 6, p. 440-8, Feb 2008. ISSN 1526-632X.

REIFLER, B. V. *et al.* Double-blind trial of imipramine in Alzheimer's disease patients with and without depression. **Am J Psychiatry,** v. 146, n. 1, p. 45-9, Jan 1989. ISSN 0002-953X.

REITZ, C.; BRAYNE, C.; MAYEUX, R. Epidemiology of Alzheimer disease. **Nat Rev Neurol,** v. 7, n. 3, p. 137-52, Mar 2011. ISSN 1759-4766.

RICHARDSON, D.; BERNHARDT, P. V.; BECKER, E. M. **Iron chelators and uses thereof**: US6989397 B1 2006.

RINK, L.; GABRIEL, P. Zinc and the immune system. **Proc Nutr Soc,** v. 59, n. 4, p. 541-52, Nov 2000. ISSN 0029-6651.

RIVA, E. *et al.* Association of mild anemia with hospitalization and mortality in the elderly: the Health and Anemia population-based study. **Haematologica,** v. 94, n. 1, p. 22-8, Jan 2009. ISSN 1592-8721.

RIVERA, E. J. *et al.* Insulin and insulin-like growth factor expression and function deteriorate with progression of Alzheimer's disease: link to brain reductions in acetylcholine. **J Alzheimers Dis,** v. 8, n. 3, p. 247-68, Dec 2005. ISSN 1387-2877.

RODRIGUES SIMÕES, M. C. *et al.* Donepezil: an important prototype to the design of new drug candidates for Alzheimer's disease. **Mini Rev Med Chem,** v. 14, n. 1, p. 2-19, Jan 2014. ISSN 1875-5607.

ROESLER, R. *et al.* Bombesin/gastrin-releasing peptide receptors in the basolateral amygdala regulate memory consolidation. **Eur J Neurosci,** v. 19, n. 4, p. 1041-5, Feb 2004. ISSN 0953-816X.

RONDEAU, V. A review of epidemiologic studies on aluminum and silica in relation to Alzheimer's disease and associated disorders. **Rev Environ Health,** v. 17, n. 2, p. 107-21, 2002 Apr-Jun 2002. ISSN 0048-7554.

RÖNNEMAA, E. *et al.* Impaired insulin secretion increases the risk of Alzheimer disease. **Neurology,** v. 71, n. 14, p. 1065-71, Sep 2008. ISSN 1526-632X.

SAHARAN, S.; MANDAL, P. K. The emerging role of glutathione in Alzheimer's disease. **J Alzheimers Dis,** v. 40, n. 3, p. 519-29, 2014. ISSN 1875-8908.

SAMPSON, E. L.; JENAGARATNAM, L.; MCSHANE, R. Metal protein attenuating compounds for the treatment of Alzheimer's dementia. **Cochrane Database Syst Rev,** v. 5, p. CD005380, 2012. ISSN 1469-493X.

SANDSTEAD, H. H. Understanding zinc: recent observations and interpretations. **J Lab Clin Med,** v. 124, n. 3, p. 322-7, Sep 1994. ISSN 0022-2143.

SATYAJIT MONDAL[A,] S. N., AYAN KUMAR DEYA, EKKEHARD SI[N]NB, CARLA ERIBALB, STEVEN R. HER[R]ONC,SHYAMAL KUMAR CHATTOPADH[Y]AYA. Mononuclear and binuclear Cu(II) complexes of some tridentate aroyl hydrazones. X-ray crystal structures of a mononuclear and a binuclear complex. **Inorganica Chimica Acta,** v. 398, p. 98-105, 2013.

SAVINI, L. *et al.* New alpha-(N)-heterocyclichydrazones: evaluation of anticancer, anti-HIV and antimicrobial activity. **Eur J Med Chem,** v. 39, n. 2, p. 113-22, Feb 2004. ISSN 0223-5234.

SAVORY, J.; HERMAN, M. M.; GHRIBI, O. Mechanisms of aluminum-induced neurodegeneration in animals: Implications for Alzheimer's disease. **J Alzheimers Dis,** v. 10, n. 2-3, p. 135-44, Nov 2006. ISSN 1387-2877.

SAYRE, L. M. *et al.* In situ oxidative catalysis by neurofibrillary tangles and senile plaques in Alzheimer's disease: a central role for bound transition metals. **J Neurochem,** v. 74, n. 1, p. 270-9, Jan 2000. ISSN 0022-3042.

SCHACTER, D. L. Implicit memory: History and current status. **Journal of Experimental Psychology: Learning, Memory, and Cognition,** v. 13, p. 501-518, 1987.

SCHNABEL, J. Amyloid: little proteins, big clues. **Nature,** v. 475, n. 7355, p. S12-4, Jul 2011. ISSN 1476-4687.

SCHRADER-FISCHER, G.; PAGANETTI, P. A. Effect of alkalizing agents on the processing of the beta-amyloid precursor protein. **Brain Res,** v. 716, n. 1-2, p. 91-100, Apr 1996. ISSN 0006-8993.

SCHWARTZ, J. R.; ROTH, T. Neurophysiology of sleep and wakefulness: basic science and clinical implications. **Curr Neuropharmacol,** v. 6, n. 4, p. 367-78, Dec 2008. ISSN 1570-159X.

SEBASTIÃO, I. *et al.* Insulin as a Bridge between Type 2 Diabetes and Alzheimer Disease - How Anti-Diabetics Could be a Solution for Dementia. **Front Endocrinol (Lausanne),** v. 5, p. 110, 2014. ISSN 1664-2392.

SELKOE, D.; MANDELKOW, E.; HOLTZMAN, D. Deciphering Alzheimer disease. **Cold Spring Harb Perspect Med,** v. 2, n. 1, p. a011460, Jan 2012. ISSN 2157-1422.

SELKOE, D. J. Amyloid beta-protein and the genetics of Alzheimer's disease. **J Biol Chem,** v. 271, n. 31, p. 18295-8, Aug 1996. ISSN 0021-9258.

_____. Soluble oligomers of the amyloid beta-protein impair synaptic plasticity and behavior. **Behav Brain Res,** v. 192, n. 1, p. 106-13, Sep 2008. ISSN 0166-4328.

_____. Alzheimer's disease. **Cold Spring Harb Perspect Biol,** v. 3, n. 7, Jul 2011. ISSN 1943-0264.

SENSI, S. L. *et al.* The neurophysiology and pathology of brain zinc. **J Neurosci,** v. 31, n. 45, p. 16076-85, Nov 2011. ISSN 1529-2401.

SERRANO-POZO, A. *et al.* Neuropathological Alterations in Alzheimer Disease. **Cold Spring Harbor Perspectives in Biology,** v. 3, n. 12, Dec 2011. ISSN 1943-0264.

SEUBERT, P. *et al.* Isolation and quantification of soluble Alzheimer's beta-peptide from biological fluids. **Nature,** v. 359, n. 6393, p. 325-7, Sep 1992. ISSN 0028-0836.

SHANKAR, A. H.; PRASAD, A. S. Zinc and immune function: the biological basis of altered resistance to infection. **Am J Clin Nutr,** v. 68, n. 2 Suppl, p. 447S-463S, Aug 1998. ISSN 0002-9165.

SHAW, G. *et al.* Preferential transformation of human neuronal cells by human adenoviruses and the origin of HEK 293 cells. **FASEB J,** v. 16, n. 8, p. 869-71, Jun 2002. ISSN 1530-6860.

SHCHERBATYKH, I.; CARPENTER, D. O. The role of metals in the etiology of Alzheimer's disease. **J Alzheimers Dis,** v. 11, n. 2, p. 191-205, May 2007. ISSN 1387-2877.

SILVA, A. G. *et al.* Synthesis and vasodilatory activity of new N-acylhydrazone derivatives, designed as LASSBio-294 analogues. **Bioorg Med Chem,** v. 13, n. 10, p. 3431-7, May 2005. ISSN 0968-0896.

SMALL, G. W. *et al.* Diagnosis and treatment of Alzheimer disease and related disorders - Consensus statement of the American Association for Geriatric Psychiatry, the Alzheimer's Association, and the American Geriatrics Society. **Jama-Journal of the American Medical Association,** v. 278, n. 16, p. 1363-1371, Oct 22 1997. ISSN 0098-7484.

SMILEY, J. F.; SUBRAMANIAN, M.; MESULAM, M. M. Monoaminergic-cholinergic interactions in the primate basal forebrain. **Neuroscience,** v. 93, n. 3, p. 817-29, 1999. ISSN 0306-4522.

SMITH, M. A. *et al.* Iron accumulation in Alzheimer disease is a source of redox-generated free radicals. **Proc Natl Acad Sci U S A,** v. 94, n. 18, p. 9866-8, Sep 1997. ISSN 0027-8424.

SMITH, M. A. C. Doença de Alzheimer. **Revista Brasileira de Psiquiatria,** v. 21, n. 2, p. 03-07, 1999.

SNOOK, R. D. **Handbook of inductively coupled plasma mass spectrometry**. Springer-Verlag, 1992. 546.

SOFOLA-ADESAKIN, O. *et al.* Lithium suppresses Aβ pathology by inhibiting translation in an adult Drosophila model of Alzheimer's disease. **Front Aging Neurosci,** v. 6, p. 190, 2014. ISSN 1663-4365.

SOREGHAN, B.; KOSMOSKI, J.; GLABE, C. Surfactant properties of Alzheimer's A beta peptides and the mechanism of amyloid aggregation. **J Biol Chem,** v. 269, n. 46, p. 28551-4, Nov 1994. ISSN 0021-9258.

SOUTHERN, E. The early days of blotting. **Methods Mol Biol,** v. 1312, p. 1-3, 2015. ISSN 1940-6029.

SPENCER, A. P.; CARSON, D. S.; CROUCH, M. A. Vitamin E and coronary artery disease. **Arch Intern Med,** v. 159, n. 12, p. 1313-20, Jun 1999. ISSN 0003-9926.

SQUIRE, L. R.; KANDEL, E. R. **Memory : from mind to molecules**. 2nd ed. Greenwood Village, Colo.: Roberts & Co., 2009. ISBN 9780981519418
0981519415.

SQUITTI, R.; SALUSTRI, C. Agents complexing copper as a therapeutic strategy for the treatment of Alzheimer's disease. **Curr Alzheimer Res,** v. 6, n. 6, p. 476-87, Dec 2009. ISSN 1875-5828.

STEEN, E. *et al.* Impaired insulin and insulin-like growth factor expression and signaling mechanisms in Alzheimer's disease--is this type 3 diabetes? **J Alzheimers Dis,** v. 7, n. 1, p. 63-80, Feb 2005. ISSN 1387-2877.

STOCKHORST, U. *et al.* Insulin and the CNS: effects on food intake, memory, and endocrine parameters and the role of intranasal insulin administration in humans. **Physiol Behav,** v. 83, n. 1, p. 47-54, Oct 2004. ISSN 0031-9384.

SUBASH, S. *et al.* Pomegranate from Oman Alleviates the Brain Oxidative Damage in Transgenic Mouse Model of Alzheimer's disease. **J Tradit Complement Med,** v. 4, n. 4, p. 232-8, Oct 2014. ISSN 2225-4110.

SYLVESTER, P. W. Optimization of the tetrazolium dye (MTT) colorimetric assay for cellular growth and viability. **Methods Mol Biol,** v. 716, p. 157-68, 2011. ISSN 1940-6029.

SZKUDELSKI, T. Streptozotocin-nicotinamide-induced diabetes in the rat. Characteristics of the experimental model. **Exp Biol Med (Maywood),** v. 237, n. 5, p. 481-90, May 2012. ISSN 1535-3699.

TALBOT, K. *et al.* Demonstrated brain insulin resistance in Alzheimer's disease patients is associated with IGF-1 resistance, IRS-1 dysregulation, and cognitive decline. **J Clin Invest,** v. 122, n. 4, p. 1316-38, Apr 2012. ISSN 1558-8238.

TAN, L. *et al.* Yeast expressed foldable quadrivalent Aβ15 elicited strong immune response against Aβ without Aβ-specific T cell response in wild

C57BL/6 mice. **Hum Vaccin Immunother,** v. 8, n. 8, p. 1090-8, Aug 2012. ISSN 2164-554X.

TOLOSA, L.; DONATO, M. T.; GÓMEZ-LECHÓN, M. J. General Cytotoxicity Assessment by Means of the MTT Assay. **Methods Mol Biol,** v. 1250, p. 333-48, 2015. ISSN 1940-6029.

TONEFF, T. *et al.* Beta-amyloid peptides undergo regulated co-secretion with neuropeptide and catecholamine neurotransmitters. **Peptides,** v. 46, p. 126-35, Aug 2013. ISSN 1873-5169.

TREIT, D.; FUNDYTUS, M. Thigmotaxis as a test for anxiolytic activity in rats. **Pharmacol Biochem Behav,** v. 31, n. 4, p. 959-62, Dec 1988. ISSN 0091-3057.

TREIT, D.; MENARD, J.; ROYAN, C. Anxiogenic stimuli in the elevated plus-maze. **Pharmacol Biochem Behav,** v. 44, n. 2, p. 463-9, Feb 1993. ISSN 0091-3057.

TÕUGU, V.; KARAFIN, A.; PALUMAA, P. Binding of zinc(II) and copper(II) to the full-length Alzheimer's amyloid-beta peptide. **J Neurochem,** v. 104, n. 5, p. 1249-59, Mar 2008. ISSN 1471-4159.

ULLMAN, M. T. Contributions of memory circuits to language: the declarative/procedural model. **Cognition,** v. 92, n. 1-2, p. 231-70, 2004 May-Jun 2004. ISSN 0010-0277.

URBANC, B. *et al.* Structural Basis for A beta(1-42) Toxicity Inhibition by A beta C-Terminal Fragments: Discrete Molecular Dynamics Study. **Journal of Molecular Biology,** v. 410, n. 2, p. 316-328, Jul 8 2011. ISSN 0022-2836.

VALKO, M. *et al.* Free radicals and antioxidants in normal physiological functions and human disease. **International Journal of Biochemistry & Cell Biology,** v. 39, n. 1, p. 44-84, 2007. ISSN 1357-2725.

VAN LEEUWEN, R. *et al.* Dietary intake of antioxidants and risk of age-related macular degeneration. **JAMA,** v. 294, n. 24, p. 3101-7, Dec 2005. ISSN 1538-3598.

VAUGHAN, D. W.; PETERS, A. The structure of neuritic plaque in the cerebral cortex of aged rats. **J Neuropathol Exp Neurol,** v. 40, n. 4, p. 472-87, Jul 1981. ISSN 0022-3069.

VICINI, P. *et al.* Synthesis and antiproliferative activity of benzo[d]isothiazole hydrazones. **Eur J Med Chem,** v. 41, n. 5, p. 624-32, May 2006. ISSN 0223-5234.

_____. Anti-HIV evaluation of benzo[d]isothiazole hydrazones. **Eur J Med Chem,** v. 44, n. 4, p. 1801-7, Apr 2009. ISSN 1768-3254.

WALSH, D. M. *et al.* Naturally secreted oligomers of amyloid beta protein potently inhibit hippocampal long-term potentiation in vivo. **Nature,** v. 416, n. 6880, p. 535-9, Apr 2002. ISSN 0028-0836.

WARRA, A. A.; JIMOH, W. L. O. OVERVIEW OF AN INDUCTIVELY COUPLED PLASMA (ICP) SYSTEM. **International Journal of Chemical Research,** v. 3, n. 2, p. 41-48, 2011. ISSN 0975-3699.

WEBB, R. L.; MURPHY, M. P. β-Secretases, Alzheimer's Disease, and Down Syndrome. **Curr Gerontol Geriatr Res,** v. 2012, p. 362839, 2012. ISSN 1687-7071.

WHITTAKER, P. Iron and zinc interactions in humans. **Am J Clin Nutr,** v. 68, n. 2 Suppl, p. 442S-446S, Aug 1998. ISSN 0002-9165.

WHITTAKER, P.; TUFARO, P. R.; RADER, J. I. Iron and folate in fortified cereals. **J Am Coll Nutr,** v. 20, n. 3, p. 247-54, Jun 2001. ISSN 0731-5724.

WILCOCK, G. K. *et al.* Alzheimer's disease. Correlation of cortical choline acetyltransferase activity with the severity of dementia and histological abnormalities. **J Neurol Sci,** v. 57, n. 2-3, p. 407-17, Dec 1982. ISSN 0022-510X.

WINKLER, J. *et al.* Essential role of neocortical acetylcholine in spatial memory. **Nature,** v. 375, n. 6531, p. 484-7, Jun 1995. ISSN 0028-0836.

WINTERGERST, E. S.; MAGGINI, S.; HORNIG, D. H. Contribution of selected vitamins and trace elements to immune function. **Ann Nutr Metab,** v. 51, n. 4, p. 301-23, 2007. ISSN 1421-9697.

WU, J. *et al.* Alzheimer's disease (AD)-like pathology in aged monkeys after infantile exposure to environmental metal lead (Pb): evidence for a developmental origin and environmental link for AD. **J Neurosci,** v. 28, n. 1, p. 3-9, Jan 2008. ISSN 1529-2401.

XU, P. X. *et al.* Rutin improves spatial memory in Alzheimer's disease transgenic mice by reducing Aβ oligomer level and attenuating oxidative stress and neuroinflammation. **Behav Brain Res,** v. 264, p. 173-80, May 2014. ISSN 1872-7549.

YAMADA, M. *et al.* Implanted cannula-mediated repetitive administration of Abeta25-35 into the mouse cerebral ventricle effectively impairs spatial working memory. **Behav Brain Res,** v. 164, n. 2, p. 139-46, Nov 2005. ISSN 0166-4328.

YAN, Z.; FENG, J. Alzheimer's disease: interactions between cholinergic functions and beta-amyloid. **Curr Alzheimer Res,** v. 1, n. 4, p. 241-8, Nov 2004. ISSN 1567-2050.

YANG, D. S. *et al.* Examining the zinc binding site of the amyloid-beta peptide. **Eur J Biochem,** v. 267, n. 22, p. 6692-8, Nov 2000. ISSN 0014-2956.

ZATTA, P. *et al.* In vivo and in vitro effects of aluminum on the activity of mouse brain acetylcholinesterase. **Brain Res Bull,** v. 59, n. 1, p. 41-5, Oct 2002. ISSN 0361-9230.

Appendix

Appendix 1. UV-Vis absorbance INHOVA profile in 10% DMSO concentration, over 30 h, in 250-400 nm range. 200-250 nm range is DMSO UV-Vis absorbance range, and 400-800 range shows no bands, then them are not shown.
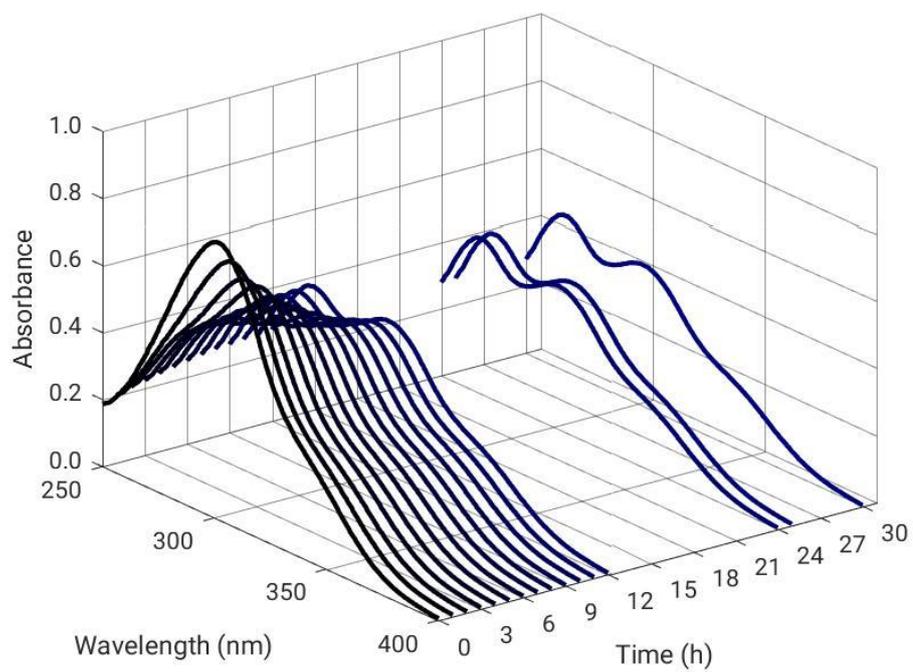
Appendix 2. Bidimensional contour plot profile of Aβ$_{1-40}$-Zn-INHHQ system in ^{1}H x ^{15}N HSQC NMR analysis. A) Aβ-free profile (black), and the profile of Aβ-Zn^{2+} (1:1) (red). B) Aβ-free profile (black), and the profile of Aβ-Zn^{2+}-INHHQ (1:1:5) (grey). C) I/I$_0$ intensity profiles for the Aβ residues in Aβ$_{1-40}$-Zn-INHHQ system. Aβ-Zn without INHHQ (violet bars), Aβ-Zn^{2+}-INHHQ system in with 1, 3, 5 and 10 INHHQ equivalents (soft brown, dark grey, grey and black bars, respectively). Adapted from Hauser-Davis *et al.*, 2015.
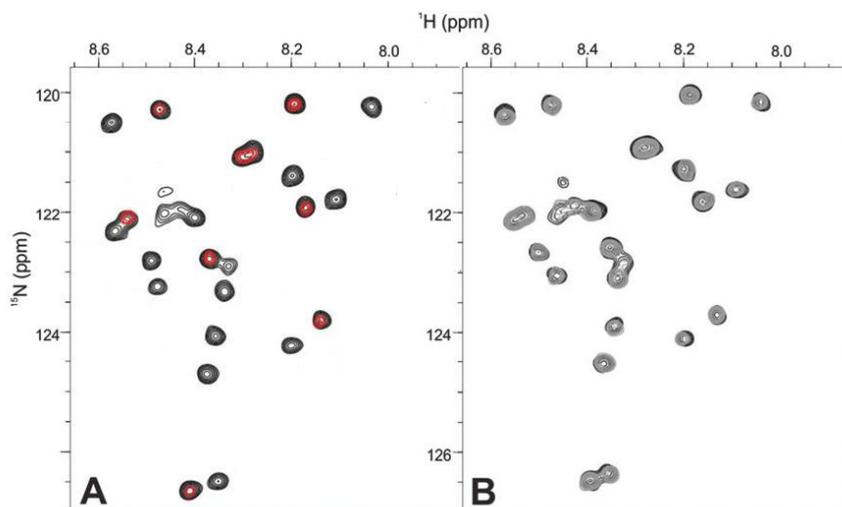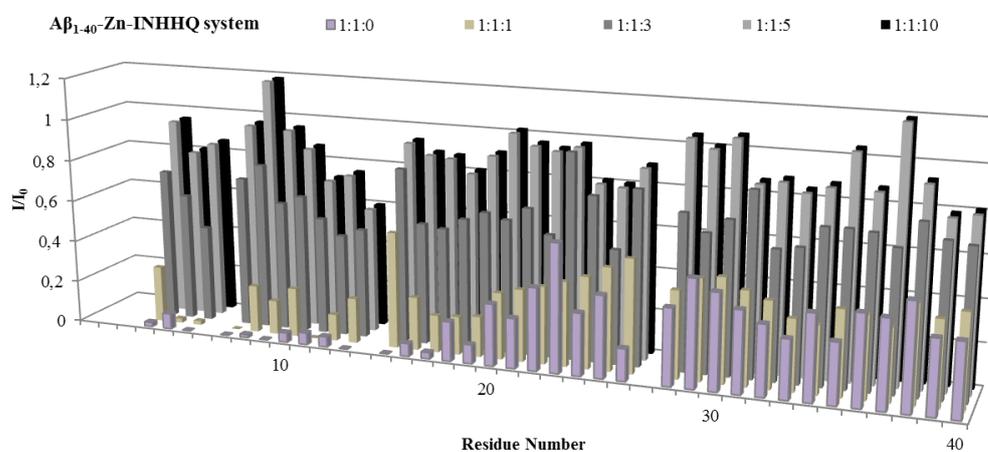
Appendix 3. Bidimensional contour plot profile of Aβ$_{1-40}$-Zn-HPCIH system in ^{1}H x ^{15}N HSQC NMR analysis. A) Aβ-free profile (black), and the profile of Aβ-Zn^{2+} (1:1) (magenta). B) Aβ-free profile (black), and the profile of Aβ-Zn^{2+}-HPCIH (1:1:5) (red). C) I/I$_0$ intensity profiles for the Aβ residues in Aβ$_{1-40}$-Zn-HPCIH system. Aβ-Zn without HPCIH (violet bars), Aβ-Zn^{2+}-HPCIH system in with 1, 3, 5 and 10 HPCIH equivalents (pink, dark red, red and black bars, respectively).